

Star Cocircularities of Knots

by

Garret Flowers
B.A., Oberlin College, 2009

A Thesis Submitted in Partial Fulfillment of the
Requirements for the Degree of

MASTER OF SCIENCE

in the Department of Mathematics

© Garret Flowers, 2011
University of Victoria

All rights reserved. This thesis may not be reproduced in whole or in part, by
photocopying or other means, without the permission of the author.

Star Cocircularities of Knots

by

Garret Flowers
B.A., Oberlin College, 2009

Supervisory Committee

Dr. Ryan Budney, Supervisor
(Department of Mathematics)

Dr. Alfonso Gracia-Saz, Departmental Member
(Department of Mathematics)

Supervisory Committee

Dr. Ryan Budney, Supervisor
(Department of Mathematics)

Dr. Alfonso Gracia-Saz, Departmental Member
(Department of Mathematics)

ABSTRACT

The study of knot invariants is a large and active area of research in the field of knot theory. In the early 1990s, Russian mathematician Victor Vassiliev developed a series of numerical knot invariants, now known as Vassiliev invariants. These invariants have sparked a great deal of interest in the mathematical community, and it is conjectured that, together, they formulate a complete knot invariant. The computation of these invariants is largely algebraic, and unfortunately the values do not appear to describe any intrinsic properties of the knot. In this thesis, a geometric interpretation of the second Vassiliev invariant is provided by examining occurrences of five distinct points on the knot that lie on a common circle in the ambient space. This process is then extended to include an analysis of six-point cocircularities of knots as well.

Contents

Supervisory Committee	ii
Abstract	iii
Table of Contents	iv
List of Figures	vi
Acknowledgements	viii
Dedication	ix
1 Introduction	1
2 Fundamental Properties of Manifolds	4
2.1 Manifolds with Boundary and Transversality	4
2.2 Orientation and Intersection Theory	10
3 Knots and Vassiliev Invariants	17
4 Quadrisecants	22
4.1 Quadrisecant Transversality	27
4.2 Quadrisecant Count as a Vassiliev Invariant	38
5 Transversality and Cocircularities	42
5.1 Adjacency and the Tubular Neighborhood	43
5.2 Perturbing the Knot	51
6 Satanic and Thelemic Points as Invariants	57
6.1 Satanic Points	58
6.2 Thelemic Points	60

7 Conclusion	72
A Vassiliev Tables	75
B Satanic Circle Code	76
C Satanic Circle Gallery	83
D Thelemic Circle Code	87
E Thelemic Circle Gallery	91

List of Figures

Figure 2.1.1	The sphere S^2 and P_b	7
Figure 2.1.2	An ε -neighborhood of a curve.	9
Figure 2.2.1	A potential example for $F^{-1}(Z)$ in $S^1 \times \mathbb{I}$	11
Figure 2.2.2	The Möbius strip	12
Figure 2.2.3	A homotopy space with orientations.	16
Figure 3.0.1	Two equivalent knots.	17
Figure 3.0.2	A particular crossing.	19
Figure 3.0.3	The crossing change operation.	20
Figure 4.0.1	A point in $C_4\mathbb{R}^2$	23
Figure 4.0.2	A point in C_3K	26
Figure 4.0.3	An alternating quadrisequant in the trefoil knot.	27
Figure 4.1.1	An extension of the knot to its normal bundle.	31
Figure 4.1.2	Bump functions on the unit interval.	32
Figure 5.0.1	Compactification of the long knot.	43
Figure 5.1.1	Satanic points.	44
Figure 5.1.2	Thelemic points.	45
Figure 5.1.3	A diagram illustrating the minimum distance between the coordinates of satanic points.	48
Figure 5.1.4	A commutative diagram extending the knot f to f^*	50
Figure 5.2.1	Bump functions on S^1	53
Figure 5.2.2	A commutative diagram incorporating g	53
Figure 6.1.1	A commutative diagram relating a knot f with its corresponding long knot f_*	59
Figure 6.1.2	A satanic circle on the trefoil knot.	60
Figure 6.2.1	C_2S^1 as a Möbius strip.	64
Figure 6.2.2	Inducing an orientation on the quotient manifold.	65

Figure 6.2.3 A commutative diagram establishing orientations on configuration spaces.	67
Figure C.0.1 The 4_1 (figure-eight) knot.	84
Figure C.0.2 The 5_1 knot.	85
Figure C.0.3 The 8_{14} knot.	86
Figure E.0.1 The 4_1 (figure-eight) knot.	91
Figure E.0.2 The 5_2 knot.	92
Figure E.0.3 The 6_2 knot.	92

ACKNOWLEDGEMENTS

I would like to thank:

Ryan Budney for his guidance, insight and patience.

University of Victoria for providing a fellowship and additional funding for my work.

DEDICATION

To my family, my friends, and Aleister Crowley.

Chapter 1

Introduction

A knot is a simple mathematical creature — it is a closed curve contained in some ambient space (usually, but not always, \mathbb{R}^3). However, the study of knots is a vast and active area of research in topology. Many questions in knot theory are able to be explained to a non-mathematician: given two knots, how can we maneuver the strands of one knot to obtain a copy of the other? The answers to these questions (including the aforementioned) remain elusive and subtle. In fact, even proving that a unknotted circle is not the same as the trefoil knot (the basic 'shoelace' knot) is highly nontrivial, and requires some background in topology, although even a child would readily agree with such a statement. These objects are appealing to study partially because of their highly geometric structure, as well as the subtleties in their distinguishing properties.

In an effort to distinguish types of knots, mathematical invariants have been established. These invariants assign to each knot an object (typically a number, group, or polynomial), with the property that two equivalent knots (informally, two knots are equivalent if the strands of one knot can be manipulated to form a copy of the other knot) are always assigned the same object. Ideally, invariants should hold three properties:

- they should be easily computable — one should be able to quickly determine the value of the invariant on a given knot,
- they should distinguish knots — if two knots take on the same value under an invariant, it should be reasonably likely that the two knots are equivalent,
- they should be descriptive — the output of the invariant should describe some

properties of the knot itself.

Unfortunately, very few knot invariants satisfy all three of these properties simultaneously. In the early 1990s, the Russian mathematician Victor Vassiliev developed a series of knot invariants, now known as Vassiliev invariants. These invariants have generated a great deal of interest in the mathematical community, and seem to be particularly good at distinguishing various types of knots. In fact, it is conjectured ([CDM]), that these invariants together form a *complete* knot invariant — two knots are equivalent if and only if all of their Vassiliev invariants agree. These invariants, while quite useful, are typically described algebraically or combinatorially, and do not appear to describe any intrinsic properties that the knot itself may possess.

Recently, an article published by Ryan Budney *et al.* ([BCSS]) provided a link between one of the Vassiliev invariants (known as the 'second-order' invariant, or v_2), and the geometric properties of knots. In this article, the authors study long knots, embeddings of the real line into \mathbb{R}^3 , and determine that the second-order Vassiliev invariant corresponds exactly to the 'signed alternating quadriseccant count' of the knot. A quadriseccant of a knot is a line in \mathbb{R}^3 that intersects the knot in four places. The quadriseccant is said to be alternating if the intersections occur in a particular order along the knot, which will be elaborated upon later. Finally, each of these alternating quadriseccants may be granted a sign of ± 1 , determined by the orientation imposed upon the knot. In this way, the v_2 invariant corresponds to the sum of these signs associated to all such alternating quadriseccants.

In this paper, this relationship is extended to closed knots. A similar geometric connection will be established between the second-order Vassiliev invariant and closed knots (embeddings of the circle in \mathbb{R}^3 , or the 3-sphere S^3). In [BCSS], quadriseccants on closed knots were examined as an extension of the original result. It will become clear later that this is not a natural extension of the quadriseccant result on long knots to closed knots, and this extension is also reasonably complex. Rather than examining quadriseccants of the knot, the object of interest in this paper will be cocircularities of the closed knot. In particular, the occurrences of five distinct points on a closed knot that all lie on a common circle in the ambient space. After this link is established, we will proceed further and study the occurrences of six distinct points on a closed knot that lie on a common circle as well, and determine what invariants arise.

The structure of this thesis is as follows. Chapter 2 provides the essential preliminaries needed in differential topology, concentrating on some fundamental transversality theorems, as well as reviewing the concept of orientability of manifolds. The

next chapter narrows the focus to knots. A description of some general properties of knots, as well as a detailed definition of Vassiliev invariants is given. Chapter 4 condenses the alternating quadriseccant result found in [BCSS]; although, the presentation and method of proof will be significantly different from the one presented in the original article. Beyond this chapter contains the bulk of the new results. Chapter 5 defines the types of five- and six-point cocircularities we will be interested in studying, and establishes invariants related to these objects. An analysis of these invariants follows in Chapter 6, and the paper concludes with some remaining open questions and conjectures.

Through the course of the proofs in Chapters 5 and 6, we will rely on some computer computations to aid in locating the appropriate five- and six-point cocircularities on particular knots. A sketch of the implementation of this code is given in the appendices, along with a verification that the code behaves correctly. The program also outputs some images of these cocircularities on knots, and a few of these images are presented in the appendices as well.

Chapter 2

Fundamental Properties of Manifolds

Our study of quadrisecants and cocircularities of knots will be primarily contained within the realm of differential topology. Knots are in some sense the simplest non-trivial examples of manifolds; however, they still provide a very rich theory, and many of the classical questions surrounding knots remain unanswered. Our descent into knot theory will begin by first describing some properties of general manifolds. After establishing preliminary terminology, a review of the fundamental transversality theorems and orientability will be presented. All of the theorems presented here are contained within most textbooks on the subject of differential topology; in particular, our presentation will coincide with [GP]. As a consequence, we omit many of their proofs. A reader well-versed in such terminology may skip this chapter.

2.1 Manifolds with Boundary and Transversality

Intuitively, a manifold is a space which is locally modeled by Euclidean space, although globally the space may behave in an indeterminate manner. The motivation behind this definition is practical: most objects one encounters in the physical world can be considered as manifolds. Spaces such as the sphere, torus, and Klein bottle are common examples of manifolds. Other familiar spaces, such as closed disks, are 'almost' manifolds — they appear locally to model Euclidean space at every point, except along the boundary, where they model the upper half-space. As these spaces are manifolds 'almost everywhere', they have many similar properties to boundary-

less manifolds, and frequently the term 'manifold' includes the possible existence of a boundary.

Definition 1. An m -dimensional *manifold (with boundary)* is a space $X \subset \mathbb{R}^k$ such that each point $x \in X$ possesses an (open) neighborhood $U \subset X$ diffeomorphic to an open subset of the upper half-space

$$H^m = \{(x_1, \dots, x_m) \in \mathbb{R}^m : x_1 \geq 0\}.$$

The *boundary* of X is denoted by ∂X , and consists of points x whose image under a local parametrization lies on the boundary of H^m (if $\partial X = \emptyset$, then X is *boundaryless*). The boundary of a manifold is itself a boundaryless manifold of dimension $m - 1$. The *interior* of X is $\text{Int}(X) = X \setminus \partial X$, and is a boundaryless manifold of dimension m .

It is important to note that the definition of boundary presented here does not agree with the typical topological notion of boundaries. The topological boundary of a manifold depends upon the ambient space the manifold lies within, while our usage of the word boundary is independent of the ambient space (although this is perhaps not immediately clear from our definition above). The following proposition is trivial:

Proposition 2. *If X is a manifold, and Y is a boundaryless manifold, then $X \times Y$ is a manifold, with $\partial(X \times Y) = \partial X \times Y$.*

Demonstrating that a given space is a manifold by finding local parametrizations around each point in the manifold is often an arduous task. A more appealing strategy is to define the space as the image (or preimage) of a map between two spaces that are already known to be manifolds. If the map is sufficiently well-behaved, we may conclude that the image (or preimage) is indeed a submanifold of the codomain (or domain).

Definition 3. An *embedding* is a map $f : X \rightarrow Y$ between two manifolds that satisfies the following three properties:

1. f is injective.
2. df_x is injective for each $x \in X$.
3. f is proper — the preimage of every compact subset of Y is compact.

Theorem 4. *If $f : X \rightarrow Y$ is an embedding between manifolds, then $f(X)$ is a submanifold of Y , and is diffeomorphic to X .*

All (closed) knots can be realized as an embedding of the circle S^1 into either \mathbb{R}^3 or the 3-sphere S^3 .

Determining if the preimage of a submanifold of the codomain is a submanifold of the domain is a more delicate problem. For this, we turn to the notion of transversality. Transversality also has its roots firmly in the physical realm: two submanifolds are said to be transverse if their intersection is 'generic'...small perturbations of either submanifold does not significantly affect the properties of their intersection. In some sense, we cannot observe anything other than transversality between spaces.

Definition 5. If $f : X \rightarrow Y$ is a (smooth) map between manifolds, and Z is a submanifold of Y , then f is *transverse* to Z , written $f \pitchfork Z$, if

$$df_x(T_xX) + T_{f(x)}Z = T_{f(x)}Y$$

for all $x \in X$ such that $f(x) \in Z$. Similarly, two submanifolds $Z_1, Z_2 \subset Y$ are transverse if $T_zZ_1 + T_zZ_2 = T_zY$, for all $z \in Z_1 \cap Z_2$.

Implicit in this definition is that $f \pitchfork Z$ if the image of f is disjoint from Z . A simple example illustrates the intuitive idea behind this formal definition.

Example 6. Let S^2 be the unit sphere embedded in \mathbb{R}^3 , and P_b a plane in \mathbb{R}^3 with normal vector $v = (0, 0, 1)$, and translation vector $(0, 0, b) \in \mathbb{R}^3$. Then P_b consists of the set of points $x \in \mathbb{R}^3$ such that $v \cdot (x - (0, 0, b)) = \mathbf{0}$, while T_xP_b consists of the set of points $y \in \mathbb{R}^3$ such that $v \cdot y = \mathbf{0}$. On the other hand, if $x \in S^2 \subset \mathbb{R}^3$, then $x \cdot x = 1$, and T_xS^2 consists of points y that satisfy the equality $x \cdot y = \mathbf{0}$.

Suppose $x \in S^2 \cap P_b$. Then T_xS^2 and T_xP are both planes containing $\mathbf{0}$, and as such they span $T_x\mathbb{R}^3 = \mathbb{R}^3$ if and only if they are not coincident. This occurs precisely when the normal vectors $v = (0, 0, 1)$ and x of the two tangent planes are scalar multiples of each other. So T_xP is coincident with T_xS^2 if and only if $x = (0, 0, \pm 1)$. But $(0, 0, 1) \in P_b$ implies that $b = 1$, while $(0, 0, -1) \in P_b$ implies that $b = -1$. Transversality between S^2 and P_b occurs for all choices of b except ± 1 . Notice that if $b \in (-1, 1)$, then $S^2 \cap P_b$ appears as a circle, and small perturbations of b results in small perturbations of the circle of intersection. On the other hand, if $b \in \mathbb{R} \setminus [-1, 1]$, then $S^2 \cap P_b$ is empty. The cases where $b = \pm 1$ are degenerate — a small change in the value of b significantly alters the intersection space. See Figure 2.1.1 on page 7.

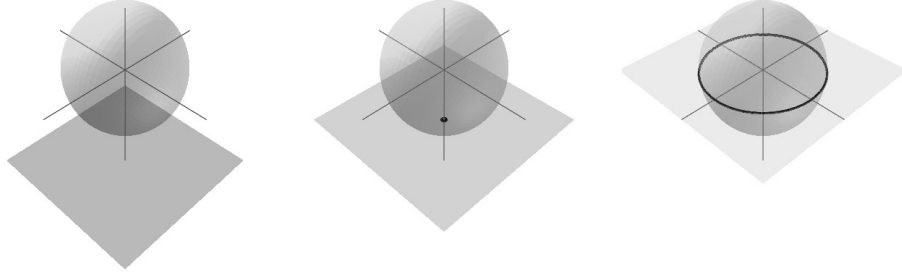


Figure 2.1.1: The sphere S^2 and P_b , for $b = -2, -1$ and 0 .

Given a map $f : X \rightarrow Y$ between manifolds, if $y \in Y$ is such that df_x is surjective for all $x \in X$ such that $f(x) = y$, then y is a *regular value* of f , while each x where df_x is surjective is a *regular point*. If every point of Y is a regular value, then f is called a *submersion*.

We now state two fundamental theorems regarding transversality that will be of vital importance to our work. The first is The Preimage Theorem, which specifies what conditions are necessary for preimage of a submanifold of the codomain to be a submanifold of the domain.

Theorem 7. (*The Preimage Theorem*) *Let $f : X \rightarrow Y$ be a (smooth) map between manifolds, where Y is boundaryless. If Z is a boundaryless submanifold of Y , and $\partial f : \partial X \rightarrow Y$ denotes the restriction of f to the boundary, then $f \pitchfork Z$ and $\partial f \pitchfork Z$ imply that $f^{-1}(Z)$ is a submanifold of X . Furthermore,*

$$\partial(f^{-1}(Z)) = (\partial X) \cap (f^{-1}(Z))$$

and the codimension of $f^{-1}(Z)$ in X is equal to the codimension of Z in Y .

The second theorem is The Transversality Theorem, which captures the notion that transversality is the only observable behavior between manifolds from a physical standpoint. Suppose that $f : X \rightarrow Y$ is a smooth map, and Z is a submanifold of Y . Due to Sard's Theorem [Sa], the regular values of f form a dense, open subset of Y — almost all values of Y are regular. We may always adjust f in an arbitrarily small manner so that the critical values (the points of Y that are not regular) 'miss' the submanifold Z of Y , resulting in a map transverse to Z .

Theorem 8. (*The Transversality Theorem*) *Let $F : X \times S \rightarrow Y$ be a smooth map between manifolds, where S and Y are boundaryless. If Z is a boundaryless submanifold of Y transverse to both F and ∂F , then for almost all $s \in S$, the maps $f_s = F|_{X \times \{s\}}$ and $\partial f_s = \partial F|_{X \times \{s\}}$ are also transverse to Z , and f_s is said to be a 'generic' map.*

Recall our previous example, with the sphere S^2 and a horizontal plane P_b embedded in \mathbb{R}^3 , with $P_b = \{(x, y, b) : x, y, b \in \mathbb{R}\}$. If we let $F : \mathbb{R}^2 \times \mathbb{R} \rightarrow \mathbb{R}^3$ be defined as the identity map, which is clearly a submersion, then $F \pitchfork S^2$, and by The Transversality Theorem, it follows that for almost all choices of $b \in \mathbb{R}$, we have that $f_b = F|_{\mathbb{R}^2 \times \{b\}}$ is transverse to S^2 . Specifically, if $b = \pm 1$, then transversality fails, as was concluded in the prior example. A generic plane parallel to the xy -plane is transverse to S^2 .

We introduce four more major theorems regarding manifolds before turning to the subject of orientations. The first pair are the ε -Neighborhood Theorem and the Tubular Neighborhood Theorem, which are of particular importance to our study of knots. The premises of the theorems will be satisfied by our definition of knots as closed curves sitting in the 3-sphere. They demonstrate that our knots can be thickened by some small amount without resulting in any self-intersections.

Theorem 9. (*The ε -Neighborhood Theorem*) *Let X be a compact boundaryless submanifold of \mathbb{R}^k , and let $N(X; \mathbb{R}^k)$ be the normal bundle of X . Then there exists a positive real number ε and a diffeomorphism h between*

$$N_\varepsilon(X; \mathbb{R}^k) = \{(x, v) : x \in X, v \in T_x \mathbb{R}^k, v \perp T_x X, |v| < \varepsilon\}$$

and the open subset

$$X_\varepsilon = \{y \in \mathbb{R}^k : \exists x \in X, \text{ such that } |x - y| < \varepsilon\}.$$

defined as

$$(x, v) \mapsto x + v.$$

Additionally, there is a submersion $\pi : X_\varepsilon \rightarrow X$ sending each point $y \in X_\varepsilon$ to the unique point in X that is closest to y in \mathbb{R}^k .

If X is not compact, then a diffeomorphism still exists, but our choice of ε must be allowed to vary over X . That is, there is a smooth function $\varepsilon : X \rightarrow (0, \infty)$, such that

$$N_\varepsilon(X; \mathbb{R}^k) = \{(x, v) : x \in X, v \in T_x \mathbb{R}^k, v \perp T_x X, |v| < \varepsilon(x)\}$$

is diffeomorphic to

$$X_\varepsilon = \{y \in \mathbb{R}^k : \exists x \in X, \text{ such that } |x - y| < \varepsilon(x)\}.$$

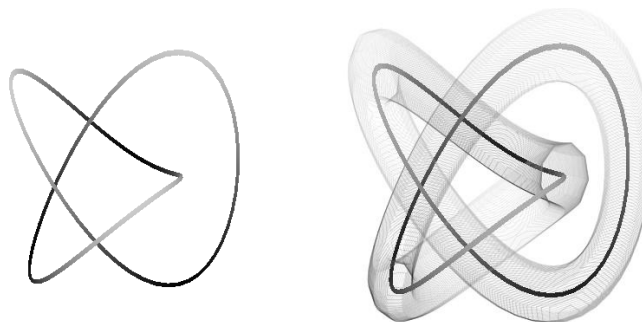


Figure 2.1.2: A closed curve in \mathbb{R}^3 , and an ε -neighborhood.

The maps π and h still exist and behave as before.

In the compact case above, the supremum over all possible ε is known as the *injective radius* of the normal bundle.

Theorem 10. (*The Tubular Neighborhood Theorem*) Let X be a boundaryless submanifold of Y , also a boundaryless manifold. There exists a diffeomorphism h between an open subset $N_\varepsilon(X; Y)$ of $(X, \mathbf{0})$ in the normal bundle $N(X; Y)$ of X in Y and an open neighborhood X_ε of X in Y . This diffeomorphism may be arranged so the zero section map $i_0 : X \rightarrow N_\varepsilon(X; Y)$ sending X to $(X, \mathbf{0})$ and the inclusion map $i : X \rightarrow X_\varepsilon$ satisfy $i_0 \circ h = i$.

Our final two theorems in this section regard transversality. The first is The Extension Theorem.

Theorem 11. (*The Extension Theorem*) Suppose Z is a closed submanifold of Y , both of which are boundaryless. If C is a closed subset of X , and $f : X \rightarrow Y$ is a smooth map, then we say that $f \pitchfork Z$ on C if

$$df_x T_x X + T_{f(x)} Z = T_{f(x)} Y$$

for each $x \in C$ such that $f(x) \in Z$. If $f \pitchfork Z$ on C , and $\partial f \pitchfork Z$ on $C \cap \partial X$, then there exists a smooth map $g : X \rightarrow Y$ homotopic to f such that $g \pitchfork Z$, $\partial g \pitchfork Z$, and $g = f$ on a neighborhood of C .

Of particular interest will be the case where $X = S \times \mathbb{I}$, for some boundaryless manifold S . Then the Extension Theorem directly proves the following corollary.

Corollary 12. *Suppose S, Z and Y are boundaryless manifolds, with $Z \subset Y$, and $F : S \times \mathbb{I} \rightarrow Y$ is a smooth homotopy. If $F_0 = F|_{S \times \{0\}}$ and $F_1 = F|_{S \times \{1\}}$ are both transverse to Z , then there exists a smooth homotopy $G : S \times \mathbb{I} \rightarrow Y$ such that $G_0 = F_0$, $G_1 = F_1$, and $G \pitchfork Z$.*

The second theorem is related to the first, and is The Isotopy Extension Theorem. The version presented here is from [Hi].

Definition 13. Let X and Y be manifolds. An *isotopy* of X in Y is a smooth map

$$F : X \times \mathbb{I} \rightarrow Y$$

such that each $F_t : X \rightarrow Y$ is an embedding. If $X = Y$, and F_0 is the identity map, then F is an *ambient isotopy* of Y .

Theorem 14. *(The Isotopy Extension Theorem) Suppose X is a compact submanifold of Y , and $F : X \times \mathbb{I} \rightarrow Y$ is an isotopy of X . If $F(X \times \mathbb{I}) \subset \text{Int}(Y)$, then F extends to an ambient isotopy of Y with compact support (that is, the isotopy is fixed for all $y \in Y$ outside of a compact subset of Y).*

2.2 Orientation and Intersection Theory

Many of the theorems above link together in a remarkable manner when studying intersection theory. Unless otherwise specified, we will assume the manifolds X, Y, Z and the smooth map f are 'appropriate for intersection theory':

- X, Y, Z are boundaryless manifolds, with $Z \subset Y$.
- X is compact.
- $f : X \rightarrow Y$ is transverse to Z .
- $\dim X + \dim Z = \dim Y$.

Under these conditions, The Preimage Theorem asserts that $f^{-1}(Z)$ is a finite collection of points. If $f_0, f_1 : X \rightarrow Y$ are homotopic maps that are each transverse to Z , then the corollary to The Extension Theorem indicates that there exists a homotopy $F : X \times \mathbb{I} \rightarrow Y$ joining f_0 with f_1 that is also transverse to Z . As a result, $F^{-1}(Z)$ is a 1-manifold: a collection of (non-intersecting) curves in $X \times \mathbb{I}$ (see Figure 2.2.1 on page

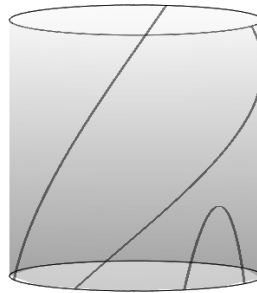


Figure 2.2.1: A potential example for $F^{-1}(Z)$ in $S^1 \times \mathbb{I}$. Here $X = S^1$. The curves intersects X_0 (the bottom of the figure) in four places, while it it intersects X_1 in two points. The parity of these intersection numbers agree.

11). Initially, it may seem that there is no strong link between $f_0^{-1}(Z)$ and $f_1^{-1}(Z)$; however, by examining $F^{-1}(Z)$, a connection may be established. The boundaryless curves in $F^{-1}(Z)$ must be contained entirely within $X \times (0, 1)$, while the curves with boundary must join two distinct points in $\partial F^{-1}(Z) = f_0^{-1}(Z) \cup f_1^{-1}(Z)$. These are the only two cases permissible, due to the nature of compact 1-manifolds. It is well-known that all connected, compact 1-manifolds are diffeomorphic to either the circle S^1 or the closed interval $[0, 1]$, and as such are either boundaryless or possess exactly two boundary points. At the very least, the parity of $f_1^{-1}(Z)$ and $f_0^{-1}(Z)$ must agree.

Definition 15. The *unoriented intersection number* $I_2(f, Z)$ is equal to the value of $|f^{-1}(Z)|$ taken modulo 2.

Proposition 16. *If $f_0, f_1 : X \rightarrow Y$ are homotopic maps, each transverse to Z , then $I_2(f_0, Z) = I_2(f_1, Z)$.*

Unfortunately, the actual numerical values of $|f_0^{-1}(Z)|$ and $|f_1^{-1}(Z)|$ need not agree, as some curves in $F^{-1}(Z)$ could have boundaries entirely contained within $f_0^{-1}(Z)$, or alternatively $f_1^{-1}(Z)$. In order to establish a more precise homotopy invariant from this data, we need to be able to distinguish these types of curves from the curves that join a point in $f_0^{-1}(Z)$ with a point in $f_1^{-1}(Z)$. Applying orientations to our manifolds is the tool required to make such distinctions.

If V is a real vector space, then we state that two bases β_1, β_2 are *equivalently ordered* if the unique linear isomorphism $A : V \rightarrow V$ sending β_1 to β_2 has a positive determinant. This establishes an equivalence relation on the set of bases of V that consists of two classes. An orientation on V is an arbitrary decision to assign to the

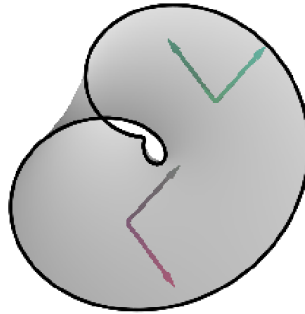


Figure 2.2.2: The Möbius strip, and a potential choice of bases for two points on the surface.

elements of one of these classes a positive sign, and the other a negative sign. In the case where V is zero-dimensional, we simply grant the point a sign of ± 1 .

The tangent space $T_x X$ of a manifold with boundary is a real vector space, so we may assign it an orientation. An *orientation* on such a manifold X is then a smooth choice of orientations for each tangent space $T_x X$. If X is connected and able to be oriented, then it admits two possible orientations, which are denoted as X and $-X$.

Example 17. All 1-manifolds are orientable. If $f : X \rightarrow Y$ is an embedding of a 1-manifold, then we may grant the basis $\{f'(x)\}$ of $T_x X$ a positive orientation (while $\{-f'(x)\}$ obtains a negative orientation).

The cylinder $S^1 \times \mathbb{I}$ is an orientable manifold. Embed $S^1 \times \mathbb{I}$ into \mathbb{R}^3 , by letting $S^1 = \{(\cos \theta, \sin \theta) \in \mathbb{R}^2 : \theta \in \mathbb{R}\}$. If $x = (\cos \theta, \sin \theta, t) \in S^1 \times \mathbb{I}$, then

$$T_x(S^1 \times \mathbb{I}) = T_{(\cos \theta, \sin \theta)} S^1 \times T_t \mathbb{I} = \{y \in \mathbb{R}^3 : (\cos \theta, \sin \theta, 0) \cdot y = 0\},$$

and we may choose $\{(-\sin \theta, \cos \theta, 0); (0, 0, 1)\}$ as a positive basis for $T_x(S^1 \times \mathbb{I})$. This choice is clearly smooth.

The classical example of a nonorientable manifold is the Möbius strip. The formal proof that it is not orientable will be omitted here, although it follows as a corollary to a later theorem (Theorem 61). However, some intuition suggests that a smooth basis cannot be found. On Figure 2.2.2 on page 12, two potential bases are depicted on the surface. As we 'push' one of them around the surface, we may ultimately arrive back at our original location, but with the orientation on the basis reversed.

We now define several different induced orientations that may be applied to specific manifolds. Although we omit the proofs, all of these induced orientations are well-

defined.

- *Product Orientation* - If X and Y are oriented manifolds, one of which is boundaryless, then we may apply an induced orientation on the product manifold $X \times Y$. If $(x, y) \in X \times Y$, then

$$T_{(x,y)}(X \times Y) = T_x X \times T_y Y.$$

If α is a basis for $T_x X$ and β is a basis for $T_y Y$, then $(\alpha \times \{\mathbf{0}\}, \{\mathbf{0}\} \times \beta)$ is a basis for $T_{(x,y)}(X \times Y)$. We assign

$$\text{sign}(\alpha \times \{\mathbf{0}\}, \{\mathbf{0}\} \times \beta) = \text{sign}(\alpha) \cdot \text{sign}(\beta).$$

- *Boundary Orientation* - If X is an oriented manifold with boundary, it induces a boundary orientation on the manifold ∂X . At every point $x \in \partial X$, the tangent space $T_x \partial X$ is a linear subspace of codimension one in $T_x X$. As a result, there are exactly two unit vectors $v, -v$ in $T_x X$ that are orthogonal to $T_x \partial X$. Let X' be a neighborhood of X , and $\phi : X' \rightarrow U$ a diffeomorphism sending X' to an open subset U of $\mathbb{R}^{\dim X}$. Furthermore, let $\phi(x) = \mathbf{0}$. Then $d\phi_x$ is a linear map with domain $T_x(X') = T_x(X)$ and codomain $\mathbb{R}^{\dim X}$, and it carries either v or $-v$ into $H^{\dim X}$. Call this vector the *inward pointing normal* of $T_x \partial X$, and the other the *outward pointing normal*. If v is the outward-pointing normal, and β is a basis for $T_x \partial X$, then we declare that the following equality must hold:

$$\text{sign}(\beta) = \text{sign}(v, \beta)$$

where $\text{sign}(v, \beta)$ is determined by our orientation on X (since $\{v, \beta\}$ is a basis for $T_x X$).

- *Preimage Orientation* - If $f : X \rightarrow Y$ is a smooth map between oriented manifolds with $f \pitchfork Z$ and $\partial f \pitchfork Z$ (where Z, Y are oriented and boundaryless, and $Z \subset Y$), then we may define a preimage orientation on the submanifold $S = f^{-1}(Z)$. If $f(x) = z \in Z$, for some $x \in X$, then $T_x S$ is the preimage of $T_z Z$ under the derivative map $df_x : T_x X \rightarrow T_z Y$ (this is demonstrated in [GP], among others).

Let $N_x(S; X)$ be the orthogonal complement to T_xS in T_xX . Then

$$N_x(S; X) \oplus T_xS = T_xX,$$

so imposing an orientation on $N_x(S; X)$ induces an orientation on T_xS via a direct sum orientation of real vector spaces. Transversality of f with Z demonstrates that

$$df_x T_xX \oplus T_zZ = T_zY.$$

It can be shown that T_xS is the entire preimage of T_zZ , so

$$df_x N_x(S; X) \oplus T_zZ = T_zY,$$

As a result, the orientations on Z and Y grant an orientation on $df_x N_x(S; X)$. The derivative df_x maps $N_x(S; X)$ diffeomorphically onto its image, and determines an orientation of $N_x(S; X)$ by examining the isomorphism df_x when restricted to $N_x(S; X)$. An orientation may then be imposed on T_xS through the following two equalities:

$$df_x N_x(S; X) \oplus T_zZ = T_zY$$

$$N_x(S; X) \oplus T_xS = T_xX.$$

As indicated earlier, an important application of these induced orientations is in examining homotopy spaces $\mathbb{I} \times X$. For every $t \in \mathbb{I}$, let $X_t = \{t\} \times X$, a diffeomorphic copy of X , with an orientation corresponding to an orientation of X .

The disjoint union $X_0 \cup X_1$ is the boundary of $\mathbb{I} \times X$, but what is the orientation of this space imposed by the boundary orientation? For X_1 , the tangent space T_xX_1 is a linear subspace of codimension one in $T_{(t,x)}(\mathbb{I} \times X)$. The outward pointing normal to T_xX_1 in $T_{(t,x)}(\mathbb{I} \times X)$ is the vector $(1, \mathbf{0})$, as determined by the product orientation $T_{(t,x)}(\mathbb{I} \times X) = T_t\mathbb{I} \times T_xX$. Thus, through the definition of the boundary orientation,

$$\text{sign}(\beta) = \text{sign}((1, \mathbf{0}), \{0\} \times \beta)$$

where β is a basis for X . By the product orientation,

$$\text{sign}((1, \mathbf{0}), \{0\} \times \beta) = \text{sign}(1) \cdot \text{sign}(\beta) = \text{sign}(\beta).$$

In other words, the boundary orientation on X_1 agrees with the orientation imposed on X_1 by considering it as a diffeomorphic copy of X . On the other hand, the outward pointing normal along X_0 is $(-1, \mathbf{0})$. By the definition of boundary orientation,

$$\text{sign}(\beta) = \text{sign}((-1, \mathbf{0}), \{0\} \times \beta).$$

But by the product orientation,

$$\text{sign}((-1, \mathbf{0}), \{0\} \times \beta) = \text{sign}(-1) \cdot \text{sign}(\beta) = -\text{sign}(\beta).$$

So the boundary orientation on X_0 does not agree with the orientation imposed on X_0 as a diffeomorphic copy of X . Therefore,

$$\partial(\mathbb{I} \times X) = X_1 \cup (-X_0)$$

which we abbreviate as $X_1 - X_0$.

In particular, if X is point with an orientation of ± 1 , then $\partial(\mathbb{I} \times X) = X_1 - X_0 = (\pm 1) - (\pm 1) = 0$. Since every compact, oriented one-manifold is diffeomorphic to either a (boundaryless) closed curve, or a closed interval,

Proposition 18. *The sum of the orientation numbers of the boundary points of any compact, oriented one-dimensional manifold is zero.*

If X, Y, Z and f_0 are appropriate for intersection theory, and f_1 is homotopic to f_0 , with $f_1 \pitchfork Z$, then there exists a homotopy $F : \mathbb{I} \times X \rightarrow Y$ also transverse to Z that joins f_0 with f_1 . Additionally, if X, Y, Z are oriented, $F^{-1}(Z)$ is a compact 1-manifold, with an orientation induced by the preimage orientation. Therefore, the sum of the orientation numbers of the boundary points of $F^{-1}(Z)$ is exactly zero. By The Preimage Theorem,

$$0 = \partial F^{-1}(Z) = f_1^{-1}(Z) - f_0^{-1}(Z)$$

$$f_1^{-1}(Z) = f_0^{-1}(Z)$$

Where $f_t^{-1}(Z)$ is the sum of the orientation signs applied to each point in the preimage of Z under f_t through the preimage orientation. Applying orientations to our manifolds establishes a more powerful homotopy invariant to X, Y, Z and f .

Definition 19. Given that X, Y, Z and f are appropriate for intersection theory, the

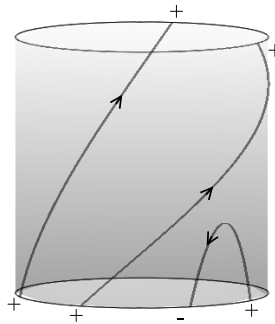


Figure 2.2.3: The homotopy space from Figure 2.2.1 on page 11, with orientations. The sum of the signs on the top of the figure ($f_1^{-1}(Z)$) agrees with the bottom ($f_0^{-1}(Z)$), for some submanifold Z of the ambient space. $I(f_0, Z) = I(f_1, Z) = +2$.

(oriented) intersection number $I(f, Z)$ is the sum of the signs applied to each point in $f^{-1}(Z)$ through the preimage orientation.

Proposition 20. *If $f_0, f_1 : X \rightarrow Y$ are both transverse to Z , with $f_0 \simeq f_1$, then $I(f_0, Z) = I(f_1, Z)$.*

In fact, by The Extension Theorem, we may define the intersection number $I(f, Z)$ for maps f that are not transverse to Z , simply defining $I(f, Z)$ to be equal to $I(g, Z)$, where g is some map homotopic to f and transverse to Z (which is well-defined and guaranteed to exist by The Extension Theorem).

Finally, if Y is connected, and is of the same dimension as X , then for any smooth map $f : X \rightarrow Y$, the intersection number $I(f, \{y\})$ at any point $y \in Y$ is defined and independent of our choice of y .

Definition 21. If $f : X \rightarrow Y$ is a smooth map between two oriented manifolds of the same dimension, then the *degree* of f is denoted by $\deg(f)$, and is equal to $I(f, \{y\})$, for any point $y \in Y$.

Note that in this case, determining the preimage orientations on each point $f^{-1}(\{y\})$ is straightforward, since $T_x\{y\} = \emptyset$, for every $x \in f^{-1}(y)$. Thus, if $x \in f^{-1}(y)$, then the sign associated to x is positive if the isomorphism df_x preserves orientation, and negative otherwise.

Chapter 3

Knots and Vassiliev Invariants

A (closed) knot is typically defined as an embedding f of the circle in the 3-sphere S^3 or \mathbb{R}^3 , or alternatively as the image of such an embedding. Here, we will let $f : S^1 \rightarrow S^3$ be such an embedding, and K will refer to the image of f . A problem at the heart of knot theory is distinguishing when two knots K and K' are equivalent. This is captured formally by applying an ambient isotopy of the knot.

Definition 22. Two embeddings $f_0, f_1 : S^1 \rightarrow S^3$ with images K_0 and K_1 are *equivalent knots* if and only if there exists a smooth map $F : S^3 \times \mathbb{I} \rightarrow S^3$ such that F_i is a diffeomorphism for all $i \in \mathbb{I}$, F_0 is the identity map, and $F_1(K_0) = K_1$. The map F is an *ambient isotopy taking f_0 to f_1* .

This definition naturally induces an equivalence relation on the set \mathcal{K} of all knot embeddings. Determining whether two knots are equivalent is a difficult problem, and

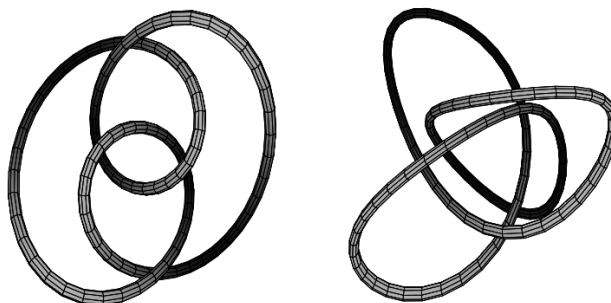


Figure 3.0.1: While not obvious, the two (thickened) knots depicted here are equivalent — we may manipulate the strands of one to obtain the other (without causing self-intersections).

much work has been done on providing algorithms to determine equivalence ([Ha]). Some of this progress is in the form of knot invariants. A *knot invariant* is formally a functor from the category of knots and ambient isotopies to any category. More informally, it may be interpreted as a function with domain \mathcal{K} and the property that any two equivalent knots share the same image. Of course, the converse need not be true (if it is, then the knot invariant is *complete*; although, there are currently no easily computable complete knot invariants). We will focus exclusively on a specific class of numerical invariants — the Vassiliev invariants. These invariants were first developed by Russian mathematician Victor Vassiliev in the early 1990s.

The invariants are commonly defined on knot diagrams — projections of knots onto a generic plane. These projections provide a beautiful transition between topological and combinatorial knot theory; however, our work will not be concerned with knot diagrams or their combinatorial nature. In order to preserve the focus of this paper, we will define Vassiliev invariants without introducing knot diagrams. As a consequence, our exposition here will be more technical and lengthy; however, this will save some energy later on, where we must apply the theorems described below.

The approach taken involves applying a form of crossing changes to the knot in the ambient space. Essentially, this operation takes two arcs of a knot in S^3 and passes them through each other, without significantly altering the rest of the knot. This action typically results in a knot that is not diffeomorphic to the original. Let D^3 be the compact 3-ball, and α_-, α_+ be two arcs (submanifolds) in D^3 , with

$$\alpha_- = \left\{ \left[\begin{array}{c} -\frac{\sqrt{3}}{3} \\ 0 \\ 0 \end{array} \right] + \left[\begin{array}{c} 0 \\ \frac{\sqrt{3}}{3} \\ \frac{\sqrt{3}}{3} \end{array} \right] t \right\} \quad \alpha_+ = \left\{ \left[\begin{array}{c} \frac{\sqrt{3}}{3} \\ 0 \\ 0 \end{array} \right] + \left[\begin{array}{c} 0 \\ -\frac{\sqrt{3}}{3} \\ \frac{\sqrt{3}}{3} \end{array} \right] t \right\} \quad (3.0.1)$$

where $t \in [-1, 1]$. Orient the arcs from $t = -1$ towards $t = +1$.

Definition 23. A *crossing* of a knot K is an orientation-preserving embedding $c : D^3 \rightarrow S^3$ with $c^{-1}(K) = \alpha_- \cup \alpha_+$. Two crossings c_0 and c_1 are equivalent if there exists a smooth map $C : S^3 \times \mathbb{I} \rightarrow S^3$ such that each $C_t \circ c_0$ is a crossing with $C_0 = \text{id}$ and $C_1 \circ c_0 = c_1$. This isotopy can be arranged so C_t is the identity map outside of an arbitrarily small neighborhood of

$$\bigcup_{0 \leq s \leq t} \text{im} c_s.$$

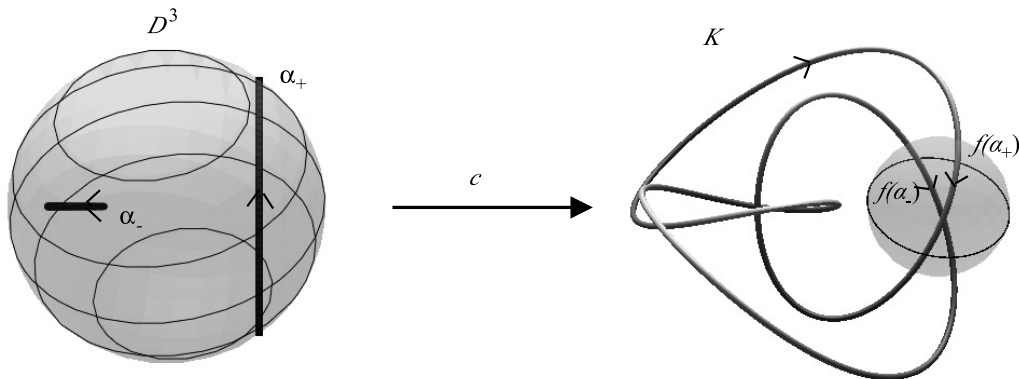


Figure 3.0.2: A particular crossing.

The set of all crossings of a knot will be denoted by \mathcal{C} , while the set of crossings with equivalent crossings identified will be denoted as $\tilde{\mathcal{C}}$. Let $\beta : \mathbb{I} \rightarrow \mathbb{R}$ be the standard bump function

$$\beta(t) = e^{-\frac{1}{1-t^2}}.$$

Definition 24. Given a knot K and a crossing c , let χ_- and χ_+ be two arcs in D^3 , with

$$\chi_- = \alpha_-(t) + \begin{bmatrix} 2 \cos(\frac{\pi t}{2})\beta(t) \\ 0 \\ 0 \end{bmatrix} \quad \chi_+ = \alpha_+(t) + \begin{bmatrix} -2 \cos(\frac{\pi t}{2})\beta(t) \\ 0 \\ 0 \end{bmatrix}$$

where t ranges from -1 to 1 . Then a *crossing change* (of K at c) transforms the knot K into a new knot K^c , where

$$K^c = (K \setminus c(\alpha_- \cup \alpha_+)) \cup c(\chi_- \cup \chi_+).$$

Figure 3.0.3 on page 20 depicts the crossing change operation. When applied, the smoothness of the knot is preserved (since χ_{\pm} , c , and K are smooth), and the orientation on the knot is preserved. The boundary points of χ_{\pm} are the same as α_{\pm} , so K^c remains a closed knot. Also, $\chi_- \cup \chi_+$ is not ambient isotopic to $\alpha_- \cup \alpha_+$ in D^3 , so K^c is not necessarily equivalent to K . It is immediately apparent that if c_0 and c_1 are equivalent crossings, then K^{c_0} and K^{c_1} are equivalent knots (through the same ambient isotopy C joining c_0 with c_1). Crossing changes are thus independent of the choice of representative of an element of $\tilde{\mathcal{C}}$. Two crossing changes on a knot



Figure 3.0.3: The crossing change operation. When applied to a knot, the arcs $c(\alpha_{\pm}) \subset K$ are replaced with $c(\chi_{\pm})$ to obtain a new knot K^c .

are *distinct* if the crossings in question are representatives of distinct elements of $\tilde{\mathcal{C}}$. Shrinking the compact 3-balls if necessary, we may assume the images of each of the distinct crossings are disjoint. If multiple distinct crossing changes are to be performed on a knot, then the crossing changes may be performed either simultaneously or in succession, without regard to order, since applying a crossing change does not affect the knot outside of the image of the crossing (which is pairwise disjoint with the other crossings in question).

We may now define what it means for a knot invariant to be Vassiliev.

Definition 25. Let $v : \mathcal{K} \rightarrow \mathbb{Z}$ be a numerical knot invariant. Then v is *Vassiliev of order $n - 1$* if, for every knot K and every choice of n disjoint crossings c_1, \dots, c_n of K , the alternating sum

$$\sum_{\sigma \subset \{1, \dots, n\}} (-1)^{|\sigma|} v(K^{\sigma})$$

vanishes, where K^{σ} is the knot obtained from K by applying crossings changes at each c_i , with $i \in \sigma$.

This definition may initially seem opaque and arbitrary; however, it has the benefit of possessing numerous properties that will be of value. It is worth noting that while this definition applies to oriented knots, there are currently no known Vassiliev invariants that are able to distinguish a knot from its inverse (the inverse being the knot obtained by reversing the orientation of the curve). A conjecture by Vassiliev states that:

Conjecture 26. [V] *The set of Vassiliev invariants is a complete knot invariant. Two knots are equivalent if and only if all of their Vassiliev invariants are identical.*

Some properties of Vassiliev invariants are obtained easily. If v is of order $n - 1$, then it is also of order n . For if K is a knot, and c_1, \dots, c_{n+1} is a choice of $n + 1$ distinct crossings, then

$$\begin{aligned} \sum_{\sigma \subset \{1, \dots, n+1\}} (-1)^{|\sigma|} v(K^\sigma) &= \sum_{\sigma \subset \{1, \dots, n\}} (-1)^{|\sigma|} v(K^\sigma) + (-1)^{|\sigma|+1} v(K^{\sigma \cup c_{n+1}}) \\ &= 0 + \left(\sum_{\sigma \subset \{1, \dots, n\}} (-1)^{|\sigma|+1} v((K^{c_{n+1}})^\sigma) \right) \\ &= 0 \end{aligned}$$

It is clear from the definition that if v, v' are Vassiliev invariants of orders n and n' , then $av + bv'$ is a Vassiliev knot invariant of order $\max\{n, n'\}$ whenever a, b are nonzero integers. The low order Vassiliev invariants are relatively well-understood, and an article by Dror Bar-Natan [B-N] proves that there are only a few Vassiliev invariants of small order.

Theorem 27. *Up to linear combinations with Vassiliev invariants of lower order, there exist unique Vassiliev invariants of orders zero, two and three. There are no Vassiliev invariants of order one (excluding the order zero invariant).*

These invariants have been standardized. The order zero invariant $v_0 : \mathcal{K} \rightarrow \mathbb{Z}$ is the constant map that assigns each knot the value one. The second-order Vassiliev invariant $v_2 : \mathcal{K} \rightarrow \mathbb{Z}$ assigns to the unknot a value of 0, and the 3_1 trefoil a value of 1. The third Vassiliev invariant $v_3 : \mathcal{K} \rightarrow \mathbb{Z}$ obtains a value of 0 on the unknot, and -1 on the 3_1 trefoil knot. A table of these values for some knots is given in Appendix A.

Chapter 4

Quadriseccants

As mentioned, these Vassiliev invariants are quite useful in distinguishing knots; however, they appear by applying local crossing changes to a knot, and seem to lack a sufficient global geometric interpretation of the knots. A recent publication by R. Budney *et al.* [BCSS] established such an interpretation for the second Vassiliev invariant v_2 on long knots. While we have not mentioned the extension of Vassiliev invariants to long knots, the idea is nearly identical, and all of the same concepts still apply. We begin by formalizing our definition of a long knot.

Definition 28. A *long knot* is an embedding $f : \mathbb{R} \rightarrow \mathbb{R}^3$, or alternatively the image K of such an embedding, with the additional property that f behave linearly outside of a compact set. By applying an ambient isotopy and reparametrizing the curve, we may apply additional restrictions on f . Here, we will always assume the following:

- $f(x) = (x, 0, 0)$, for all $x \in \mathbb{R} \setminus (0, 1)$,
- $f'(0) = f'(1) = (1, 0, 0)$,
- $f((0, 1)) \subset (0, 1) \times \mathbb{R}^2$.

With these conditions in mind, the 'interesting' portion of the knot is captured when we restrict the domain to \mathbb{I} . Thus, we may instead consider f as an embedding $f : \mathbb{I} \rightarrow \mathbb{I} \times \mathbb{R}^2$, with endpoints $f(0) = (0, 0, 0)$ and $f(1) = (1, 0, 0)$. We retain the condition that $f'(0) = f'(1) = (1, 0, 0)$ as well. To reduce notational complications, let $\mathbf{0} = (0, 0, 0) \in \mathbb{R}^3$, and $\mathbf{1} = (1, 0, 0) \in \mathbb{R}^3$. The image of f is a submanifold of $\mathbb{I} \times \mathbb{R}^2$, with boundary $\{\mathbf{0}, \mathbf{1}\}$.

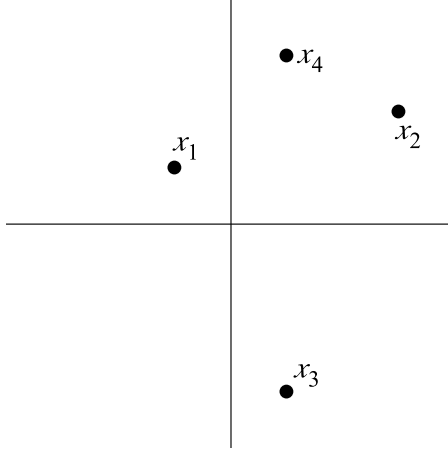


Figure 4.0.1: The point (x_1, x_2, x_3, x_4) is an element of $C_4\mathbb{R}^2$. Any arrangement of the subscripts also results in an element of $C_4\mathbb{R}^2$.

Our interpretation of the v_2 invariant counts the number of alternating quadrise-cants on the knot — four distinct, collinear points on K that satisfy a special ‘alter-nating’ condition to be clarified momentarily. In order to discuss distinct points on the knot effectively, we turn to configuration spaces.

Definition 29. Given a manifold M , the n -point configuration space of M is the space of n distinct points in M^n , and is denoted by C_nM . That is,

$$C_nM := \{(x_1, \dots, x_n) \in M^n : x_i \neq x_j, \forall i \neq j\}$$

C_nM is an open subset of M^n ; so C_nM is an mn -dimensional submanifold of M^n , where $m = \dim M$. When M is connected and 1-dimensional, then C_nM is disconnected when $n > 2$. Each component in this case corresponds to a particular ‘ordering’ of the n points on M .

Proposition 30. *The manifold $C_n\mathbb{I}$ is diffeomorphic to the disjoint union of $n!$ half-open n -simplices*

$$\Lambda_n = \{(t_1, \dots, t_n) \in \mathbb{R}^n : 0 \leq t_1 < \dots < t_n \leq 1\}.$$

Proof. Consider the symmetric group Σ_n on the set $\{1, \dots, n\}$, and associate to each permutation $\sigma \in \Sigma_n$ a point $\mathbf{s}_\sigma = (\frac{\sigma 1}{n}, \dots, \frac{\sigma n}{n}) \in C_n\mathbb{I}$. For each $\mathbf{t} = (t_1, \dots, t_n) \in C_n\mathbb{I}$, there exists a unique $\sigma_{\mathbf{t}} \in \Sigma_n$ such that $0 \leq t_{\sigma 1} < \dots < t_{\sigma n} \leq 1$. We first demonstrate the existence of a path joining \mathbf{t} with $\mathbf{s}_{\sigma_{\mathbf{t}}}$. Let P_0 be the linear path that maps \mathbf{t} to

$\frac{1}{n}\mathbf{t}$. Then let P_i be the path that linearly sends the $\sigma(n-i)$ th coordinate to $\frac{n-i+1}{n}$, and keeps all other coordinates fixed. The composition $P_n \circ \cdots \circ P_0$ is our desired path. At the end of P_0 , all the coordinates of \mathbf{t} are contained within the interval $[0, \frac{1}{n}]$. The map P_1 moves the largest coordinate, $\frac{1}{n}t_{\sigma n}$, to 1. Then P_2 moves the next largest coordinate, $\frac{1}{n}t_{\sigma(n-1)}$ to $\frac{n-1}{n}$. Repeating this process, we find the path is entirely contained within $C_n\mathbb{I}$, and its terminal point is $\mathbf{s}_{\sigma\mathbf{t}}$.

If σ and τ are two distinct permutations of Σ_n , then \mathbf{s}_σ and \mathbf{s}_τ are in separate components of $C_n\mathbb{I}$. Since σ and τ are distinct, it follows that there exists $i, j \in \{1, \dots, n\}$ such that $\sigma i < \sigma j$, but $\tau i > \tau j$. Suppose P is a path joining \mathbf{s}_σ with \mathbf{s}_τ , and let P' be the restriction of this path to just observing the behavior of the i th and j th coordinates along the path. That is, there exists a continuous map $P' : \mathbb{I} \rightarrow C_2\mathbb{I}$, where $P'(0) = (\frac{\sigma i}{n}, \frac{\sigma j}{n})$ and $P'(1) = (\frac{\tau i}{n}, \frac{\tau j}{n})$. But $C_2\mathbb{I}$ is clearly diffeomorphic to \mathbb{I}^2 minus the main diagonal, which consists of two components:

$$A = \{(x, y) \in \mathbb{I}^2 : x < y\} \quad B = \{(x, y) \in \mathbb{I}^2 : x > y\}$$

where $A \cup B = C_2\mathbb{I}$ and $A \cap B = \emptyset$. Since $\sigma i < \sigma j$ and $\tau i > \tau j$, $P'(0) \in A$, but $P'(1) \in B$, which contradicts the continuity of our path P' , and thus the continuity of P as well. This contradiction ensures \mathbf{s}_σ and \mathbf{s}_τ are not elements of a common component. Thus, $C_n\mathbb{I}$ contains precisely $n!$ components — one corresponding to each permutation in Σ_n . Let $\Lambda_n^\sigma = \{(t_1, \dots, t_n) \in \mathbb{R}^n : 0 \leq t_{\sigma 1} < \cdots < t_{\sigma n} \leq 1\}$. Then Λ_n^σ is diffeomorphic to Λ_n through the map

$$\lambda_\sigma : \Lambda_n \rightarrow \Lambda_n^\sigma \quad (t_1, \dots, t_n) \mapsto (t_{\sigma 1}, \dots, t_{\sigma n}).$$

This completes the proposition. □

Corollary 31. $C_n\mathbb{R}$ is diffeomorphic to the disjoint union of $n!$ copies of

$$\Lambda'_n = \{(t_1, \dots, t_n) \in \mathbb{R}^n : t_1 < \cdots < t_n\}.$$

Also, C_nS^1 is diffeomorphic to the disjoint union of $(n-1)!$ copies of

$$\Lambda_n^\circ = \{(t_1, \dots, t_n) \in (S^1)^n : t_1, \dots, t_n \text{ are arranged in counter-clockwise order}\}.$$

Proof. For $C_n\mathbb{R}$, we use a very similar argument as in Proposition 30. Here, use the arctangent map to first send points in $C_n\mathbb{R}$ to $C_n((0, 2))$. Then replace the

path P_0 above, with the linear map that scales by $\frac{1}{2n}$. Now the same points \mathbf{s}_σ and paths P_1, \dots, P_n may be utilized as before.

For each $t \in C_n S^1$, let $\rho_t : S^1 \setminus \{t\} \rightarrow \mathbb{R}$ be the standard smooth stereographic projection map. Then $C_n S^1$ is diffeomorphic to $S^1 \times C_{n-1} \mathbb{R}$ through the map

$$\phi : C_n S^1 \rightarrow S^1 \times C_{n-1} \mathbb{R} \quad (t_1, \dots, t_n) \mapsto (t_1, \rho_{t_1} t_2, \dots, \rho_{t_1} t_n),$$

which is in turn diffeomorphic to $(n-1)!$ copies of $S^1 \times \Lambda'_{n-1}$. By applying the inverse stereographic projection map on the Λ'_{n-1} component, based at the point given by the S^1 component, we obtain $(n-1)!$ diffeomorphic copies of Λ_n° . \square

By an abuse of notation, we will relabel the spaces $C_n \mathbb{I}$, $C_n \mathbb{R}$, and $C_n S^1$ to be Λ_n , Λ'_n and Λ_n° respectively — we are considering only the 'identity' components of these three spaces from this point forward. If M is a connected manifold of dimension greater than one, then $C_n M$ consists only of one component, so we are not altering our definition of configuration spaces when $\dim M > 1$. When $f : \mathbb{I} \rightarrow \mathbb{I} \times \mathbb{R}^2$ is a long knot with image K , then $C_n K$ is the image of $C_n \mathbb{I}$ under the *evaluation map of f* ,

$$C_n f : C_n \mathbb{I} \rightarrow C_n(\mathbb{I} \times \mathbb{R}^2) \quad (t_1, \dots, t_n) = (f(t_1), \dots, f(t_n)).$$

Let us reiterate our modified definition of these configuration spaces and evaluation maps.

Definition 32. Let

$$C_n \mathbb{I} = \{(t_1, \dots, t_n) \in \mathbb{I}^n : 0 \leq t_1 < \dots < t_n \leq 1\}$$

$$C_n \mathbb{R} = \{(t_1, \dots, t_n) \in \mathbb{R}^n : t_1 < \dots < t_n\}$$

$$C_n S^1 = \{(t_1, \dots, t_n) \in S^n : t_1, \dots, t_n \text{ are ordered counter-clockwise along } S^1\}$$

If $f : \mathbb{I} \rightarrow \mathbb{I} \times \mathbb{R}^2$ is a long knot with image K , then

$$C_n f : C_n \mathbb{I} \rightarrow C_n(\mathbb{I} \times \mathbb{R}^2) \quad (t_1, \dots, t_n) \mapsto (f(t_1), \dots, f(t_n))$$

$$C_n K = \text{im } C_n f.$$

If $f : S^1 \rightarrow S^3$ is a closed knot, then we have similar definitions for $C_n f$ and $C_n K$.

The interpretation of v_2 as a quadriseccant count is first discussed in [BCSS], but

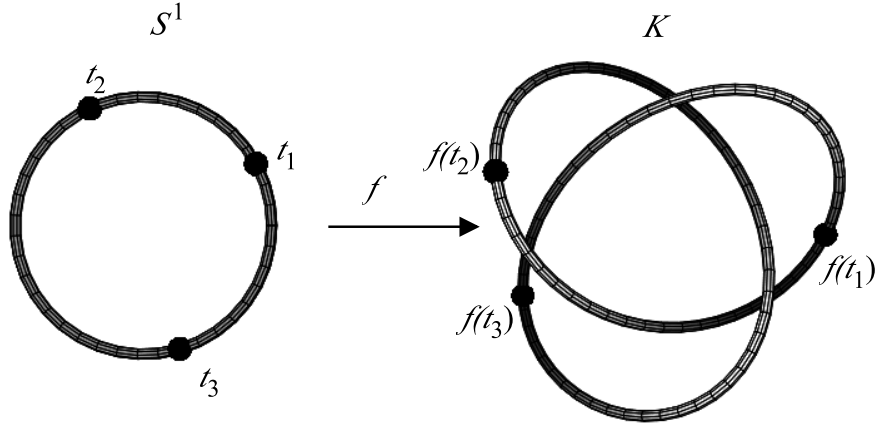


Figure 4.0.2: The point (t_1, t_2, t_3) is an element of C_3S^1 , as is (t_2, t_3, t_1) ; however, (t_3, t_2, t_1) is not, because the coordinates are not in counter-clockwise order. The point $C_3(f)(t_1, t_2, t_3) = (f(t_1), f(t_2), f(t_3))$ is an element of C_3K .

the direction we take here to prove this result is significantly different. The inspiration for this method derives from a lecture by Michael Polyak [P], although it remains unpublished.

Given a long knot K , the image of $f : \mathbb{I} \rightarrow \mathbb{I} \times \mathbb{R}^2$, consider the map $\xi : C_4(K) \rightarrow (S^2)^3$, defined by

$$\xi(x_1, x_2, x_3, x_4) = (\|x_1 - x_3\|, \|x_4 - x_1\|, \|x_2 - x_4\|). \quad (4.0.1)$$

Each point \mathbf{x} in C_4K is the image of a unique point $\mathbf{t} = (t_1, \dots, t_4)$ in $C_4\mathbb{I}$, where $t_1 < \dots < t_4$. The map ξ sends $\mathbf{x} = (x_1, \dots, x_4)$ in C_4K to a collection of three unit vectors. The first can be considered as a unit vector originating at x_3 on the knot and pointing towards x_1 , the second originates at x_1 and points towards x_4 , while the final coordinate is a unit vector from x_4 towards x_2 .

Definition 33. An *alternating quadriseccant* of the knot K is a point $\mathbf{x} = (x_1, \dots, x_4) \in C_4K$ such that $\xi(\mathbf{x})$ is contained within the diagonal Δ of $(S^2)^3$. That is, $\xi(\mathbf{x}) = (y, y, y) \in (S^2)^3$ for some $y \in S^2$.

From this definition, if $\xi(\mathbf{x}) \in \Delta \subset (S^1)^3$, then the points x_1, \dots, x_4 are all collinear. We may alternatively describe an alternating quadriseccant as the line intersecting the knot at x_1, \dots, x_4 . The term *alternating* comes from the observation that x_i and x_{i+1}

are never adjacent on the quadrisequant line, for any $i \in \{1, 2, 3\}$. Later, we will elaborate upon why this particular alternating sequence is utilized, and why other arrangements of the subscripts in the map ξ fail to be of any importance in our interpretation of v_2 .

The space C_4K is a four-dimensional submanifold of the 12-dimensional ambient manifold $(\mathbb{I} \times \mathbb{R}^2)^4$. As we will prove momentarily, its image under ξ is a four-dimensional submanifold of the 6-dimensional ambient manifold $(S^2)^3$. By intersecting the image of ξ with the main diagonal Δ of $(S^2)^3$, we are intersecting a four-dimensional space with a two-dimensional space in $(S^2)^3$. Assuming that this intersection is sufficiently generic, transversality is expected and the intersection is a zero-dimensional manifold — a finite collection of points. By orienting our spaces in the natural manner, we can associate to each point a sign of ± 1 . This signed intersection number is precisely the knot invariant that we wish to derive.

4.1 Quadrisequant Transversality

Let Δ be the 2-dimensional main diagonal of $(S^2)^3$, and ξ be the map mentioned in Equation (4.0.1), with the corresponding long knot K being implied through context. The coordinates of a point \mathbf{x} in C_nK will be referred to by x_1, \dots, x_n , and its preimage under the long knot embedding f will be referred to by $\mathbf{t} = (t_1, \dots, t_n) \in C_n\mathbb{I}$. That is, $C_n f(\mathbf{t}) = \mathbf{x}$. We now state the main theorem of this section.

Theorem 34. *If $f : \mathbb{I} \rightarrow \mathbb{I} \times \mathbb{R}^2$ is a generic knot, then we have that $\xi \circ C_4 f \pitchfork \Delta$.*

The following definition and subsequent lemma will make several reappearances in later chapters, and is vital to our progress.

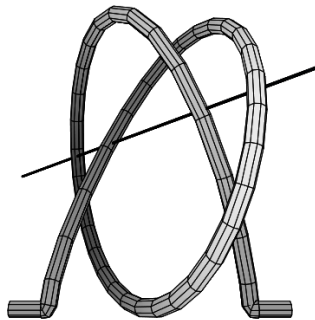


Figure 4.0.3: An example of an alternating quadrisequant for the long trefoil knot.

Definition 35. Suppose M is a connected curve, and $\mathbf{x} = (x_1, \dots, x_n)$ is an element of $C_n M$. Then the points x_i, x_j are said to be *adjacent* if there exists a path in M joining x_i with x_j that does not contain any other x_k , where i, j and k are all distinct elements of $\{1, \dots, n\}$.

Through our redefinition of the space $C_n \mathbb{I}$, it follows that two coordinates x_i and x_j of a point $\mathbf{x} \in C_n K$ are adjacent if and only if i and j are consecutive. Two coordinates x_i and x_j are adjacent in a point \mathbf{x} of $C_n S^1$ if and only if i and j are consecutive modulo n . Intuitively, if a point \mathbf{x} lies in $C_n K$, then we may begin at $\mathbf{0}$ and travel along the knot towards $\mathbf{1}$, and we will encounter the coordinates of \mathbf{x} in order, that is, x_1 comes 'before' x_2 , and so on, when travelling along the knot.

Lemma 36. *For every long knot K , there exists an $\varepsilon > 0$ such that, if \mathbf{x} is an alternating quadrisecant of K , then $|x_i - x_j| \geq \varepsilon$, for all distinct $i, j \in \{1, 2, 3, 4\}$.*

Proof. Temporarily extend our knot K to a knot K' contained within all of \mathbb{R}^3 (that is, $K = K'$ in $\mathbb{I} \times \mathbb{R}^2$, and K' behaves linearly outside of this region). Then we may apply the ε -Neighborhood Theorem to K' to obtain a smooth function $\varepsilon' : K' \rightarrow (0, \infty)$. Let $\varepsilon = \min\{\varepsilon(x) : x \in K\}$. Since K is compact, such a minimum exists. A submersion $\pi : K'_{\varepsilon'} \rightarrow K'$ and diffeomorphism $h : N_{\varepsilon'}(K'; \mathbb{R}^3) \rightarrow K'_{\varepsilon'}$ is also determined by the ε -Neighborhood Theorem. We now claim that our choice of ε may be shrunk sufficiently so that the image of $N_{\varepsilon}(K; \mathbb{I} \times \mathbb{R}^2) = N_{\varepsilon}(K; \mathbb{R}^3)$ under h is entirely contained within $\mathbb{I} \times \mathbb{R}^2$. In other words, we wish to apply the ε -Neighborhood Theorem on K , even though the ambient space is not \mathbb{R}^3 .

Let $\pi_2 : K_{\varepsilon/2} \rightarrow K$ be the restriction of π to $K_{\varepsilon/2}$. Let $J_{\mathbf{0}}$ be the open segment of $K \subset \mathbb{R}^3$ beginning at $\mathbf{0}$, and of arc length $\varepsilon/2$, but not containing its boundary points. Let $B_{\mathbf{0}} = \pi_2^{-1}(J_{\mathbf{0}})$. If $y \in B_{\mathbf{0}}$ and $y \notin \mathbb{I} \times \mathbb{R}^2$, then the line joining y with $\pi_2(y) = \pi(y)$ must cross the plane $\{0\} \times \mathbb{R}^2$, so by the definition of π , there must exist a point $y_0 \in B_{\mathbf{0}}$ such that $y_0 \in \{0\} \times \mathbb{R}^2$, and $\pi(y_0) = \pi(y) \in J_{\mathbf{0}}$. By the definition of π_2 , the point y_0 is of distance less than $\varepsilon/2$ from $\pi_2(y_0) = \pi(y_0) \in J_{\mathbf{0}}$. The point $\pi(y_0)$ is also of distance less than $\varepsilon/2$ from $\mathbf{0}$. By the Triangle Inequality, $|y_0 - \mathbf{0}| < \varepsilon$.

Since $f'(\mathbf{0}) = (1, 0, 0)$, it follows that the section S of $N_{\varepsilon}(K; \mathbb{R}^3)$:

$$S = \{(\mathbf{0}, v) : v \perp f'(\mathbf{0}) = (1, 0, 0), |v| < \varepsilon\}$$

under h contains y_0 . By the definition of h , the $h(S) \subset \{0\} \times \mathbb{R}^2$, and $y_0 \in h(S)$. But then $\pi(y_0) = \mathbf{0}$, which contradicts the fact that $\pi(y_0) \in J_{\mathbf{0}}$, which does not contain

0. Thus, there cannot exist a point $y \in B_0$ with $y \notin \mathbb{I} \times \mathbb{R}^2$. A similar argument proves that B_1 is contained within $\mathbb{I} \times \mathbb{R}^2$. Now consider the closed, compact arc of $K \setminus \{J_0, J_1, \mathbf{0}, \mathbf{1}\}$. Since it is properly contained within $\mathbb{I} \times \mathbb{R}^2$, there exists a minimum positive distance ε^* between this arc and $\partial(\mathbb{I} \times \mathbb{R}^2)$. Thus, by shrinking our choice of ε by a factor of 2 (to ensure B_0 and B_1 are contained in $\mathbb{I} \times \mathbb{R}^2$), and shrinking if further so that it is smaller than ε^* , it follows that $h(N_\varepsilon(K; \mathbb{R}^3))$ is entirely contained within $\mathbb{I} \times \mathbb{R}^2$. Thus, $h(N_\varepsilon(K; \mathbb{I} \times \mathbb{R}^2)) \subset \mathbb{I} \times \mathbb{R}^2$. Let

$$N_\varepsilon(K; \mathbb{I} \times \mathbb{R}^2) = \{(x, v) \in N(K; \mathbb{I} \times \mathbb{R}^2) : |v| < \varepsilon\}$$

and $K_\varepsilon = h(N_\varepsilon(\mathbb{I}; \mathbb{I} \times \mathbb{R}^2))$. The space K_ε is an ε -neighborhood of K in $\mathbb{I} \times \mathbb{R}^2$. Restrict our map π above to the domain K_ε , so $\pi : K_\varepsilon \rightarrow K$ remains a submersion that sends a point to its closest point on K .

Suppose \mathbf{x} is an alternating quadriseccant of K , so $\xi(\mathbf{x}) \in \Delta$. Furthermore, let L be the line containing the coordinates of \mathbf{x} in $\mathbb{I} \times \mathbb{R}^2$, and ℓ be the segment of L beginning at x_1 and terminating at x_2 . By definition, $\|x_1 - x_3\| = \|x_4 - x_1\| = \|x_2 - x_4\|$, so if we consider \mathbf{x} as a point in C_4L , then the pairs (x_1, x_3) , (x_1, x_4) and (x_4, x_2) all contain adjacent coordinates. Thus, x_4 must lie on ℓ . Assume that $|x_1 - x_2| < \varepsilon$. Then ℓ is entirely contained within K_ε , and as such π is defined on ℓ . If we restrict π to ℓ , then π is the identity on the boundary of ℓ , and $\pi(x_4) = x_4$, since $x_4 \in \ell \cap K$. By the Intermediate Value Theorem, there must exist a point p on the segment of ℓ between x_1 and x_4 such that $\pi(p) = x_2$. However, π maps points on ℓ to the closest point on K . The point p is mapped to x_2 , but clearly the point x_4 is closer to p than x_2 , since it lies between p and x_2 on ℓ . This contradiction ensures that $|x_1 - x_2| \geq \varepsilon$. A similar argument can be applied to guarantee that $|x_i - x_j| \geq \varepsilon$ whenever i and j are consecutive.

Now suppose $|x_1 - x_3| < \varepsilon$. Then let L again be the alternating quadriseccant line for \mathbf{x} , and let ℓ be the line segment joining x_1 with x_3 . As before, π is a continuous submersion, with $\pi(x_1) = x_1$ and $\pi(x_3) = x_3$. There exists a point p on ℓ such that $\pi(p) = x_2$, again from the Intermediate Value Theorem. However, x_2 lies on $L \setminus \ell$, since x_3 and x_1 are adjacent on L . This is a contradiction of our definition of π , as p must be closer to either x_1 or x_3 than x_2 . Thus, $|x_1 - x_3| \geq \varepsilon$. This argument applies for all i, j that are not consecutive, completing the proof. \square

The lemma above gives a bit of insight on our motivation behind examining this particular type of quadriseccant. If $\xi(\mathbf{x}) \in \Delta$, and L is the line containing the coordi-

nates of \mathbf{x} , then x_i and x_j cannot be consecutive on both L and K . It is this property that allows Lemma 36 to hold, and a quick combinatorial check demonstrates that an alternating quadriseccant is the only type of quadriseccant with this property.

In Lemma 36, the Tubular Neighborhood Theorem was applied to obtain an $\varepsilon > 0$ and the spaces

$$N_\varepsilon(K; \mathbb{I} \times \mathbb{R}^2) = \{(x, v) \in N(K; \mathbb{I} \times \mathbb{R}^2) : |v| < \varepsilon\}$$

and K_ε , as well as a diffeomorphism h and a submersion π :

$$N_\varepsilon(K; \mathbb{I} \times \mathbb{R}^2) \xrightarrow{h} K_\varepsilon \xrightarrow{\pi} K,$$

where $h(x, v) = x + v$. By embedding \mathbb{I} in $\mathbb{I} \times \mathbb{R}^2$ in the standard manner (mapping t to $(t, 0, 0)$), we may extend f to a diffeomorphism f^* between $N_\varepsilon(\mathbb{I}; \mathbb{I} \times \mathbb{R}^2)$ and $N_\varepsilon(K; \mathbb{I} \times \mathbb{R}^2)$. While many such diffeomorphisms exist, we will provide a technique for constructing one in the paragraphs that follow.

Since f is an embedding, $f'(t)$ is always a nonzero vector contained within the one-dimensional tangent space $T_{f(t)}(K) \subset \mathbb{R}^3$. Let $\phi_\pm : \mathbb{I} \rightarrow \mathbb{I} \times S^2$ be the embeddings that send t to $(t, \|\pm f'(t)\|)$, with $X_\pm = \text{im}\phi_\pm$. Then X_+ and X_- are two disjoint 1-manifolds in $\mathbb{I} \times S^2$. As such, the image of the projection map from $\mathbb{I} \times S^2$ to the second component S^2 , when restricted to $X_+ \cup X_-$, is not surjective. In other words, there exists a vector $w \in S^2$ such that $w \neq \|\pm f'(t)\|$, for all $t \in \mathbb{I}$. Let w_t be the projection of w onto the plane $N_{f(t)}(K)$ in \mathbb{R}^3 . Since w is not contained in $T_{f(t)}(K)$, for any t , it follows that w_t is always nonzero. Finally, let $A_t \in SO_3\mathbb{R}$ be a rotation matrix that sends the vectors $(1, 0, 0)$ and $(0, 1, 0)$ to the vectors $\|f'(t)\|$ and $\|w_t\|$, respectively. The matrix A_t is well-defined, and varies smoothly with t ; it carries the normal space $N_t(\mathbb{I})$ diffeomorphically onto $N_{f(t)}(K)$. Define f^* by sending (t, v) to $(f(t), A_t v)$.

The diagram indicated in Figure 4.1.1 on page 31 commutes, where the vertical arrows and left horizontal arrows are diffeomorphisms, and the right horizontal arrows are submersions.

Theorem 34 requires that we only consider generic knots. So for a family of perturbations of any knot, almost all such perturbations result in a knot that satisfies the transversality indicated in the theorem. Our perturbations will be characterized by applying bump functions to a given knot. We may choose almost any bump

$$\begin{array}{ccccc}
N_\varepsilon(\mathbb{I}; \mathbb{I} \times \mathbb{R}^2) & \longrightarrow & \mathbb{I}_\varepsilon & \longrightarrow & \mathbb{I} \\
f^* \downarrow & & \downarrow & & f \downarrow \\
N_\varepsilon(K; \mathbb{I} \times \mathbb{R}^2) & \xrightarrow{h} & K_\varepsilon & \xrightarrow{\pi} & K
\end{array}$$

Figure 4.1.1: A commutative diagram extending the knot f to f^* .

function we wish, but let us standardize our choice somewhat. Let $\beta : \mathbb{R} \rightarrow [0, 1]$ be a smooth bump function that is identically zero on $\mathbb{R} \setminus (-1, 1)$, and nonzero on $(-1, 1)$. It reaches its height of 1 only at the point 0 on the domain, and is increasing on the interval $(-1, 0)$, and decreasing on $(0, 1)$. We say here that our bump function has both height and radius 1. For instance,

$$\beta(t) = \begin{cases} e^{\frac{-1}{1-t^2}} & t \in (-1, 1) \\ 0 & \text{otherwise} \end{cases}$$

is a potential choice for such a bump function.

Given a long knot $f : \mathbb{I} \rightarrow \mathbb{I} \times \mathbb{R}^2$, shrink our ε sufficiently to satisfy both Lemma 36 and the commutative diagram in Figure 4.1.1 on page 31. The domain of f is compact, so there exists an upper bound on the 'speed' $|f'(t)|$ of the knot, which we will denote as F . This means that if two points $f(t_1)$ and $f(t_2)$ are of distance ε from each other in the ambient space $\mathbb{I} \times \mathbb{R}^2$ of the knot, then $|t_1 - t_2| \geq \varepsilon/F$.

The diffeomorphism h is a restriction of a linear map, so $dh_{(x,v)}$ can be represented by a square matrix with determinant H , whose values are independent of our choice of $(x, v) \in N_\varepsilon(K; \mathbb{I} \times \mathbb{R}^2)$.

The derivative of f^* is

$$df_{((t,0,0),v)}^* : T_{((t,0,0),v)}N_\varepsilon(\mathbb{I}; \mathbb{I} \times \mathbb{R}^2) \rightarrow T_{f^*((t,0,0),v)}N_\varepsilon(K; \mathbb{I} \times \mathbb{R}^2)$$

and can therefore be represented as a square matrix as well. Since $|v| < \varepsilon$, and \mathbb{I} is compact, $|\det(df_{((t,0,0),v)}^*)|$ is bounded by some positive value F^* .

Set $n \in \mathbb{N}$ to be any value such that

$$\frac{2}{n} < \frac{\varepsilon}{2HF^*(1 + \varepsilon^2)}.$$

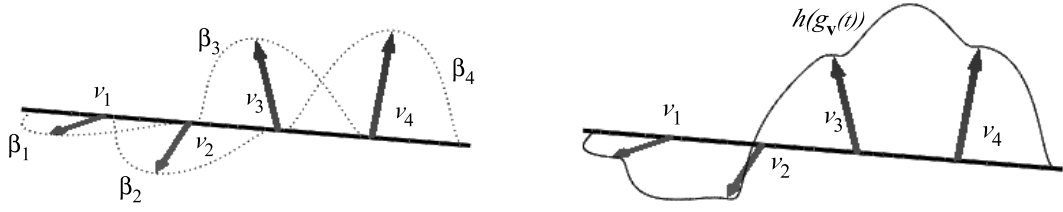


Figure 4.1.2: A possible choice of $\mathbf{v} = (v_1, v_2, v_3, v_4)$, when $n = 5$. Each bump function β_i is pushed in the direction of v_i off of the unit interval $\mathbb{I} \times \{0\}^2$ in an orthogonal direction. The curve on the right shows the final perturbed curve as it sits in \mathbb{I}_ε .

This seemingly arbitrary choice will become apparent in the following paragraphs. Define a collection of bump functions

$$\beta_i : \mathbb{R} \rightarrow [0, \frac{1}{n^2\bar{\beta}}] \quad t \mapsto \frac{1}{n^2\bar{\beta}}\beta(nt - i),$$

where $\bar{\beta} = \sup_{t \in \mathbb{I}} |\beta'(t)|$, and $i \in \{1, \dots, n-1\}$. This is a bump function with height $1/n^2\bar{\beta}$, radius $1/n$, and center i/n . The family of perturbations is defined by:

$$g : \mathbb{I} \times (\varepsilon D)^{n-1} \rightarrow N_\varepsilon(\mathbb{I}; \mathbb{I} \times \mathbb{R}^2)$$

$$g(t, \mathbf{v}) = g_k(t, v_1, \dots, v_{n-1}) = ((t, 0, 0), \sum_{i=1}^{n-1} \beta_i(t)v_i)$$

where D is the set of vectors v on the yz -plane of \mathbb{R}^3 , such that $|v| < 1$. Essentially, we are applying a series of tiny bump functions β_i to \mathbb{I} , and each one is 'pushed' in a direction v_i that is orthogonal to the x -axis.

Below are a few critical observations regarding this family of perturbations:

- $g(0, \mathbf{v}) = (\mathbf{0}, \mathbf{0})$, and $g(1, \mathbf{v}) = (\mathbf{1}, \mathbf{0})$ for all $\mathbf{v} \in (\varepsilon D)^{n-1}$.
- $h \circ f^* \circ g(t, \mathbf{0}) = f(t)$
- For a fixed $\mathbf{v} \in (\varepsilon D)^{n-1}$, the map $h \circ f^* \circ g_{\mathbf{v}}$ is an embedding of \mathbb{I} in K_ε , and is a long knot.
- For any $t \in \mathbb{I}$, there exists at least one i such that $\beta_i(t) \neq 0$.
- For any $t \in \mathbb{I}$, there exist at most two distinct i, j such that $\beta_i(t), \beta_j(t) \neq 0$.

For any $\mathbf{v} \in (\varepsilon D)^{n-1}$,

$$d(g_{\mathbf{v}})_t = \begin{bmatrix} 1 \\ 0 \\ 0 \\ d(\beta_1)_t \cdot v_1 + \cdots + d(\beta_{n-1}) \cdot v_{n-1} \end{bmatrix}$$

and

$$\begin{aligned} |d(g_{\mathbf{v}})_t| &= \left| 1^2 + \left(\sum_{i=1}^{n-1} d(\beta_i)_t \cdot v_i \right)^2 \right| \\ &\leq 1 + \left(\sum_{i=1}^{n-1} |v_i| |d(\beta_i)_t| \right)^2 \\ &< 1 + \left(\sum_{i=1}^{n-1} \left(\varepsilon \left| \frac{nd(\beta_{nt-i})}{n^2\bar{\beta}} \right| \right) \right)^2 \\ &< 1 + (\varepsilon)^2 \left(\sum_{i=1}^{n-1} \left| \frac{\sup_{t \in \mathbb{I}} \beta'(t)}{n\bar{\beta}} \right| \right)^2 \\ &< 1 + \varepsilon^2 \end{aligned}$$

Therefore, the speed of a long knot $h \circ f^* \circ g_{\mathbf{v}}$ in our family of perturbations is bounded by $HF^*(1 + \varepsilon^2)$.

Given $h \circ f^* \circ g_{\mathbf{v}}$, this long knot may have alternating quadriseccants as well. We may apply Lemma 36 to ensure that if \mathbf{x} is an alternating quadriseccant, then $|x_i - x_j| \geq \varepsilon_{\mathbf{v}}$, where $\varepsilon_{\mathbf{v}}$ is the injective radius of the tubular neighborhood of the perturbed long knot. Since $\varepsilon_{\mathbf{v}}$ depends on \mathbf{v} , it is potentially much smaller than the original $\varepsilon = \varepsilon_{\mathbf{0}}$. Thus, alternating quadriseccants have the potential to have coordinates that are much closer in distance than ε . We would like to prevent this situation from occurring. There must exist some $\delta \in (0, \varepsilon)$ such that, for each \mathbf{v} if $|v_i| < \delta$ for all $i \in \{1, \dots, n-1\}$, then $\varepsilon_{\mathbf{v}} > \varepsilon/2$. Thus, we may shrink our choice of ε even further so that ε is smaller than this δ value. As a result, every long knot in the collection $h \circ f^* \circ g_{\mathbf{v}}$ possesses a tubular neighborhood of radius greater than $\varepsilon/2$. It follows that we have a family of long knots

$$G_{\mathbf{v}} = h \circ f^* \circ g_{\mathbf{v}}$$

such that, if \mathbf{x} is an alternating quadriseccant in the image of $C_4G_{\mathbf{v}}$, then $|x_i - x_j| \geq \varepsilon/2$, for all $\mathbf{v} \in (\varepsilon D)^{n-1}$.

Theorem 37. *For all \mathbf{v} , if \mathbf{x} is an alternating quadriseccant in the image of $C_4G_{\mathbf{v}}$, with preimage $\mathbf{t} = (t_1, t_2, t_3, t_4)$, then $\beta_i(t_j) \neq 0$ implies that $\beta_i(t_k) = 0$, for all distinct $j, k \in \{1, 2, 3, 4\}$, and $i \in \{1, \dots, n-1\}$.*

Proof. We have just shown that, for all \mathbf{v} , if \mathbf{x} is an alternating quadriseccant in the image of $C_4G_{\mathbf{v}}$, then $|x_i - x_j| \geq \varepsilon/2$. In other words, the distance between any two coordinates in an alternating quadriseccant of the image of $C_4G_{\mathbf{v}}$ is at least $\varepsilon/2$. Now let us compute the 'speed' of $G_{\mathbf{v}}$.

$$|d(G_{\mathbf{v}})_t| = |d(h \circ f^* \circ g_{\mathbf{v}})_t|$$

Our bounds for H and F^* for dh and df^* allow us to apply a bound to $dG_{\mathbf{v}}$:

$$|d(G_{\mathbf{v}})_t| \leq HF^* |d(g_{\mathbf{v}})_t| < HF^*(1 + \varepsilon^2).$$

The speed of the long knot $G_{\mathbf{v}}$ cannot exceed $HF^*(1 + \varepsilon^2)$. Since $|x_i - x_j|$ is of distance at least $\varepsilon/2$, it follows that the amount of time $|t_i - t_j|$ to travel along the knot from x_i to x_j must be at least

$$\frac{\varepsilon}{2} \cdot \frac{1}{HF^*(1 + \varepsilon^2)}.$$

But recall that our choice of n was such that

$$\frac{\varepsilon}{2HF^*(1 + \varepsilon^2)} > \frac{2}{n}$$

which implies that

$$|t_i - t_j| > \frac{\varepsilon}{2} \cdot \frac{1}{HF^*(1 + \varepsilon^2)} > \frac{2}{n}.$$

The bump functions β_i were chosen to have radius $2/n$, so the theorem follows immediately. \square

This theorem is the key to proving the main result in this section. By an abuse of notation, let C_4g and C_4G be defined as

$$C_4g : C_4\mathbb{I} \times (\varepsilon D)^{n-1} \rightarrow C_4N_\varepsilon(\mathbb{I}; \mathbb{I} \times \mathbb{R}^2)$$

$$C_4g(\mathbf{t}, \mathbf{v}) = C_4(g_{\mathbf{v}})(\mathbf{t}) = (g_{\mathbf{v}}t_1, g_{\mathbf{v}}t_2, g_{\mathbf{v}}t_3, g_{\mathbf{v}}t_4)$$

$$C_4G = C_4h \circ C_4f^* \circ C_4g$$

Note that C_4h and C_4f^* are diffeomorphisms, so the maps dC_4h and dC_4f^* are isomorphisms between 12-dimensional tangent spaces. The domain of $dC_4g(\mathbf{t}, \mathbf{v})$ is precisely

$$\mathbb{R}^4 \times \prod_{i=1}^{n-1} T_{v_i}D = \mathbb{R}^4 \times (\{0\} \times \mathbb{R}^2)^{n-1}$$

while the codomain is

$$\prod_{i=1}^4 (\mathbb{R} \times T_{w_i}D) = (\mathbb{R} \times \{0\} \times \mathbb{R}^2)^4$$

If $dC_4g(\mathbf{t}, \mathbf{v})$ is of rank 12, then $dC_4G(\mathbf{t}, \mathbf{v})$ is also of rank 12.

Theorem 38. *For any $\mathbf{v} \in (\varepsilon D)^{n-1}$, if \mathbf{t} is the preimage of an alternating quadrise-cant in the image of $C_4G_{\mathbf{v}}$, then (\mathbf{t}, \mathbf{v}) is a regular point of C_4G .*

Proof. Suppose \mathbf{t} is the preimage of an alternating quadrise-cant in the image of $C_4G_{\mathbf{v}}$. Consider the transformation

$$dC_4g(\mathbf{t}, \mathbf{v}) : \mathbb{R}^4 \times \prod_{i=1}^{n-1} T_{v_i}D \rightarrow (\mathbb{R} \times \{0\} \times \mathbb{R}^2)^4$$

$$dC_4g(\mathbf{t}, \mathbf{v}) = \begin{bmatrix} \frac{\partial g_{\mathbf{v}}}{\partial t_1} & & 0 & \frac{\partial g_{t_1}}{\partial v_1} & \cdots & \frac{\partial g_{t_1}}{\partial v_{n-1}} \\ & \ddots & & \vdots & \ddots & \vdots \\ 0 & & \frac{\partial g_{\mathbf{v}}}{\partial t_4} & \frac{\partial g_{t_4}}{\partial v_1} & \cdots & \frac{\partial g_{t_4}}{\partial v_{n-1}} \end{bmatrix}$$

where

$$\frac{\partial g_{\mathbf{v}}}{\partial t_i} = \begin{bmatrix} 1 \\ \sum_{j=1}^{n-1} \beta'_j(t_i)v_j \end{bmatrix} \quad \frac{\partial g_{t_i}}{\partial v_j} = \begin{bmatrix} 0 & 0 & 0 \\ 0 & 0 & 0 \\ 0 & \beta_j(t_i) & 0 \\ 0 & 0 & \beta_j(t_i) \end{bmatrix}$$

By relabeling our bump functions β_i and their corresponding vectors v_i , suppose without loss to generality that $\beta_i(t_i) \neq 0$. By Theorem 37, it follows that $\beta_j(t_i) = 0$,

for any i, j distinct in $\{1, 2, 3, 4\}$. Then

$$dC_4g(\mathbf{t}, \mathbf{v}) = \begin{bmatrix} \frac{\partial g_{\mathbf{v}}}{\partial t_1} & 0 & \frac{\partial g_{t_1}}{\partial v_1} & 0 & \frac{\partial g_{t_1}}{\partial v_5} & \cdots & \frac{\partial g_{t_1}}{\partial v_{n-1}} \\ & \ddots & & \ddots & \vdots & \ddots & \vdots \\ 0 & \frac{\partial g_{\mathbf{v}}}{\partial t_4} & 0 & \frac{\partial g_{t_4}}{\partial v_4} & \frac{\partial g_{t_4}}{\partial v_5} & \cdots & \frac{\partial g_{t_4}}{\partial v_{n-1}} \end{bmatrix}.$$

But the matrix

$$\begin{bmatrix} \frac{\partial g_{\mathbf{v}}}{\partial t_1} & \frac{\partial g_{t_1}}{\partial v_1} \end{bmatrix} = \begin{bmatrix} 1 & 0 & 0 & 0 \\ 0 & 0 & 0 & 0 \\ \beta'_1(t_1)v_1 & 0 & \beta_1(t_1) & 0 \\ 0 & 0 & 0 & \beta_1(t_1) \end{bmatrix}$$

has rank 3. Therefore, $dC_4g(\mathbf{t}, \mathbf{v})$ has rank 12. Since the codomain is of dimension 12, it follows that (\mathbf{t}, \mathbf{v}) is a regular point of C_4g , and is thus a regular point of C_4G as well. \square

Theorem 39. *For a generic knot $f : \mathbb{I} \rightarrow \mathbb{I} \times \mathbb{R}^2$, the composition map $\xi \circ C_4f$ is transverse to Δ .*

Proof. Given f , let $G : \mathbb{I} \times (\varepsilon D)^{n-1} \rightarrow K_\varepsilon \subset \mathbb{I} \times \mathbb{R}^2$ be the associated family of perturbations just constructed. Extend our map $\xi : C_4K \rightarrow (S^2)^3$,

$$\Xi : C_4K_\varepsilon \rightarrow (S^2)^3 \quad \mathbf{x} \mapsto (\|x_3 - x_1\|, \|x_1 - x_4\|, \|x_4 - x_2\|).$$

Suppose (\mathbf{t}, \mathbf{v}) is such that $\Xi \circ G(\mathbf{t}, \mathbf{v}) \in \Delta$. Then by definition, \mathbf{t} is the preimage of an alternating quadriseccant \mathbf{x} of the long knot $G_{\mathbf{v}}$. Theorem 38, proves that (\mathbf{t}, \mathbf{v}) is a regular point of C_4G , and the image of $dC_4G(\mathbf{t}, \mathbf{v})$ is all of $T_{\mathbf{x}}K_\varepsilon = \mathbb{R}^{12}$.

Now compute $d\Xi_{\mathbf{x}} : T_{\mathbf{x}}K_\varepsilon \rightarrow (T_y S^2)^3$, where $y = \|x_3 - x_1\| = \|x_1 - x_4\| = \|x_4 - x_2\|$.

$$\begin{aligned} \frac{\partial \|x_3 - x_1\|}{\partial x_1} &= \frac{1}{|x_3 - x_1|^3} ((x_3 - x_1) \cdot (x_3 - x_1)^T - |x_3 - x_1|^2 I_3) \\ &= \frac{1}{|x_3 - x_1|} (y \cdot y^T - I_3) \\ \frac{\partial \|x_3 - x_1\|}{\partial x_3} &= \frac{-1}{|x_3 - x_1|^3} ((x_3 - x_1) \cdot (x_3 - x_1)^T - |x_3 - x_1|^2 I_3) \\ &= \frac{-1}{|x_3 - x_1|} (y \cdot y^T - I_3) \end{aligned}$$

where I_3 is the 3×3 identity matrix. Then

$$d\Xi_{\mathbf{x}} = \begin{bmatrix} \frac{\partial \|x_3 - x_1\|}{\partial x_1} & 0 & -\frac{\partial \|x_3 - x_1\|}{\partial x_1} & 0 \\ -\frac{\partial \|x_1 - x_4\|}{\partial x_4} & 0 & 0 & \frac{\partial \|x_1 - x_4\|}{\partial x_4} \\ 0 & \frac{\partial \|x_4 - x_2\|}{\partial x_2} & 0 & -\frac{\partial \|x_4 - x_2\|}{\partial x_2} \end{bmatrix}$$

which simplifies and column-reduces to the matrix

$$\begin{bmatrix} -y \cdot y^T + I_3 & 0 & y \cdot y^T - I_3 & 0 \\ -y \cdot y^T + I_3 & 0 & 0 & y \cdot y^T - I_3 \\ 0 & y \cdot y^T - I_3 & 0 & -y \cdot y^T + I_3 \end{bmatrix},$$

and further reduces to

$$\begin{bmatrix} 0 & 0 & y \cdot y^T - I_3 & 0 \\ 0 & 0 & 0 & y \cdot y^T - I_3 \\ 0 & y \cdot y^T - I_3 & 0 & 0 \end{bmatrix}.$$

If $y \cdot y^T - I_3$ has rank 2, then $d\Xi_{\mathbf{x}}$ has rank 6. Suppose $y = (y_1, y_2, y_3) \in S^2 \subset \mathbb{R}^3$,

$$y \cdot y^T - I_3 = \begin{bmatrix} y_1^2 - 1 & y_1 y_2 & y_1 y_3 \\ y_1 y_2 & y_2^2 - 1 & y_2 y_3 \\ y_1 y_3 & y_2 y_3 & y_3^2 - 1 \end{bmatrix},$$

and if y_1, y_2 or y_3 are equal to 0, then the remaining two coordinates cannot both be zero, which directly implies that $y \cdot y^T - I_3$ has rank 2. Assume $y_1, y_2, y_3 \neq 0$. Then we may reduce this matrix to

$$\begin{bmatrix} 1 - \frac{1}{y_1^2} & 1 & 1 \\ 1 & 1 - \frac{1}{y_2^2} & 1 \\ 1 & 1 & 1 - \frac{1}{y_3^2} \end{bmatrix}$$

which, through further reduction, can be shown to have rank 2. Since the codomain of Ξ is six dimensional, and the rank of $d\Xi_{\mathbf{x}}$ is always six whenever $\mathbf{x} = G(\mathbf{t}, \mathbf{v})$ it follows that (\mathbf{t}, \mathbf{v}) is a regular point of $\Xi \circ C_4G$. Thus,

$$\Xi \circ C_4G \pitchfork \Delta.$$

The Transversality Theorem applies, so for almost all choices of $\mathbf{v} \in (\varepsilon D)^{n-1}$, the composition $\Xi \circ C_4 G_{\mathbf{v}}$ is transverse to Δ . This is equivalent to the statement of the theorem. \square

Now we may assume that a generic knot f is such that $\xi \circ C_4 f \pitchfork \Delta$. The spaces $C_4 \mathbb{I}$, Δ , and $(S^2)^3$ are all orientable manifolds of dimensions 4, 2, and 6 respectively. These spaces, together with $\xi \circ C_4 f$ are almost appropriate for intersection theory, with the minor issue that $C_4 \mathbb{I}$ is not boundaryless. However, we may essentially ignore this issue. Let ε be the radius of the tubular neighborhood about f in $\mathbb{I} \times \mathbb{R}^2$. Then partition \mathbb{I} into three segments, $[0, \delta_0) = f^{-1}([0, \varepsilon) \times \mathbb{R}^2)$, $(\delta_1, 1] = f^{-1}((1 - \varepsilon, 1] \times \mathbb{R}^2)$, and $[\delta_0, \delta_1]$, where $\delta_0, \delta_1 \in \mathbb{I}$. Suppose \mathbf{t} is the preimage of an alternating quadriseccant \mathbf{x} of $C_4 f$. If $t_1 \in [0, \delta_0)$, then $x_1 \in [0, \varepsilon) \times \mathbb{R}^2$. However, our alternating quadriseccant line ensures that either x_3 or x_4 must also lie in $[0, \varepsilon) \times \mathbb{R}^2$ as well. This is not possible, as our tubular neighborhood, along with the fact that $|x_3 - x_1| \geq \varepsilon$, forces x_3 to be at least distance ε away from the boundary of $\mathbb{I} \times \mathbb{R}^2$. This contradiction implies $t_1 \notin [0, \delta_0)$, and a similar argument shows that $t_4 \notin (\delta_1, 1]$. Thus, our preimage points $(\xi \circ C_4 f)^{-1}(\Delta)$ are not close to the boundary of $C_4 \mathbb{I}$, the domain $C_4 \mathbb{I}$ may be restricted to some open interval $C_4(\delta_0, \delta_1)$ instead, without affecting our alternating quadriseccant count.

We then derive a signed intersection number

$$v_Q : \mathcal{K} \rightarrow \mathbb{Z} \quad v_Q(f) = I(\xi \circ C_4 f, \Delta),$$

which is by definition a knot invariant (see the paragraph following 20). Intuitively, we are attaching to each alternating quadriseccant of K a sign of ± 1 , induced by the preimage orientation. The sum of these signs is the intersection number.

4.2 Quadriseccant Count as a Vassiliev Invariant

We have established the invariance of the signed alternating quadriseccant count; however, it is useful to check if this invariant coincides with any well-known knot invariants. We will verify that v_Q is equal to the second-order Vassiliev invariant v_2 .

Proposition 40. *v_Q is a Vassiliev invariant of order two.*

Proof. Define \mathcal{L} to be the subspace

$$\mathcal{L} = \{(x_1, x_2, x_3) \in C_4\mathbb{R}^3 : x_1, x_2, x_3 \text{ are colinear}\}.$$

It is an 7-dimensional submanifold of $C_3\mathbb{R}^3$, as it is diffeomorphic to

$$C_2\mathbb{R}^3 \times ((-\infty, 0) \cup (0, 1) \cup (1, \infty))$$

through the map that sends (x_1, x_2, x_3) to $((x_1, x_2); \frac{|x_3 - x_1|}{|x_2 - x_1|})$.

Let f be a generic knot, and c_1, c_2, c_3 be a collection of three distinct crossings, with domains D_1, D_2, D_3 respectively. Let

$$D = \prod_{i=1}^3 D_i \quad c = \prod_{i=1}^3 c_i : D \rightarrow S^3$$

First the generic existence of three equivalent crossings, such that no triple in the product space $c_1(D_1) \times c_2(D_2) \times c_3(D_3)$ contains three colinear coordinates will be demonstrated. A generic choice of three points in the interiors of D_1, D_2, D_3 are such that their images under c_1, c_2, c_3 are not collinear. Since \mathcal{L} is closed, these points may be thickened in a small manner to obtain three compact 3-balls V_1, V_2, V_3 each contained within the interiors of D_1, D_2, D_3 . Let V be the (disjoint) union of V_1, V_2 and V_3 , and $b : D \times \mathbb{I} \rightarrow D$ be a smooth isotopy such that b_0 is the identity, and $b_1(D_i) = V_i$. Then the diagram

$$\begin{array}{ccc} D \times \mathbb{I} & \xrightarrow{b} & D \\ c \times \text{id} \downarrow & & \downarrow c \\ c(D) \times \mathbb{I} & \xrightarrow{b^*} & c(D) \subset S^3 \end{array}$$

commutes, where the bottom horizontal map b^* is determined by the diffeomorphism between D and $c(D)$. Because b_t is an embedding for all $t \in \mathbb{I}$, it follows that b_t^* is also an embedding, and b^* is an isotopy of $c(D)$. The Isotopy Extension Theorem may be applied to obtain an ambient isotopy $B^* : S^3 \times \mathbb{I} \rightarrow S^3$, such that B_0^* is the identity, and

$$B_1^*(c(D)) = c(V).$$

Since B^* is an ambient isotopy, the two curves $\alpha_{\pm, i}$ in D_i (defined in (3.0.1)) are sent to two curves in V_i . Each V_i is diffeomorphic to the compact 3-ball D^3 , and an

ambient isotopy of V_i can be arranged to manipulate the strands $B_1^*(c_i(\alpha_{\pm,i}))$ so that they lie in the appropriate position to apply a crossing change (i.e. they are sent to a position in V_i so that the diffeomorphism sending V_i to D^3 maps the curves to $\alpha_{\pm} \subset D^3$). These crossing changes in V_1, V_2, V_3 are equivalent to D_1, D_2, D_3 , while no three points x_1, x_2, x_3 in V_1, V_2, V_3 (respectively) are collinear.

The choice of three initial points was generic. We may assume that a generic choice of three distinct crossing changes c_1, c_2, c_3 with domains D_1, D_2, D_3 are such that no triple in $c_1(D_1) \times c_2(D_2) \times c_3(D_3)$ contains collinear coordinates.

With such crossings in mind, consider the Vassiliev sum

$$\sum_{\sigma \subset \{1,2,3\}} (-1)^{|\sigma|} v_Q(K^\sigma),$$

where $v_Q(K^\sigma)$ returns the signed alternating quadriseccant count for the knot K^σ defined in Chapter 3. Given any σ , let L be an alternating quadriseccant of K^σ . The space $\prod_{i=1}^3 c_i(D_i)$ contains no collinear triples, so L cannot pierce all three $c_i(D_i)$. Assume, without loss to generality, that L is disjoint from $c_3(D_3)$. Then applying a crossing change at c_3 results in the knot $K^{\sigma \ominus \{3\}}$, where L remains an alternating quadriseccant with the same sign (the operator \ominus denotes the symmetric difference). So, for every alternating quadriseccant of K^σ , there exists an $i \in \{1, 2, 3\}$ such that L is an alternating quadriseccant of $K^{\sigma \ominus \{i\}}$. However, $|\sigma| - |\sigma \ominus \{i\}| = \pm 1$. These alternating quadriseccants 'cancel' each other in the Vassiliev sum. Our choices of the knot K and three crossings were arbitrary, so the sum

$$\sum_{\sigma \subset \{1,2,3\}} (-1)^{|\sigma|} v(K^\sigma)$$

is zero, and v_Q , the signed alternating quadriseccant count, is a Vassiliev invariant of order two. \square

From Theorem 27 we now know how v_Q behaves: it is of the form $av_2 + bv_0$, where v_2 and v_0 are the standard Vassiliev invariants of orders two and zero respectively, and $a, b \in \mathbb{Z}$. It is obvious that the unknot has no alternating quadriseccants. Therefore,

$$0 = v_Q(\bigcirc) = av_2(\bigcirc) + bv_0(\bigcirc) = a(0) + b(1) = b$$

and $v_Q = av_2$. If the signed number of alternating quadriseccants for any nontrivial

knot with nonzero v_2 value can be computed, then this value can be compared with the v_2 knot invariant for this knot, and a may be determined.

Theorem 41. *[BCSS]* $v_Q = v_2$.

A proof of this will follow from a result in Chapter 6.

Chapter 5

Transversality and Cocircularities

The above results for quadriseccants of long knots provides an elegant geometric description of the second Vassiliev invariant v_2 in terms of the (signed) number of alternating quadriseccants of the knot. There is a bijective correspondence between the isotopy classes of long knots and oriented closed knots through a stereographic projection at a point on the knot, so one might expect a similar geometric description of the v_2 invariant on closed knots. By taking the naive one-point compactification on both the domain and codomain of a long knot, we begin to see how the quadriseccants are transformed. Any alternating quadriseccants in \mathbb{R}^3 become circles in S^3 intersecting the point-at-infinity. Our focus now shifts from quadriseccant lines on long knots in \mathbb{R}^3 to circles in S^3 that intersect a closed knot in five places. It is possible to examine these cocircularities purely through our previous results regarding long knots. That is, we may relate cocircularities of a closed knot to quadriseccants of the corresponding long knot; however, that is not the approach we will take. While it may have the immediate advantage of brevity, this course does not generalize to an examination of six-point cocircularities. Furthermore, it will be helpful to establish the result independently to provide the appropriate perspective, without reliance on long knots.

The procedure shares many similarities to the quadriseccant case. The space C_5K is a five dimensional submanifold of C_5S^3 , which is of dimension fifteen. Demanding that five distinct points in S^3 be cocircular is a codimension four condition: we first choose three arbitrary points in S^3 (a dimension 9 condition), and this determines the circle that the remaining two points must lie upon (a dimension 2 condition). By intersecting this space with C_5K , a 1-dimensional subspace of C_5S^3 may be expected. This 1-manifold will be the object of study for five-point cocircularities.

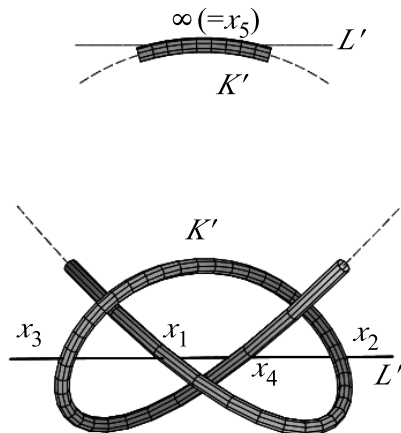


Figure 5.0.1: A long knot K , when compactified becomes a closed knot K' in S^3 . The alternating quadriseccant line L is compactified to a circle L' in S^3 that intersects the point-at-infinity ∞ .

As a natural extension to the five-point cocircularity case, we will also examine occurrences of six points on a closed knot that are cocircular in S^3 . Here, the ambient space is now C_6S^3 , and the space of six ordered distinct points on K is the submanifold C_6K . Demanding that six points in S^3 be cocircular is a dimension twelve condition: three arbitrary points in S^3 may be selected initially to determine the circle that the remaining three points must lie upon. By intersecting C_6K with this cocircularity space in a generic way, a 0-manifold emerges in C_6S^3 . This manifold gives rise to another knot invariant. The proof for transversality of C_5K against the five-point cocircularity space is nearly identical to the proof of transversality between C_6K and the six-point cocircularity space. In this chapter, we will largely present the transversality arguments in tandem.

5.1 Adjacency and the Tubular Neighborhood

All our knots will be closed knots in S^3 . When the context is appropriate, subscripts will be treated cyclically (for example, if $\mathbf{x} = (x_1, \dots, x_5)$, then x_{i+1} will refer to x_1 if $i = 5$). As before, if \mathbf{x} is a point in a configuration space, then x_i denotes the i th coordinate of \mathbf{x} .

Alternating quadriseccants in \mathbb{R}^3 , once compactified, indicate exactly what type of five-point cocircularity will be of interest. We may intuitively think of the point-at-infinity as the 'fifth' point of the knot that the alternating quadriseccant line touches.

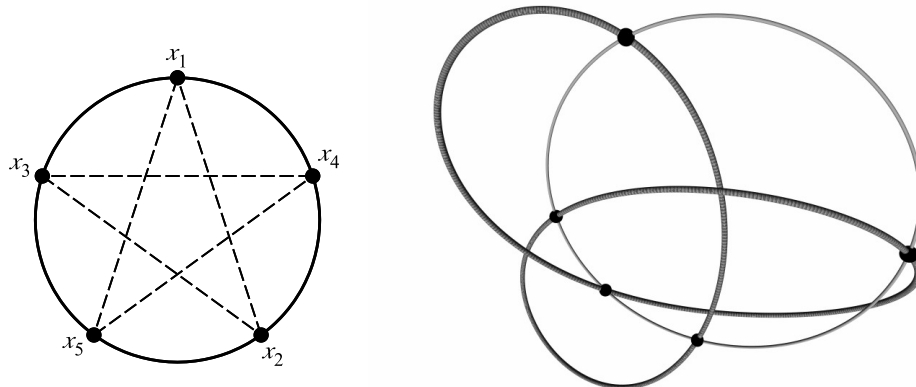


Figure 5.1.1: The necessary arrangement of subscripts for a satanic point, and an example of a satanic circle on the trefoil knot.

In the compactified quadriseccant line (a circle in S^3), if two coordinates of $\mathbf{x} \in C_5K$ are adjacent on the knot, then they are not adjacent on the common circle.

Definition 42. A point $\mathbf{x} = (x_1, \dots, x_5) \in C_5S^3$ is considered a *satanic point* if

- x_1, \dots, x_5 lie on a common circle \mathcal{C} in S^3 .
- For all $i \in \{1, \dots, 5\}$, x_i is not adjacent to x_{i-1} and x_{i+1} when \mathbf{x} is considered as a point in $C_5\mathcal{C}$ (with subscripts working modulo 5).

The common circle \mathcal{C} will be referred to as the *satanic circle* (of \mathbf{x}). Let \mathcal{P} denote the space of all satanic points in C_5S^3 .

The diagram indicates why the term 'satanic' is chosen. The critical observation that will allow transversality is the following:

Fact 43. Let $\mathbf{x} \in C_5K$ be a satanic point, and \mathcal{C} is its corresponding satanic circle. If x_i and x_j are adjacent on \mathcal{C} , then they are not adjacent on K .

Our examination of six-point cocircularities will rely on the same fact. This adjacency requirement will specify what types of six-point cocircularities are to be inspected.

Definition 44. A point $\mathbf{x} = (x_1, \dots, x_6) \in C_6S^3$ is considered a *thelemic point* if

- x_1, \dots, x_6 lie on a common circle \mathcal{C} in S^3 .

- For all $i \in \{1, \dots, 6\}$, the coordinate x_i is not adjacent to x_{i-1} and x_{i+1} on \mathcal{C} (with subscripts working modulo 6).

The common circle \mathcal{C} will be referred to as the *thelemic circle* of \mathbf{x} . Let \mathcal{H} denote the space of all thelemic points in C_6S^3 .

A quick combinatorial check verifies that there are three potential types of thelemic points, indicated in Figure 5.1.2 on page 45. In each type, there exists an $i \in \{1, 2, 3\}$ such that each component of $\mathcal{C} \setminus \{x_i, x_{i+3}\}$ contains two coordinates of \mathbf{x} . If (x_1, \dots, x_6) is a thelemic point of one type, then $(x_2, x_3, x_4, x_5, x_6, x_1)$ is also a thelemic point, but of a different type. This fact will play a critical role later.

Theorem 45. \mathcal{P} is an orientable, boundaryless 11-dimensional submanifold of C_5S^3 , while \mathcal{H} is an orientable, boundaryless 12-dimensional submanifold of C_6S^3 .

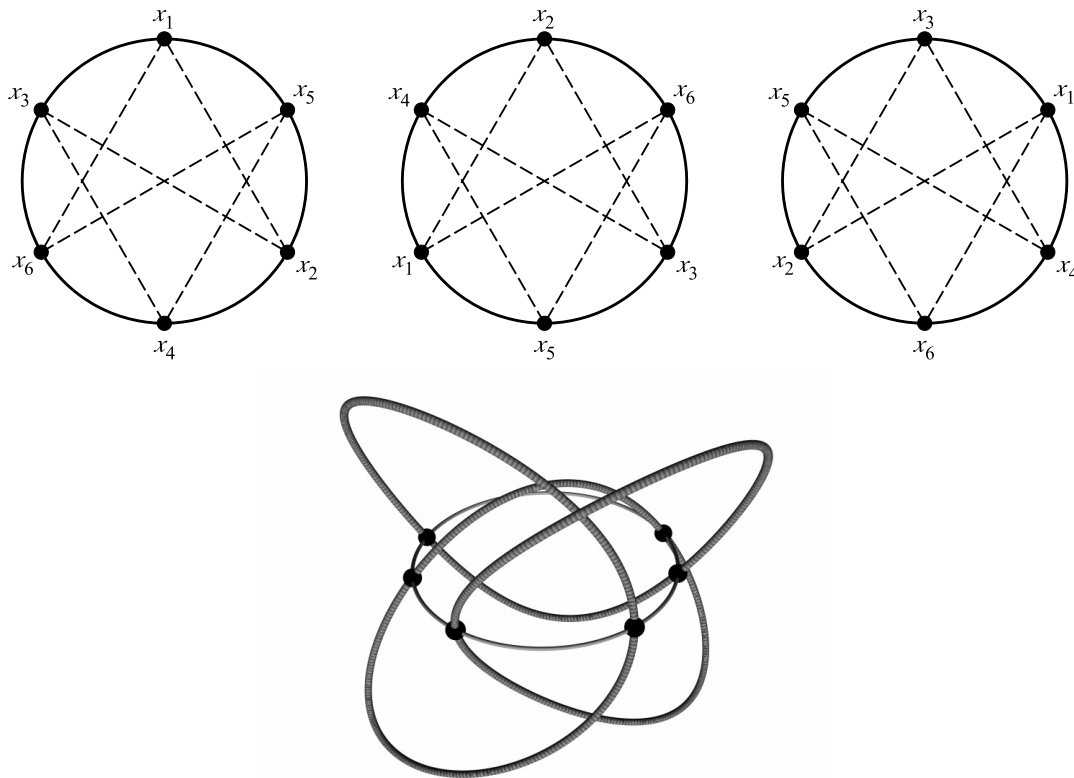


Figure 5.1.2: The necessary arrangements of subscripts for a thelemic point, and an example of a thelemic circle on the figure-eight knot.

Proof. The following map ϕ is a diffeomorphism between \mathcal{P} and $C_3S^3 \times (0, \infty)^2$:

$$\mathbf{x} = (x_1, \dots, x_5) \mapsto \left(x_1, x_2, x_3, \frac{|x_4 - x_1|}{|x_4 - x_2|}, \frac{|x_5 - x_2|}{|x_5 - x_3|} \right).$$

The map is smooth on C_3S^3 . If $\mathbf{x}, \mathbf{y} \in \mathcal{P}$, and $\phi(\mathbf{x}) = \phi(\mathbf{y})$, then trivially $x_i = y_i$ for $i \in \{1, 2, 3\}$. Let \mathcal{C} be the circle containing the coordinates of \mathbf{x} (and thus of \mathbf{y} as well, since the circle is uniquely determined by x_1, x_2, x_3). Because $\mathbf{x}, \mathbf{y} \in \mathcal{P}$, it follows that x_4 and y_4 are contained on the arc of \mathcal{C} between $x_1 = y_1$ and $x_2 = y_2$, that does not contain $x_3 = y_3$. Assume without loss of generality, that the points x_1, x_4, y_4, x_2 are cyclically ordered (that is, that the lines $\overline{x_1y_4}$ and $\overline{x_4x_2}$ intersect). A classical theorem of geometry by the Greek mathematician Ptolemy states that four vertices A, B, C, D in \mathbb{R}^n form a cyclic quadrilateral (the four vertices are cocircular and the diagonals \overline{AC} and \overline{BD} intersect) if and only if

$$|\overline{AB}||\overline{CD}| + |\overline{BC}||\overline{DA}| = |\overline{AC}||\overline{BD}|,$$

where degeneracies such as the four vertices being colinear or two (or more) vertices colliding to form a triangle are permitted. The points x_1, x_4, y_4, x_2 are cyclically ordered:

$$|x_1 - x_4||y_4 - x_2| + |x_1 - x_2||x_4 - y_4| = |x_1 - y_4||x_4 - x_2|.$$

Because $\phi(\mathbf{x}) = \phi(\mathbf{y})$,

$$|x_1 - x_4| = \frac{|y_4 - x_1||x_4 - x_2|}{|y_4 - x_2|}.$$

Substituting this into Ptolemy's Equation,

$$|x_1 - x_2||x_4 - y_4| = 0.$$

The points x_1 and x_2 are not equal, so $x_4 = y_4$. A similar argument dictates that $x_5 = y_5$ as well, so $\mathbf{x} = \mathbf{y}$, and ϕ is injective. It is also surjective, as if $\mathbf{y} = (y_1, y_2, y_3, y_4, y_5) \in C_3S^3 \times (0, \infty)^2$, then we may set $x_i = y_i$, for $i \in \{1, 2, 3\}$. Consider the circle containing x_1, x_2 and x_3 , and the closed arc c of the circle joining x_1 and x_2 , but not containing x_3 . As a point y travels along c , beginning at x_1 and moving towards x_2 , the value $\frac{|y-x_1|}{|y-x_2|}$ continuously increases from 0 to ∞ . The Intermediate Value Theorem demonstrates that there must exist some $x_4 \in c$ such that $\frac{|x_4-x_1|}{|x_4-x_2|} = y_4$. By constructing a point x_5 in a similar fashion, then $\mathbf{x} \in \mathcal{P}$ and $\phi(\mathbf{x}) = \mathbf{y}$, so ϕ is

surjective. This technique also demonstrates the smooth invertability of ϕ . Thus ϕ is a diffeomorphism, and \mathcal{P} is a submanifold of C_5S^3 with $\dim \mathcal{P} = \dim(C_3S^3 \times (0, \infty)^2) = 11$. Orientability follows from the orientability of $C_3S^3 \times (0, \infty)^2$.

The space \mathcal{H} contains three components, each corresponding to a different type of cocircularity. A cyclic permutation of the coordinates of one type of cocircularity results in a different type, so the components are diffeomorphic to each other through this permutation map. It suffices to show that any one component is a submanifold; let \mathcal{H}' be the component where x_1 is adjacent to x_3 , and x_3 is adjacent to x_6 . Let $\psi : \mathcal{H}' \rightarrow C_3S^3 \times (0, \infty)^3$ be defined as:

$$\mathbf{x} = (x_1, \dots, x_6) \mapsto \left(x_1, x_2, x_3, \frac{|x_4 - x_6|}{|x_4 - x_2|}, \frac{|x_5 - x_2|}{|x_5 - x_1|}, \frac{|x_6 - x_3|}{|x_6 - x_4|} \right).$$

The map ψ is a diffeomorphism (for the same reason ϕ is), so \mathcal{H}' is an orientable submanifold of C_6S^3 with $\dim \mathcal{H}' = \dim(C_3S^3 \times (0, \infty)^3) = 12$. It immediately follows that \mathcal{H} is also an orientable submanifold with the same dimension. \square

We now state the main theorem for this section.

Theorem 46. *If f is a generic knot, then $C_5f \pitchfork \mathcal{P}$, and $C_6f \pitchfork \mathcal{H}$.*

This theorem will ultimately be proven by finding an appropriate family of ambient isotopic knots, and demonstrate transversality for the entire family. As with the quadriseccant case, an application of The Transversality Theorem will ensure that almost every knot is such that C_5f and C_6f are transverse to \mathcal{P} and \mathcal{H} respectively.

The knot K is a submanifold of the ambient space S^3 . The Tubular Neighborhood Theorem grants a diffeomorphism h between the injective radius of the normal bundle $N(K; S^3)$ of K and an open neighborhood U of K in S^3 . By embedding S^3 in \mathbb{R}^4 in the usual fashion, an application of the ε -Neighborhood Theorem on K as a submanifold of \mathbb{R}^4 provides an $\varepsilon > 0$, an open neighborhood $V_\varepsilon \subset \mathbb{R}^4$ of K consisting of points with distance less than ε from K , and a submersion $\pi : V_\varepsilon \rightarrow K$ that sends a point in V_ε to its unique closest point on the knot. By compactness, we may shrink our choice of ε small enough so that $V_\varepsilon \cap S^3 \subset U$. Let $K_\varepsilon = V_\varepsilon \cap S^3$, and $N_\varepsilon(K; S^3) = h^{-1}(K_\varepsilon)$. Then K_ε is the set of points of distance less than ε from K on S^3 . Restrict the domains of h and π to $N_\varepsilon(K; S^3)$ and K_ε respectively, so h remains a diffeomorphism and π is a submersion.

We now ensure that the coordinates of satanic and thelemic points in C_5K or C_6K are sufficiently far apart in S^3 . This separation will provide enough freedom

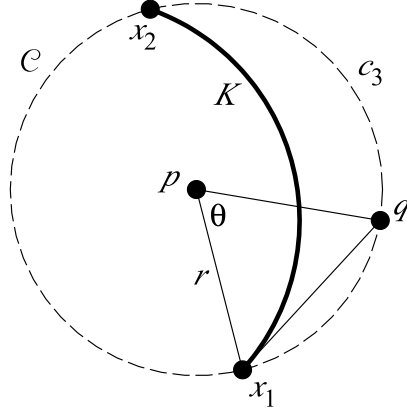


Figure 5.1.3: A diagram illustrating the minimum distance between the coordinates of satanic points.

to perturb a knot without adversely affecting the satanic and thelemic points of the knot.

Lemma 47. *For every knot K , there exists an $\varepsilon > 0$ such that, if \mathbf{x} is a satanic point of K , then $|x_i - x_j| \geq \varepsilon$ for all distinct $i, j \in \{1, \dots, 5\}$. If \mathbf{x} is a thelemic point of K , then $|x_i - x_j| \geq \varepsilon$ for all distinct $i, j \in \{1, \dots, 6\}$.*

Proof. Suppose \mathbf{x} is a satanic point of K , so $\mathbf{x} \in \mathcal{P} \cap C_5 K$, and assume $|x_1 - x_2| < \varepsilon$. The coordinates of \mathbf{x} lie on a common circle $\mathcal{C} \subset S^3$. Let c_3 and c_4 be the closed arcs of \mathcal{C} joining x_1 and x_2 , with $x_3 \in c_3$, and $x_4 \in c_4$. Additionally, let B be the closed ball of radius $|x_1 - x_2|$, centered at x_1 . A geometric argument will be used to show that either $c_3 \subset B$ or $c_4 \subset B$.

Let p be the center of \mathcal{C} , and r the radius. Without loss to generality, suppose that the arclength of c_4 is greater than or equal to the arclength of c_3 , and let q be an arbitrary point on c_3 (see Figure 5.1.3 on page 48). If θ is the angle with vertex p and edges incident with x_1 and q , then by the Law of Cosines,

$$|q - p|^2 + |x_1 - p|^2 - 2|q - p||x_1 - p| \cos \theta = |q - x_1|^2.$$

Equivalently,

$$2r^2 - 2r^2 \cos \theta = |q - x_1|^2,$$

which implies that

$$|q - x_1| = r \sqrt{2(1 - \cos \theta)}. \quad (5.1.1)$$

But the angle θ is bounded above by the measure of the angle $\angle x_1 p x_2$, which will be denoted as $\bar{\theta}$. Again, by the Law of Cosines,

$$\varepsilon \geq |x_2 - x_1| = r\sqrt{2(1 - \cos \bar{\theta})}.$$

Dividing both sides by $r\sqrt{2}$,

$$\sqrt{1 - \cos \bar{\theta}} \leq \frac{\varepsilon}{\sqrt{2}r}.$$

Since θ is bounded above by $\bar{\theta}$, which is less than or equal to π (the arclength of c_3 is less than the arclength of c_4), and the cosine function is decreasing on $(0, \pi)$, it follows that $1 - \cos \theta < 1 - \cos \bar{\theta}$. Applying this inequality to (5.1.1),

$$|q - x_1| = r\sqrt{2(1 - \cos \theta)} \leq r\sqrt{2(1 - \cos \bar{\theta})} \leq r\sqrt{2} \left(\frac{\varepsilon}{\sqrt{2}r} \right) \leq \varepsilon.$$

Thus, $q \in B$. Our choice of $q \in c_3$ was arbitrary, so $c_3 \subset B$. Because $c_3 \subset B \subset K_\varepsilon$, each point in c_3 is projected onto K via the map π . The image of the projection forms a path along K beginning at x_1 and terminating at x_2 . By definition, $x_3 \in c_3$, and $\pi(x_3) = x_3$, so the path must contain x_3 , but not x_4 (since $x_4 \notin c_3$). The Intermediate Value Theorem then proves the existence of a point s on the segment of c_3 between x_1 and x_3 such that $\pi(s) = x_2$. This is a contradiction of the definition of π , as s should be sent to the closest point on K to s , but clearly either x_1 or x_3 is closer to s than x_2 . This contradiction asserts that $|x_1 - x_2| \geq \varepsilon$, and a similar argument shows that $|x_i - x_{i+1}| \geq \varepsilon$, for all $i \in \{1, 2, 3, 4, 5\}$.

If we instead assume that $|x_1 - x_3| < \varepsilon$, and let c_1, c_2 be arbitrary arcs of \mathcal{C} such that $c_1 \cup c_2 = \mathcal{C}$, and $c_1 \cap c_2 = \{x_1, x_3\}$. Then as before, one of the arcs, say c_1 , is entirely contained within a ball of radius $|x_1 - x_3|$ that is centered at x_1 . The point \mathbf{x} is satanic, so x_1 and x_3 are adjacent on \mathcal{C} . Therefore, either $\{x_1, \dots, x_5\} \subset c_1$, or $\{x_1, \dots, x_5\} \cap c_1 = \{x_1, x_3\}$. In the former case, a contradiction arises, as $x_2 \in c_1 \subset B$, so $|x_1 - x_2| < \varepsilon$. In the latter case, there must exist a point $s \in c_1$ such that $\pi(s) = x_2$, or $\pi(s) = x_4$, since $\pi(c_1)$ is a path along K joining x_1 with x_3 . However, s lies between x_1 and x_3 on \mathcal{C} , which are adjacent, so s must be closer to either x_1 or x_3 than both x_2 and x_4 in our ambient space. This again contradicts the definition of π , and it follows that $|x_1 - x_3| \geq \varepsilon$. We may apply this argument to demonstrate that $|x_i - x_j| \geq \varepsilon$ for nonconsecutive, distinct $i, j \in \{1, \dots, 5\}$.

If \mathbf{x} is a thelemic point, then identical arguments demonstrate that $|x_i - x_j| \geq \varepsilon$ for any distinct $i, j \in \{1, \dots, 6\}$. \square

Previously, a diffeomorphism h was established between $N_\varepsilon(K; S^3)$ and K_ε . By embedding the unit circle S^1 in the standard manner into S^3 , a diffeomorphism may be fashioned between $N_\varepsilon(S^1; S^3)$ and $S_\varepsilon^1 \subset S^3$ as well.

As an embedding, the map f is a diffeomorphism onto its image K . Its extension to a map f^* can be constructed as a diffeomorphism that will cause the diagram in Figure 5.1.4 to commute. An example of one such construction is outlined below.

Choose a point $\infty \in S^3$ that is not on K . Apply a stereographic projection $\rho : S^3 \setminus \infty \rightarrow \mathbb{R}^3$ at this point to obtain an embedding $\rho \circ f$ of the knot into \mathbb{R}^3 . Let $\phi_\pm : S^1 \rightarrow S^1 \times S^2$ be the embeddings that map t to $(t, \|\pm(\rho \circ f)'(t)\|)$, with $X_\pm = \text{im}\phi_\pm$. Then X_+ and X_- are two disjoint 1-manifolds contained within $S^1 \times S^2$. Therefore, the image of $X_+ \cup X_-$ under the standard projection map of $S^1 \times S^2$ onto the second component, S^2 , is not surjective. Choose an arbitrary vector $w \in S^2$ that is not contained within this image. Then $w \neq \|\pm(\rho \circ f)'(t)\|$, for all $t \in S^1$. Let w_t^* be the projection of w as a vector in \mathbb{R}^3 onto the plane $N_{(\rho \circ f)(t)}(\rho(K))$ in \mathbb{R}^3 , and $w_t = d(\rho^{-1})(w_t^*)$. Then w_t^* , and w_t are both nonzero. Furthermore, w_t is contained within $N_{f(t)}(K)$, and smoothly varies with t . Let $t' \in \mathbb{R}^4$ be the unit tangent vector of $t \in S^1 \subset S^3$. Then define $A_t \in SO_4\mathbb{R}$ to be a rotation matrix of \mathbb{R}^4 that sends the orthogonal vectors $t', (0, 0, 1, 0)$ and $(0, 0, 0, 1)$ to the vectors $\|f'(t)\|, \|w_t\|$ and $\|f'(t) \times w_t\|$, respectively. The matrix A_t is uniquely determined, well-defined, and varies smoothly with t . Thus, we may define f^* as the map sending (t, v) to $(f(t), A_t v)$.

Additionally, the compactness of S^1 ensures that $|f'(t)|$ is bounded by some finite value. From our construction of f^* , a finite bound on $|\det df^*|$ also exists. Let $F^* \in \mathbb{R}$ be such a bound.

A bound for $|\det dh|$ can be computed as well. Although it is possible to prove

$$\begin{array}{ccccc}
 N_\varepsilon(S^1; S^3) & \longrightarrow & S_\varepsilon^1 & \longrightarrow & S^1 \\
 f^* \downarrow & & \downarrow & & f \downarrow \\
 N_\varepsilon(K; S^3) & \xrightarrow{h} & K_\varepsilon & \xrightarrow{\pi} & K
 \end{array}$$

Figure 5.1.4: A commutative diagram extending the knot f to f^*

directly that a finite bound exists, we will sidestep this issue by shrinking our choice of radius ε if necessary to restrict our domain and codomain. Then our restricted h is such that $|\det dh|$ is bounded, as h is defined on the closure of these spaces, which are compact and proper subsets of our original domain and codomain of h . Let $H \in \mathbb{R}$ be a bound on $|\det dh|$.

Proposition 48. $N_\varepsilon(S^1; S^3)$ is diffeomorphic to $S^1 \times (\varepsilon D^2)$, where D^2 is the 2-dimensional open unit disk.

Proof. First parametrize S^3 and S^1 temporarily as submanifolds of \mathbb{R}^4 with

$$S^3 = \{(x_1, x_2, x_3, x_4) \in \mathbb{R}^4 : |(x_1, x_2, x_3, x_4)| = 1\}$$

and

$$S^1 = \{(x_1, x_2, 0, 0) \in \mathbb{R}^4 : |(x_1, x_2, 0, 0)| = 1\}.$$

Then if $x \in S^3$, then $T_x(S^3)$ is the linear subspace of \mathbb{R}^4 consisting of points y such that $y \cdot x = 0$. If x lies within S^1 as well, then the points $(0, 0, 1, 0)$ and $(0, 0, 0, 1)$ are contained within $N_x(S^1; S^3)$, as are all linear combinations of these two points. The map $j : \varepsilon D^2 \rightarrow N_\varepsilon(S^1; S^3)$ sending (y_1, y_2) to $(0, 0, y_1, y_2)$ is well-defined and smooth. It is also a diffeomorphism, as $N_\varepsilon(S^1; S^3)$ is a linear subspace of dimension 2, containing $(0, 0, 1, 0)$ and $(0, 0, 0, 1)$, so the map is a bijection, with a smooth inverse. \square

Just as with h , compactness of S^1 and the ability to shrink ε if desired ensures that $|\det dj|$ is bounded by some finite value $J \in \mathbb{R}$.

5.2 Perturbing the Knot

As the distance between the coordinates of a satanic or thelemic point are sufficiently far apart (Lemma 47), we may apply a series of bump functions to the knot, where each bump function affects at most one coordinate of each satanic or thelemic point. Each of these bump functions will be a variant of a 'base' bump function $\beta : S^1 \rightarrow [0, 1]$. For reasons that will become apparent momentarily, let $n \in \mathbb{N}$ be such that

$$\frac{2}{n} < \frac{\varepsilon}{2F^*HJ(1 + \varepsilon^2)},$$

and temporarily identify the circle with $[-1, 1]/\{-1, 1\}$. Let β be a bump function that is centered at 0, with radius 1 and height 1, and $\beta_i : S^1 \rightarrow [0, 1]$ be defined as

$$\beta_i(t) = \begin{cases} \frac{1}{n^2\bar{\beta}}\beta(nt - i) & \text{if } t \in [\frac{i-1}{n}, \frac{i+1}{n}] \\ 0 & \text{otherwise} \end{cases},$$

where $\bar{\beta} = \sup_{t \in S^1} \{\beta'(t)\}$, and $i \in \{1, \dots, n\}$. Note that β_i is a bump function with radius $\frac{1}{n}$, centered at $\frac{i}{n}$. Thus, for each $t \in S^1$, there exist at most two and at least one bump function that is nonzero at t . Define

$$g : S^1 \times \left(\frac{\varepsilon}{2}D^2\right)^n \rightarrow S^1 \times \varepsilon D^2$$

$$(t, v_1, \dots, v_n) = (t, \mathbf{v}) = \left(t, \sum_{i=1}^n \beta_i(t) \cdot v_i\right)$$

as our perturbation map. For any fixed $\mathbf{v} \in \left(\frac{\varepsilon}{2}D^2\right)^n$,

$$d(g_{\mathbf{v}})_t : T_t S^1 \rightarrow T_{g_{\mathbf{v}}t}(S^1 \times \varepsilon D^2) \quad d(g_{\mathbf{v}})_t = \begin{bmatrix} 1 \\ \sum_{i=1}^n \beta'_i(t) \cdot v_i \end{bmatrix}$$

so

$$\begin{aligned} |d(g_{\mathbf{v}})_t| &= \left\| \begin{bmatrix} 1 \\ \sum_{i=1}^n \beta'_i(t) \cdot v_i \end{bmatrix} \right\| \\ &< 1 + \varepsilon^2 \sum_{i=1}^n \beta'_i(t) \\ &< 1 + (\varepsilon^2) \sum_{i=1}^n \left(\frac{n\beta'(t)}{n^2\bar{\beta}} \right) \\ &< 1 + \varepsilon^2. \end{aligned}$$

Consider the chain of maps given in Figure 5.2.2, and define

$$G : S^1 \times \left(\frac{\varepsilon}{2}D^2\right)^n \rightarrow K_\varepsilon \quad G = h \circ f^* \circ j \circ g$$

as a family of knots. For every fixed $\mathbf{v} \in \left(\frac{\varepsilon}{2}D^2\right)^n$, the map $G_{\mathbf{v}}$ is a closed knot perturbation of f . Also, $|\det dh|$, $|\det df^*|$, $|\det dj|$ and $|dg_{\mathbf{v}}|$ are all bounded by finite values, so $|dG_{\mathbf{v}}|$ is bounded above by $HF^*J(1 + \varepsilon^2)$. The maps $G_{\mathbf{v}}$ are each closed

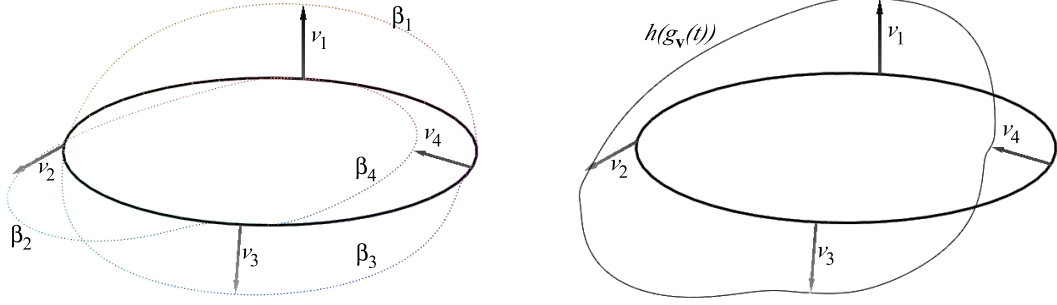


Figure 5.2.1: A collection of bump functions, when $n = 4$. The left picture depicts each bump function β_i individually, along with its corresponding perturbed vector v_i . The right picture indicates the image of such a selection of bump functions and vectors under the map g . The result is a curve in $S^1 \times \varepsilon D^2$.

knots, and as such, there exists an $\varepsilon_{\mathbf{v}} > 0$ such that, if \mathbf{x} is a satanic or thelemic point of $G_{\mathbf{v}}$, then $|x_i - x_j| \geq \varepsilon_{\mathbf{v}}$, for all i, j distinct in $\{1, \dots, 5\}$ or $\{1, \dots, 6\}$ (Lemma 47). Unfortunately, the value of $\varepsilon_{\mathbf{v}}$ may vary widely depending on our choice of \mathbf{v} ; however, it can be made to smoothly vary with \mathbf{v} . If $\mathbf{v} = \mathbf{0}$, then $G_{\mathbf{v}} = f$, and $\varepsilon_{\mathbf{0}}$ can be set to ε . By choosing a small enough open ball about $\mathbf{0}$ in $(\frac{\varepsilon}{2}D^2)^n$, we may ensure that all such \mathbf{v} in this ball are such that $\varepsilon_{\mathbf{v}} > \frac{\varepsilon}{2}$. Shrink our choice of ε sufficiently to ensure that $\varepsilon_{\mathbf{v}}$ is always greater than $\varepsilon_0/2$, for all $\mathbf{v} \in (\frac{\varepsilon}{2}D^2)^n$. From this, if \mathbf{x} is a satanic or thelemic point of the knot $G_{\mathbf{v}}$, then $|x_i - x_j| \geq \varepsilon/2$, for all distinct $i, j \in \{1, \dots, 6\}$.

Since the 'speed' of $G_{\mathbf{v}}$ is bounded by $HF^*J(1 + \varepsilon^2)$, and the distance between any two coordinates x_i and x_j of a satanic or thelemic point \mathbf{x} of $G_{\mathbf{v}}$ is at least $\varepsilon/2$, it follows that the 'time' required to travel to any two coordinates of a satanic or thelemic point is at least

$$\frac{\varepsilon}{2} \cdot \frac{1}{HF^*J(1 + \varepsilon^2)}.$$

$$\begin{array}{ccccccc}
 S^1 \times (\frac{\varepsilon}{2}D^2)^n & \xrightarrow{g} & S^1 \times (\varepsilon D^2) & \xrightarrow{j} & N_{\varepsilon}(S^1; S^3) & \longrightarrow & S^1_{\varepsilon} & \longrightarrow & S^1 \\
 & & & & f^* \downarrow & & \downarrow & & f \downarrow \\
 & & & & N_{\varepsilon}(K; S^3) & \xrightarrow{h} & K_{\varepsilon} & \xrightarrow{\pi} & K
 \end{array}$$

Figure 5.2.2: A commutative diagram incorporating g .

If \mathbf{t} is the preimage of a satanic or thelemic point \mathbf{x} under $G_{\mathbf{v}}$, then

$$|t_i - t_j| > \frac{\varepsilon}{2HF^*J(1 + \varepsilon^2)}$$

for all i, j distinct. However, we chose $n \in \mathbb{N}$ to be such that

$$\frac{2}{n} < \frac{\varepsilon}{2HF^*J(1 + \varepsilon^2)} < |t_i - t_j|.$$

The radius of each bump function β_i is $\frac{1}{n}$, so it is nonzero only on an interval of length $\frac{2}{n}$. The following lemma is proven.

Lemma 49. *If \mathbf{t} is the preimage of a satanic or thelemic point \mathbf{x} of the knot $G_{\mathbf{v}}$, then there does not exist two distinct $i, j \in \{1, \dots, 6\}$ and a $k \in \{1, \dots, n\}$ such that $\beta_k(t_i)$ and $\beta_k(t_j)$ are both nonzero.*

By an abuse of notation, let $C_5g : C_5(S^1) \times (\frac{\varepsilon}{2}D^2)^n \rightarrow C_5(S^1 \times (\varepsilon D^2))$ be the map

$$(\mathbf{t}, \mathbf{v}) = (t_1, \dots, t_5, v_1, \dots, v_n) \mapsto \left(\left(t_1, \sum_{i=1}^n \beta_i(t_1) \cdot v_i \right), \dots, \left(t_5, \sum_{i=1}^n \beta_i(t_5) \cdot v_i \right) \right)$$

and

$$C_5G = C_5h \circ C_5f^* \circ C_5j \circ C_5g.$$

Similarly, let $C_6g : C_6S^1 \times (\frac{\varepsilon}{2}D^2)^n \rightarrow C_6(S^1 \times (\varepsilon D^2))$ be defined as

$$(\mathbf{t}, \mathbf{v}) = (t_1, \dots, t_5, t_6, v_1, \dots, v_n) \mapsto \left(\left(t_1, \sum_{i=1}^n \beta_i(t_1) \cdot v_i \right), \dots, \left(t_6, \sum_{i=1}^n \beta_i(t_6) \cdot v_i \right) \right)$$

and

$$C_6G = C_6h \circ C_6f^* \circ C_6j \circ C_6g.$$

For notational purposes, we now let the path for transversality between C_5f and \mathcal{P} diverge only slightly from the transversality argument for C_6f and \mathcal{H} . Their proofs will remain the same.

Theorem 50. *If \mathbf{t} is the preimage of a satanic point \mathbf{x} under $C_5G_{\mathbf{v}}$, for some fixed $\mathbf{v} \in (\frac{\varepsilon}{2}D^2)^n$, then (\mathbf{t}, \mathbf{v}) is a regular value of C_5g .*

Proof. Assume the hypotheses of the lemma are valid. The derivative of C_5g has domain $(\prod_{i=1}^5 T_{t_i}S^1) \times \mathbb{R}^{2n}$ and codomain $\prod_{i=1}^5 (T_{t_i}S^1 \times \mathbb{R}^2)$, and may be represented

by

$$dC_5g_{(\mathbf{t}, \mathbf{v})} = \begin{bmatrix} \frac{\partial g_{\mathbf{v}}}{\partial t_1} & & 0 & \frac{\partial g_{t_1}}{\partial v_1} & \cdots & \frac{\partial g_{t_1}}{\partial v_n} \\ & \ddots & & \vdots & \ddots & \vdots \\ 0 & & \frac{\partial g_{\mathbf{v}}}{\partial t_5} & \frac{\partial g_{t_5}}{\partial v_1} & \cdots & \frac{\partial g_{t_5}}{\partial v_n} \end{bmatrix}$$

$$\frac{\partial g_{\mathbf{v}}}{\partial t_i} = \begin{bmatrix} 1 \\ \sum_{j=1}^n \beta'_j(t_i) \cdot v_j \end{bmatrix} \quad \frac{\partial g_{t_i}}{\partial v_j} = \begin{bmatrix} 0 \\ \beta_j(t_i) I_2 \end{bmatrix}$$

There exists at least one β_j such that $\beta_j(t_i)$ is nonzero. Assume, without loss to generality, that $\beta_i(t_i) \neq 0$. Then Lemma 49 implies that, $\beta_j(t_i) = 0$, for all $j \in \{1, 2, 3, 4, 5\} \setminus \{i\}$. The derivative $dC_5g_{(\mathbf{t}, \mathbf{v})}$ is a linear function that may be represented as the matrix

$$\begin{bmatrix} 1 & & 0 & & 0 & \frac{\partial g_{t_1}}{\partial v_6} & \cdots & \frac{\partial g_{t_1}}{\partial v_n} \\ \sum_{j=1}^n \beta'_j(t_1) \cdot v_j & & 0 & \beta_1(t_1) I_2 & & 0 & & \\ & \ddots & & & \ddots & & \vdots & \ddots & \vdots \\ 0 & & 1 & & 0 & & & \\ 0 & & \sum_{j=1}^n \beta'_j(t_5) \cdot v_j & & 0 & \beta_5(t_5) I_2 & \frac{\partial g_{t_5}}{\partial v_6} & \cdots & \frac{\partial g_{t_5}}{\partial v_n} \end{bmatrix},$$

which has rank 15, and is certainly surjective. \square

Corollary 51. *If \mathbf{t} is the preimage of a thelemic point \mathbf{x} under $C_6G_{\mathbf{v}}$, for some fixed \mathbf{v} , then (\mathbf{t}, \mathbf{v}) is a regular value of C_6g .*

Proof. The proof is identical. Here the derivative of C_6g has domain $(\prod_{i=1}^6 T_{t_i} S^1) \times \mathbb{R}^{2n}$ and codomain $\prod_{i=1}^6 (T_{t_i} S^1 \times \mathbb{R}^2)$, and is equal to

$$\begin{bmatrix} 1 & & 0 & & 0 & \frac{\partial g_{t_1}}{\partial v_7} & \cdots & \frac{\partial g_{t_1}}{\partial v_n} \\ \sum_{j=1}^n \beta'_j(t_1) \cdot v_j & & 0 & \beta_1(t_1) I_2 & & 0 & & \\ & \ddots & & & \ddots & & \vdots & \ddots & \vdots \\ 0 & & 1 & & 0 & & & \\ 0 & & \sum_{j=1}^n \beta'_j(t_6) \cdot v_j & & 0 & \beta_6(t_6) I_2 & \frac{\partial g_{t_6}}{\partial v_7} & \cdots & \frac{\partial g_{t_6}}{\partial v_n} \end{bmatrix},$$

which has rank 18, and is surjective. \square

Since j , f^* , and h are all diffeomorphisms, it follows that $dC_5G_{(\mathbf{t}, \mathbf{v})}$ and $dC_6G_{(\mathbf{t}, \mathbf{v})}$ are both surjective whenever \mathbf{t} is the preimage of a satanic (respectively, thelemic) point under $G_{\mathbf{v}}$.

Theorem 46 is an immediate consequence of Theorem 50 and Corollary 51. If $\mathbf{t} \in C_5S^1$, and $G_{\mathbf{v}}(\mathbf{t}) = \mathbf{x} \in \mathcal{P}$ for some $\mathbf{v} \in (\frac{\varepsilon}{2}D^2)^n$, then

$$dC_5G_{(\mathbf{t},\mathbf{v})} \left(\left(\prod_{i=1}^5 T_{t_i} S^1 \right) \times \mathbb{R}^{2n} \right) = T_{G(\mathbf{t},\mathbf{v})} C_5S^3.$$

Thus, $C_5G \pitchfork \mathcal{P}$. Similarly $C_6G \pitchfork \mathcal{H}$.

By the Transversality Theorem, almost all choices of \mathbf{v} guarantee that $C_5G_{\mathbf{v}} \pitchfork \mathcal{P}$ and $C_6G_{\mathbf{v}} \pitchfork \mathcal{H}$.

Chapter 6

Satanic and Thelemic Points as Invariants

Transversality implies that we may study the preimage manifolds of \mathcal{P} and \mathcal{H} under C_5f and C_6f . An examination of the dimensions of these submanifolds dictates that $C_5f^{-1}(\mathcal{P})$ is a 1-manifold of C_5S^1 , and $C_6f^{-1}(\mathcal{H})$ is a 0-manifold of C_6S^1 . We will first study the properties of $C_5f^{-1}(\mathcal{P})$, and relate it to the signed alternating quadriscant count for the corresponding long knot.

For ease in notation, all knots will be generic, and $\mathcal{P}_f = C_5f^{-1}(\mathcal{P})$ and $\mathcal{H}_f = C_6f^{-1}(\mathcal{H})$. In order to invoke intersection theory, compactness of \mathcal{P}_f and \mathcal{H}_f must first be demonstrated.

Proposition 52. *\mathcal{P}_f and \mathcal{H}_f are compact.*

Proof. The maps f , C_5f , and C_6f are all proper. Let

$$Z_5 = \{\mathbf{x} \in \mathcal{P} : |x_i - x_j| \geq \varepsilon, \text{ for all (distinct) } i, j \in \{1, \dots, 5\}\}$$

be a closed subset of \mathcal{P} and

$$Z_6 = \{\mathbf{x} \in \mathcal{H} : |x_i - x_j| \geq \varepsilon, \text{ for all (distinct) } i, j \in \{1, \dots, 6\}\}$$

be a closed subset of \mathcal{H} . Then Z_5 and Z_6 are both compact as subsets of $(S^3)^5$ and $(S^3)^6$ respectively. As a result, $C_5f^{-1}(Z_5)$ and $C_6f^{-1}(Z_6)$ are compact subsets of C_5S^1 and C_6S^1 . By Lemma 47, each satanic or thelemic point of the knot is contained

within Z_5 or Z_6 . Therefore,

$$C_5 f^{-1}(Z_5) = C_5 f^{-1}(\mathcal{P}) = \mathcal{P}_f \quad C_6 f^{-1}(Z_6) = C_6 f^{-1}(\mathcal{H}) = \mathcal{H}_f.$$

□

Even though the domains of $C_5(f)$ and $C_6(f)$ are not compact, the compactness of \mathcal{P}_f and \mathcal{H}_f allow intersection theory to be applied regardless, as points in these submanifolds must lie within a compact subset of the ambient space.

6.1 Satanic Points

The manifolds $C_5 S^1$ and $C_5 S^3$ each obtain an induced orientation as open subsets of $(S^1)^5$ and $(S^3)^5$. The submanifold \mathcal{P} of $C_5 S^3$ is also orientable, as indicated in Theorem 45. Transversality between $C_5 f$ and \mathcal{P} , implies that \mathcal{P}_f is an orientable manifold (with orientation induced through the preimage) of dimension

$$\dim(C_5 S^1) + \dim(\mathcal{P}) - \dim(C_5 S^3) = 5 + 11 - 15 = 1$$

in $C_5 S^1$. If f and f' are equivalent knots, then \mathcal{P}_f and $\mathcal{P}_{f'}$ are ambient isotopic. Consider the projection map

$$\pi_f : \mathcal{P}_f \rightarrow S^1 \quad \mathbf{t} = (t_1, \dots, t_5) \mapsto t_1.$$

Since \mathcal{P}_f is a 1-manifold, we may examine the degree of π_f . Recall the motivation for studying such satanic cocircularities — they are the result of the compactification of alternating quadriseccants for the corresponding long knot. The degree of π_f will be precisely what links these two geometric objects together. Let $s \in S^1$ be a generic point, so by definition $\deg(\pi_f) = I(\pi_f, s)$. Let $\rho_1 : S^1 \rightarrow \mathbb{R} \cup \{\infty_1\}$ and $\rho_3 : S^3 \rightarrow \mathbb{R}^3 \cup \{\infty_3\}$ be the (orientation preserving) stereographic projections that send s to ∞_1 and $f(s)$ to ∞_3 . Then the diagram in Figure 6.1.1 on page 59 is obtained, where the lower vertical maps are inclusions.

The map f_* indicated in Figure 6.1.1 on page 59 is an embedding that, once compactified to a closed knot, is isotopic to f . Through ambient isotopy, f can be placed in a position so that f_* satisfies the criteria for a long knot.

Theorem 53. $\deg \pi_f = I(\xi \circ C_4 f_*, \Delta)$.

Proof. Suppose $\mathbf{t} \in \mathcal{P}_f$ is such that $\pi_f(\mathbf{t}) = s$. By definition, \mathbf{t} is the preimage of a satanic point \mathbf{x} of K such that $x_1 = f(s)$. Then $C_5\rho_1(\mathbf{t}) = (\infty_1, \rho_1 t_2, \dots, \rho_1 t_5)$, and this point is mapped to $C_5\rho_3(\mathbf{x}) = (\infty_3, \rho_3 x_2, \dots, \rho_3 x_5)$ by the middle arrow in Figure 6.1.1 on page 59. If \mathbf{t}_* is defined as $C_4\rho_1(t_2, t_3, t_4, t_5)$, and $\mathbf{x}_* = C_4\rho_3(x_2, x_3, x_4, x_5)$, then \mathbf{t}_* is contained in C_4S^1 , and the coordinates of \mathbf{x}_* are collinear. In fact, $\xi(\mathbf{x}_*) \in \Delta$, since $C_4f_*(\mathbf{t}_*) = \mathbf{x}_*$, so \mathbf{t}_* is the preimage of an alternating quadrisequant of f_* . This process is reversible: an alternating quadrisequant of f_* is mapped to a satanic point of f with first coordinate $f(s)$ when compactified. Our orientations all agree as well, since all of the vertical maps in the diagram are orientation preserving. The evaluation maps also preserve orientation, so the orientation imposed on the point $\mathbf{t}_* \in (\xi \circ C_4f)^{-1}(\Delta)$ agrees with the orientation imposed on its corresponding point $\mathbf{t} \in \pi_f^{-1}(s)$. \square

This, combined with Proposition 40, yields the next corollary.

Corollary 54. *The degree of π_f is a Vassiliev invariant of order 2. In particular, $\deg \pi_f = av_2$, where a is an integer.*

The value of a will be determined by explicitly computing the degree of π_f for a non-trivial knot (specifically, a non-trivial knot such that v_2 is nonzero). The knot of choice will be the usual one — the trefoil. Computing cocircularities of a knot explicitly is quite difficult by hand. However, a computer algorithm may be implemented to find the desired cocircularities. The technique uses a variation of Newton’s Method to locate the cocircularities. The pseudocode is presented in Appendix B, along with some relevant theorems to verify its completeness.

Figure 6.1.2 on page 60 depicts a satanic circle on the trefoil knot, as well as a projection of \mathcal{P}_f onto C_2S^1 by forgetting the last three coordinates. The space C_2S^1

$$\begin{array}{ccc}
 S^1 & \xrightarrow{f} & S^3 \\
 \rho_1 \downarrow & & \rho_3 \downarrow \\
 \mathbb{R} \cup \{\infty_1\} & \longrightarrow & \mathbb{R}^3 \cup \{\infty_3\} \\
 \uparrow & & \uparrow \\
 \mathbb{R} & \xrightarrow{f_*} & \mathbb{R}^3
 \end{array}$$

Figure 6.1.1: A commutative diagram relating a knot f with its corresponding long knot f_* .

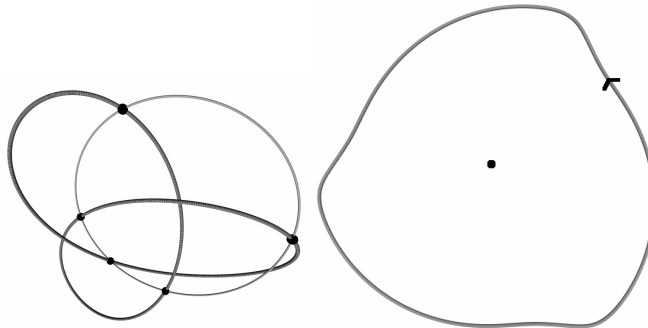


Figure 6.1.2: A satanic circle on the trefoil knot.

is represented by $S^1 \times (0, 1)$ — a punctured disk. The number of times the curve winds around the origin (marked with a dot in the center) is precisely the degree of π_f . The orientation of the curve is marked with an arrow. In the case of the trefoil, the curve winds once around the origin in the positive direction, so $\deg \pi_f = +1$. The standard second Vassiliev invariant v_2 also takes on the value $+1$ for the trefoil knot.

$$v_2(\text{trefoil}) = +1 = \deg \pi_f = av_2(\text{trefoil}) = a.$$

Theorem 55. $I(\xi \circ C_4 f, \Delta) = \deg \pi_f = v_2$.

This theorem establishes an elegant connection between the second Vassiliev invariant and the collection of satanic points on closed knots and alternating quadriseccants on long knots. While the definition of a Vassiliev invariant is somewhat obtuse, the second order invariant has a nice geometric representation as the signed alternating quadriseccant count for long knots, or as the signed number of satanic points of the knot that intersect a particular generic point $f(s)$. Appendix B contains more information regarding the computation of satanic points on various knots, while Appendix C presents a gallery of satanic circles on various knots of higher complexity.

6.2 Thelemic Points

The space $C_6 f^{-1}(\mathcal{H})$ is a collection of isolated points in $C_6 S^1$, and is denoted as \mathcal{H}_f . Recall that if \mathbf{x} is a thelemic point, then so is (x_2, \dots, x_6, x_1) . If $\phi : C_6 S^3 \rightarrow C_6 S^3$ maps (x_1, \dots, x_6) to (x_2, \dots, x_6, x_1) , then $\phi(\mathcal{H}) = \mathcal{H}$, and $\phi(C_6 K) = C_6 K$.

Proposition 56. ϕ is an orientation reversing diffeomorphism.

Proof. The map ϕ is linear. If $\mathbf{x} \in C_6S^1$, then

$$d\phi_{\mathbf{x}} = \begin{bmatrix} 0 & I_3 & 0 & 0 & 0 & 0 \\ 0 & 0 & I_3 & 0 & 0 & 0 \\ 0 & 0 & 0 & I_3 & 0 & 0 \\ 0 & 0 & 0 & 0 & I_3 & 0 \\ 0 & 0 & 0 & 0 & 0 & I_3 \\ I_3 & 0 & 0 & 0 & 0 & 0 \end{bmatrix},$$

and $\det d\phi_{\mathbf{t}} = -1$. Thus, ϕ is orientation-reversing. \square

Let \mathbf{t} be the preimage of some thelemic point \mathbf{x} , and let $\mathbf{t}' = (t_2, \dots, t_6, t_1)$, and $\mathbf{x}' = C_6f(\mathbf{t})$. Furthermore, let $\varepsilon_{\mathbf{t}}$ denote the orientation of ± 1 associated to \mathbf{x} determined by whether the orientation of

$$d(C_6f)_{\mathbf{t}}T_{\mathbf{t}}(C_6S^1) \oplus T_{\mathbf{x}}\mathcal{H} = T_{\mathbf{x}}C_6K \oplus T_{\mathbf{x}}\mathcal{H}$$

agrees with the orientation of $T_{\mathbf{x}}C_6S^3$. Since $\phi(\mathbf{x}) = \mathbf{x}'$, it follows that $\varepsilon_{\mathbf{t}'}$ is determined by whether the orientation

$$d(\phi \circ C_6f)_{\mathbf{t}}T_{\mathbf{t}}(C_6S^1) \oplus T_{\phi_{\mathbf{x}}}\mathcal{H} = T_{\phi_{\mathbf{x}}}C_6K \oplus T_{\phi_{\mathbf{x}}}\mathcal{H} = d\phi_{\mathbf{x}}T_{\mathbf{x}}C_6K \oplus d\phi_{\mathbf{x}}T_{\mathbf{x}}\mathcal{H}$$

agrees with the orientation of $T_{\phi_{\mathbf{x}}}C_6S^3 = d\phi_{\mathbf{x}}T_{\mathbf{x}}C_6S^3$. If $\beta_K, \beta_{\mathcal{H}}$ and β_S are positive bases for $T_{\mathbf{x}}C_6K, T_{\mathbf{x}}\mathcal{H}$ and $T_{\mathbf{x}}C_6S^3$, then

$$\beta_K \oplus \beta_{\mathcal{H}} = (\varepsilon_{\mathbf{t}})\beta_S.$$

The map ϕ is orientation-reversing, so $d\phi_{\mathbf{x}}T_{\mathbf{x}}C_6K$, $d\phi_{\mathbf{x}}T_{\mathbf{x}}\mathcal{H}$, and $d\phi_{\mathbf{x}}T_{\mathbf{x}}C_6S^3$ can be represented by positive bases $-\beta_K, -\beta_{\mathcal{H}}$ and $-\beta_S$ respectively. We have

$$(\varepsilon_{\mathbf{t}'})(-\beta_S) = -\beta_K \oplus -\beta_{\mathcal{H}} = \beta_K \oplus \beta_{\mathcal{H}} = (\varepsilon_{\mathbf{t}})\beta_S$$

and $\varepsilon_{\mathbf{t}'} = -\varepsilon_{\mathbf{t}}$. If \mathbf{t} is the preimage of a thelemic point, then

$$\varepsilon_{\mathbf{t}} = \varepsilon_{(t_3, t_4, t_5, t_6, t_1, t_2)} = \varepsilon_{(t_5, t_6, t_1, t_2, t_3, t_4)} = \pm 1$$

$$\varepsilon_{\mathbf{t}'} = \varepsilon_{(t_4, t_5, t_6, t_1, t_2, t_3)} = \varepsilon_{(t_6, t_1, t_2, t_3, t_4, t_5)} = \mp 1.$$

For each thelemic circle of the knot K , there exist three associated thelemic points with an orientation of $+1$ attached to them, and three thelemic points with an orientation of -1 attached to them. The next theorem is an immediate consequence.

Theorem 57. $I(C_6f, \mathcal{H}) = \sum_{\mathbf{t} \in \mathcal{H}_f} \varepsilon_{\mathbf{t}} = 0$.

It initially seems then, that our attempt to expand the alternating quadriseccant and satanic circle invariants to derive a thelemic circle invariant for knots is unsuccessful. However, the reason the knot invariant fails is because, for each thelemic circle, there are six corresponding thelemic points — three with a sign of $+1$ and three with a sign of -1 . These thelemic points all define the same circle, so there perhaps is some hope in identifying these points together; we create an equivalence class to identify (t_1, \dots, t_6) and (t_2, \dots, t_6, t_1) in C_6S^3 . We must first verify that this quotient space is indeed a manifold. Even with this verification, we must also ensure that C_6K and \mathcal{H} are not adversely affected, and the two submanifolds remain transverse in the new ambient space.

Definition 58. Given a manifold M , let the *cyclic configuration space* $Z_nM = C_nM/\mathbb{Z}_n$ be equal to the space C_nM , where the points (x_1, \dots, x_n) and (x_2, \dots, x_n, x_1) are identified together. Given a map $f : M \rightarrow N$ between two boundaryless manifolds, the *cyclic evaluation map* $Z_nf : Z_nM \rightarrow Z_nN$ maps a point of Z_nM to Z_nN in the usual sense — if $\mathbf{x} = (x_1, \dots, x_n) \in Z_nM$, then $Z_nf(\mathbf{x}) = (f(x_1), \dots, f(x_n))$.

Before we can carry the notion of transversality over between Z_6K and \mathcal{H}/\mathbb{Z}_6 are carried over, we demonstrate that Z_nM is indeed a manifold. This can be interpreted as a simple application of the powerful Quotient Manifold Theorem, presented in [L]. Theorem 59 is a remodelling of this theorem to suit the intended application.

A finite group G can be considered as a Lie group with the discrete topology attached. The group is said to act *freely on the left* on a manifold M if there exists a smooth map $\theta : G \times M \rightarrow M$ such that each orbit is of order $|G|$. In particular this means that $|\theta^{-1}x| = |G|$, for all $x \in M$.

Theorem 59. [L] *If G is a finite group acting freely on a boundaryless manifold M of dimension m embedded in \mathbb{R}^k , then the orbit space M/G is a boundaryless manifold also of dimension m , and the quotient map $\pi : M \rightarrow M/G$ is a submersion.*

Proof. If $x \in M$, let $x_g = \theta(g, x)$. For each x , the existence of an open neighborhood U^x of x such that the collection of open sets

$$U_g^x = \theta(g, U^x)$$

are pairwise disjoint open neighborhoods of each x_g will be proved. Suppose the converse, let $U^x \subset M$ be an open ball of radius $\varepsilon > 0$ about x , for some $\varepsilon \in (0, \infty)$. Then assume that for all choices of ε , there exist $g, g' \in G$ and $y \in M$ such that $y \in U_g^x \cap U_{g'}^x$. Then from this assumption, there exist points $y^g, y^{g'} \in U^x$ such that $\theta(g, y^g) = y = \theta(g', y^{g'})$. As ε is shrunk, the points y^g and $y^{g'}$ converge towards x , and the smoothness of θ dictates that $\theta(g, y^g)$ and $\theta(g', y^{g'})$ must converge towards x_g and $x_{g'}$ respectively. However, $\theta(g, y^g) = \theta(g', y^{g'})$, so this limiting process implies that $x_g = x_{g'}$ — a contradiction of the fact that G acts freely. Therefore, there exists an open neighborhood U^x about each x such that $\{U_g^x\}_{g \in G}$ are pairwise disjoint. The finiteness of G allows us to further assume that $U_g^x = U^{g \cdot x}$. Let $\phi^x : U^x \rightarrow V$ be a diffeomorphism onto an open subset of \mathbb{R}^m with $\phi^x(x) = \mathbf{0}$ and $\phi^{g \cdot x} = \phi^x \circ \theta_{g^{-1}}$.

For any $[x] \in M/G$, choose a representative $x \in M$, and let $[U] = \pi(U^x)$. Since $U_g^x = U^{g \cdot x}$, this operation is well-defined, and $[U]$ is an open neighborhood of $[x]$ in M/G . Now map $[U]$ to $\phi^x(U^x)$. This map is again independent of the choice of representative, as

$$\phi^{g \cdot x}(U^{g \cdot x}) = \phi^x \circ \theta_{g^{-1}}(U^{g \cdot x}) = \phi^x(U^x)$$

for all $g \in G$. This map is a diffeomorphism because ϕ^x is a diffeomorphism. Therefore, $[U]$ appears locally to model an open subset of \mathbb{R}^m , and is therefore a boundaryless manifold of dimension m .

If $x \in M$, then U^x is diffeomorphic to $[U] = \pi(U^x)$ through the map $\pi|_{U^x}$. It follows that

$$d\pi_x = d(\pi|_{U^x})_x,$$

and $\pi|_{U^x}$ is a diffeomorphism, so $d(\pi|_{U^x})$ is surjective. The derivative $d\pi_x$ is surjective for all $x \in M$, and π is a submersion. \square

If $G = \mathbb{Z}_n$, then we have the following corollary.

Corollary 60. *$Z_n M$ is a boundaryless manifold, and \mathcal{H}/\mathbb{Z}_6 is a boundaryless submanifold of $Z_6 S^3$.*

While this corollary ensures that $Z_6(M)$ is indeed a manifold, the intuitive visualization of the space that we had for configuration spaces is lost. The case where $M = S^1$ is of particular interest, so a model for $Z_n S^1$ will be provided by examining the low-dimensional cases: $n = 1, 2, 3$. If $n = 1$, then $Z_1 S^1$ is trivially diffeomorphic to the circle.

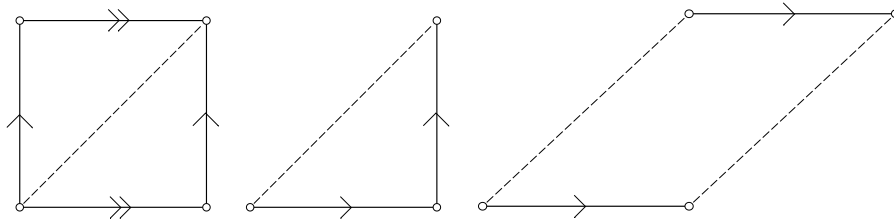


Figure 6.2.1: On the left is a representation of C_2S^1 as the square $[0, 1]^2$ with opposite edges identified, and the diagonal removed. The other two images are possible representations of Z_2S^1 as the Möbius strip.

If $n = 2$, then parametrize the circle as \mathbb{R}/\mathbb{Z} , so C_2S^1 may be parametrized by $(\mathbb{R}^2/\mathbb{Z}^2)\setminus X$, where $X = \{(n + x, m + x) : x \in \mathbb{R}, n, m \in \mathbb{Z}\}$. This is diffeomorphic to $[0, 1]^2 \setminus \Delta$, with opposite edges identified (and Δ is the main diagonal). When quotienting by \mathbb{Z}_2 , the point (x, y) is identified with (y, x) . The result is a Möbius strip (see Figure 6.2.1 on page 64).

If $n = 3$, then choose an arbitrary point s on S^1 to label as 0, and identify the circle with $[0, 1]$. Each point in Z_3S^1 may be identified as a point (x, y, z) in the partially open 3-simplex:

$$\Delta_3^p = \{(x, y, z) : 0 \leq x < y < z \leq 1\}.$$

This representation is unique unless $x = 0$ or $z = 1$, in which case $(0, x_2, x_3)$ is identified with $(x_2, x_3, 1)$. In other words, Z_3S^1 is isomorphic as a manifold to Δ_3^p / \sim , where $(x_1, x_2, x_3) \sim (y_1, y_2, y_3)$ if $x_1 = 0, y_3 = 1, x_2 = y_1$, and $x_3 = y_2$. This may be represented as a triangular prism, with the two triangular faces identified with a 120° twist. Or equivalently, as the interior of a filled torus, where the cross sections appear as triangles, and the torus has a 120° twist. This space may be embedded as an open subset of \mathbb{R}^3 .

In general Z_nS^1 has the appearance as a prism $\Delta_{n-1}^o \times [0, 1]$ where Δ_{n-1}^o is the interior of an $n - 1$ -simplex, and the two simplices $\Delta_{n-1}^o \times \{0\}$ and $\Delta_{n-1}^o \times \{1\}$ are identified by a cyclic permutation of coordinates.

That Z_2S^1 is the Möbius strip perhaps sparks some concern — it is not necessarily true that Z_nS^1 be orientable.

Theorem 61. *If G is a finite group acting freely through the map $\theta : G \times M \rightarrow M$ on a boundaryless orientable manifold M of dimension m , then M/G is orientable if and only if θ_g is an orientation-preserving diffeomorphism for all $g \in G$.*

$$\begin{array}{ccc}
M & \xrightarrow{\theta_g} & M \\
\pi \downarrow & & \pi \downarrow \\
M/G & \xlongequal{\quad} & M/G
\end{array}
\qquad
\begin{array}{ccc}
T_x M & \xrightarrow{d\theta_g} & T_{g \cdot x} M \\
d\pi \downarrow & & d\pi \downarrow \\
T_{[x]} M/G & \xlongequal{\quad} & T_{[x]} M/G
\end{array}$$

Figure 6.2.2: Inducing an orientation on the quotient manifold.

Proof. Impose an orientation on M . Figure 6.2.2 on page 65 shows two commutative diagrams. Assume that M/G is orientable, and let $[\beta]$ is a positively-oriented basis for the tangent space of M/G at an arbitrary point $[x]$. The map π preserves orientations, so for each $g \in G$ and $x_g \in M$ such that $\pi(x_g) = [x]$, there exists a positively-oriented basis β_g of $T_{x_g} M$ such that $d\pi_{x_g} \beta_g = [\beta]$. If there exists a $g' \in G$ such that $\theta_{g'}$ is orientation-reversing, then $\theta_{g'} \beta_g = -\beta_{g' \cdot g}$. However, by the commutativity of the diagram,

$$\text{sign}([\beta]) = \text{sign}(\beta_g) = -\text{sign}(\beta_{g \cdot g'}) = -\text{sign}([\beta]),$$

which is a contradiction of the orientability of M/G . Therefore, if M/G is orientable, all diffeomorphisms θ_g must be orientation-preserving. Conversely, if θ_g is orientation-preserving for all $g \in G$, then an orientation may be imposed upon M/G . Following the notation in Theorem 59, for each $x \in M$, there exists an open neighborhood U^x such that $U^{g \cdot x}$ is diffeomorphic to U^x . Furthermore, let $\phi^x : U_x \rightarrow V$ be an orientation-preserving diffeomorphism, with V an open subset of \mathbb{R}^m . Note that $\phi^{g \cdot x} U^{g \cdot x} = \phi^x U^x$.

For each $[x] \in M/G$, let x be an arbitrary choice of representative in M , and let $[U] = \pi(U^x)$. Then define $\bar{\phi} : [U] \rightarrow V$ as the composition $\phi_x \circ \pi^{-1}|_{U^x}$. The map $\bar{\phi}$ is independent of our choice of representative, as if x' is a different representative, then there exists $g \in G$ such that $g \cdot x' = x$, and $\phi^x \circ \pi^{-1}|_{U^x} = \phi^x \circ \theta_{g^{-1}} \circ \pi^{-1}|_{U^{x'}} = \phi^{g^{-1} \cdot x} \circ \pi^{-1}|_{U^{x'}} = \phi^{x'} \circ \pi^{-1}|_{U^{x'}}$. Let β_x be a positively-oriented basis of $T_x M$ such that $d\theta_g \beta_x = \beta_{g \cdot x}$ for each $g \in G$, which is possible because θ_g is always orientation-preserving. Then define the positively-oriented basis of $T_{[x]} M/G$ to be equal to $d\pi_x \beta_x$. This choice of basis is independent of our choice of representative for $[x]$, by the commutativity of the diagram and the fact that θ_g is orientation-preserving. This successfully imposes an orientation on M/G . \square

Corollary 62. *Given an orientable manifold $M \subset \mathbb{R}^k$ of dimension m , then the cyclic configuration space $Z_n M$ is orientable if and only if $m(n-1)$ is even. In particular,*

Z_6S^1 and Z_6S^3 are not orientable.

Proof. Let $\theta : \mathbb{Z}_n \times C_n M \rightarrow C_n M$ be the action of \mathbb{Z}_n upon $C_n M$, sending (i, x_1, \dots, x_n) to (x_i, \dots, x_{n+i}) , where subscripts work modulo n . For each $i \in \mathbb{Z}_n$,

$$\theta_i = (\theta_1)^i.$$

If θ_1 is orientation-preserving, then θ_i is orientation-preserving for all i . Conversely, if θ_1 is orientation-reversing, then θ_i is orientation-reversing only when i is odd. Thus, $Z_n M$ is orientable if and only if θ_1 preserves orientation.

The map $\theta_n = (\theta_1)^n$ is the identity map. If n is odd, then θ_1 cannot be orientation-reversing, as otherwise $\theta_n = \text{id}$ would be orientation-reversing as well. By Theorem 61, n odd implies that $Z_n(M)$ is orientable.

For every $x \in M$, the space $T_x M$ is an m -dimensional linear subspace of \mathbb{R}^k , and for all $\mathbf{x} = (x_1, \dots, x_n) \in C_n M$,

$$T_{\mathbf{x}} C_n M = \prod_{i=1}^n T_{x_i} M$$

Let $\mathbf{x}' = \theta_1 \mathbf{x}$. Because θ_1 is linear,

$$d(\theta_1)_{\mathbf{x}} : T_{\mathbf{x}} C_n M \rightarrow T_{\mathbf{x}'} C_n M \quad (y_1, \dots, y_n) \mapsto (y_2, \dots, y_n, y_1).$$

Let $A_i : T_{x_i} M \rightarrow \mathbb{R}^m \times \{0\}^{k-m}$ be a rotation matrix in $SO_k(\mathbb{R})$. Then A_i is an orientation preserving, linear diffeomorphism. The product maps $A = A_1 \times \dots \times A_n$, and $A' = A_2 \times \dots \times A_n \times A_1$ are also orientation-preserving diffeomorphisms. As a consequence, the diagram in Figure 6.2.3 on page 67 commutes, with $\tau = A' \circ d(\theta_1)_{\mathbf{x}} \circ A^{-1}$. The derivative $d(\theta_1)_{\mathbf{x}}$ preserves orientations if and only if τ does. By construction, $\tau(y_1, \dots, y_n) = (y_2, \dots, y_n, y_1)$, where $y_i \in \mathbb{R}^m \times \{0\}^{m-k}$. Thus, τ can be represented as the $mn \times mn$ matrix

$$\begin{bmatrix} \mathbf{0} & I_m & & \mathbf{0} \\ \vdots & & \ddots & \\ \mathbf{0} & \mathbf{0} & & I_m \\ I_m & \mathbf{0} & \cdots & \mathbf{0} \end{bmatrix},$$

which has determinant $(-1)^{m(n-1)}$. The linear map τ preserves orientation if and only if $m(n-1)$ is even, and $Z_n M$ is orientable if and only if $m(n-1)$ is even. In

other words, either M is even-dimensional or n is odd. For Z_6S^1 or Z_6S^3 , neither of these two conditions are satisfied. \square

This corollary is disastrous to the study of oriented intersection theory. Even with transversality established between Z_6K and \mathcal{H}/\mathbb{Z}_6 , we are unable to associate signs to the isolated intersection points, as the manifolds are not all orientable. The only thing we can hope to salvage is a parity invariant. If $f : S^1 \rightarrow S^3$ is a closed knot, then the parity of $Z_6f^{-1}(\mathcal{H}/\mathbb{Z}_6)$ will remain a knot invariant. But first transversality must be verified between Z_6f and \mathcal{H}/\mathbb{Z}_6 .

A point $[\mathbf{x}] \in Z_6S^3$ is *thelemic* if $\pi^{-1}[\mathbf{x}]$ contains a thelemic point (and thus it contains *only* thelemic points).

Theorem 63. *For a generic knot, $Z_6f \pitchfork \mathcal{H}/\mathbb{Z}_6$ in Z_6S^3 .*

Proof. Borrowing from the terminology of the previous chapter, recall our family of perturbations $G : S^1 \times (\frac{\varepsilon}{2}D^2)^n \rightarrow N_\varepsilon(K; S^3)$, for a given knot f . From Corollary 51, C_6G thelemic points are regular. By Theorem 59, there exists a smooth submersion $\sigma : C_6N_\varepsilon(K; S^3) \rightarrow Z_6N_\varepsilon(K; S^3)$. Since $C_6N_\varepsilon(K; S^3)$ is diffeomorphic to C_6K_ε , it follows that $Z_6N_\varepsilon(K; S^3)$ is diffeomorphic to Z_6K_ε — an open subset of Z_6S^3 . As a result, thelemic points are regular under the composition map $\sigma \circ C_6G$ as well. Therefore,

$$\sigma \circ C_6G \pitchfork \mathcal{H}/\mathbb{Z}_6.$$

By the Transversality Theorem, almost all choices of $\mathbf{v} \in (\frac{\varepsilon}{2}D^2)^n$ result in a map $\sigma \circ C_6G_{\mathbf{v}} = Z_6G_{\mathbf{v}}$ transverse to \mathcal{H}/\mathbb{Z}_6 . \square

So transversality is maintained between our submanifolds, and the intersection number modulo 2 of these submanifolds is a knot invariant. Let $(\mathcal{H}/\mathbb{Z}_6)_f = (\sigma \circ C_6f)^{-1}(\mathcal{H}/\mathbb{Z}_6)$. Notice that each thelemic point $[\mathbf{x}] \in Z_6K$ corresponds to exactly six

$$\begin{array}{ccc} T_{\mathbf{x}}C_nM & \xrightarrow{d(\theta_1)_{\mathbf{x}}} & T_{\mathbf{x}'}C_nM \\ A \downarrow & & A' \downarrow \\ (\mathbb{R}^m \times \{0\}^{k-m})^n & \xrightarrow{\tau} & (\mathbb{R}^m \times \{0\}^{k-m})^n \end{array}$$

Figure 6.2.3: A commutative diagram establishing orientations on configuration spaces.

unique thelemic points in $\sigma^{-1}[\mathbf{x}]$. In particular,

$$\mathcal{H}_f/\mathbb{Z}_6 = (\mathcal{H}/\mathbb{Z}_6)_f,$$

and

$$|(\mathcal{H}/\mathbb{Z}_6)_f| = |\mathcal{H}_f/\mathbb{Z}_6| = \frac{|\mathcal{H}_f|}{6}.$$

Formally, the parity invariant of $|(\mathcal{H}/\mathbb{Z}_6)_f|$ is denoted by $I_2(Z_6 f, \mathcal{H}/\mathbb{Z}_6)$. For brevity, this invariant will be represented by the map $v_T : \mathcal{K} \rightarrow \mathbb{Z}_2$.

Theorem 64. *v_T is a Vassiliev invariant modulo 2 of order three.*

Proof. The proof of this holds many similarities to Proposition 40. Define \mathcal{C} to be the subspace

$$\mathcal{C} = \{(x_1, x_2, x_3, x_4) \in C_4 S^3 : x_1, x_2, x_3, x_4 \text{ are cocircular}\}.$$

It is a 10-dimensional submanifold of $C_4 S^3$, as it is diffeomorphic to

$$C_3 S^3 \times ((-\infty, 0) \cup (0, 1) \cup (1, \infty))$$

through the map that sends (x_1, x_2, x_3, x_4) to $((x_1, x_2, x_3); y)$, where

$$y = \begin{cases} -\frac{|x_2-x_4|}{|x_1-x_4|} & \text{if } x_4 \text{ lies between } x_1 \text{ and } x_2 \text{ on the common circle} \\ \frac{|x_2-x_4|}{|x_2-x_3|} & \text{if } x_4 \text{ lies between } x_2 \text{ and } x_3 \text{ on the common circle} \\ \frac{|x_1-x_3|}{|x_1-x_4|} & \text{if } x_4 \text{ lies between } x_3 \text{ and } x_1 \text{ on the common circle} \end{cases}.$$

Let f be a generic knot, and c_1, c_2, c_3, c_4 be a collection of four distinct crossings, with domains D_1, D_2, D_3, D_4 respectively. Define

$$D = \prod_{i=1}^4 D_i \quad c = \prod_{i=1}^4 c_i : D \rightarrow S^3$$

A generic choice of four points in the interiors of D_1, D_2, D_3, D_4 are such that their images under c_1, c_2, c_3, c_4 are not cocircular. Since \mathcal{C} is closed, it follows that we may 'thicken' these points in a sufficiently small manner to obtain four compact 3-balls V_1, V_2, V_3, V_4 each contained within the interiors of D_1, D_2, D_3, D_4 , and no four points y_1, y_2, y_3, y_4 in V_1, V_2, V_3, V_4 (respectively) are cocircular. Let V be the (disjoint) union

of V_1, V_2, V_3 and V_4 , and $b : D \times \mathbb{I} \rightarrow D$ be a smooth isotopy such that b_0 is the identity, and $b_1(D_i) = V_i$. Then the diagram

$$\begin{array}{ccc} D \times \mathbb{I} & \xrightarrow{b} & D \\ c \times \text{id} \downarrow & & \downarrow c \\ c(D) \times \mathbb{I} & \xrightarrow{b^*} & c(D) \subset S^3 \end{array}$$

commutes, where the bottom horizontal map b^* is determined by the diffeomorphism between D and $c(D)$. Because b_t is an embedding for all $t \in \mathbb{I}$, it follows that b_t^* is also an embedding, and b^* is an isotopy of $c(D)$. The Isotopy Extension Theorem provides an ambient isotopy $B^* : S^3 \times \mathbb{I} \rightarrow S^3$, with B_0^* the identity, and

$$B_1^*(c(D)) = c(V).$$

Since B^* is an ambient isotopy, the two curves $\alpha_{\pm, i}$ in D_i (defined in (3.0.1)) are sent to two curves in V_i . Each V_i is diffeomorphic to the compact 3-ball D^3 , and an ambient isotopy of V_i can be arranged to manipulate the strands $B_1^*(c_i(\alpha_{\pm, i}))$ so that they lie in the appropriate position to apply a crossing change (i.e. they are sent to a position in V_i so that the diffeomorphism sending V_i to D^3 maps the curves to $\alpha_{\pm} \subset D^3$). Now the crossing changes may be applied to V rather than D .

The choice of the four original points was generic. Thus, we may assume that a generic choice of four distinct crossing changes c_1, c_2, c_3, c_4 with domains D_1, D_2, D_3, D_4 are such that no quadruple in $c_1(D_1) \times c_2(D_2) \times c_3(D_3) \times c_4(D_4)$ contains cocircular coordinates.

With such crossings in mind, consider the Vassiliev sum

$$\sum_{\sigma \subset \{1, 2, 3, 4\}} v_T(K^\sigma),$$

where $v_T(K^\sigma)$ returns the parity of the thelemic circle count for the knot K^σ . Given any σ , let C be a thelemic circle of K^σ . The space $\prod_{i=1}^4 c_i(D_i)$ contains no cocircular quadruples, so it follows that C cannot puncture all four $c_i(D_i)$. Assume, without loss to generality, that C is disjoint from $c_4(D_4)$. Applying a crossing change at c_4 results in the knot $K^{\sigma \ominus \{4\}}$, where C remains a thelemic circle with the same sign. For every thelemic circle of K^σ , there exists an $i \in \{1, 2, 3, 4\}$ such that C is a thelemic circle of $K^{\sigma \ominus \{i\}}$. However, $|\sigma| - |\sigma \ominus \{i\}| = \pm 1$. Thus, the two thelemic circles 'cancel'

each other in the Vassiliev sum. The choices of the knot K and four crossings were generic, so the sum

$$\sum_{\sigma \subset \{1,2,3,4\}} (-1)^{|\sigma|} v(K^\sigma)$$

is zero. Thus, v_T , the parity of the thelemic circle count is a Vassiliev invariant of order two. \square

From the above theorem, and Theorem 27,

$$v_T(K) = |(\mathcal{H}/\mathbb{Z}_6)_K| \equiv av_3(K) + bv_2(K) + cv_0(K) \quad (\text{modulo } 2)$$

for some integers a, b, c . However, the generic unknot has no thelemic circles. Since $v_3(\bigcirc) = v_2(\bigcirc) = 0$, it follows that $c = 0$. We once again turn to computers to evaluate the number of thelemic points on a knot and determine the values of a and b .

On the 3_1 trefoil knot, there are no thelemic points, so by using the actuality table in Appendix A,

$$\begin{aligned} |(\mathcal{H}/\mathbb{Z}_6)_{3_1}| &\equiv av_3(3_1) + bv_2(3_1) \\ 0 &\equiv -a + b \\ 0 &\equiv a + b \end{aligned}$$

On the 4_1 figure-eight knot, there are two thelemic circles, so again, $|(\mathcal{H}/\mathbb{Z}_6)_{4_1}|$ is congruent to 0 modulo 2, and

$$\begin{aligned} |(\mathcal{H}/\mathbb{Z}_6)_{4_1}| &\equiv av_3(4_1) + bv_2(4_1) \\ 0 &\equiv 0 - b \\ 0 &\equiv b \end{aligned}$$

Since $b \equiv 0$, it follows that a and b are both identically zero. We arrive at the conclusion of our study of thelemic circles.

Theorem 65. *If K is generic, then $|(\mathcal{H}/\mathbb{Z}_6)_K| \equiv 0$ modulo two. The number of thelemic circles of a generic knot is always even.*

Unfortunately, a nontrivial Vassiliev invariant cannot be found through thelemic circles; however, the triviality of the invariant does establish a nice result that is

common to all knots. In fact, this result is in some sense nicer than the possibility of $|(\mathcal{H}/\mathbb{Z}_6)_K|$ being a nontrivial invariant. Modulo two invariants are generally not particularly useful in distinguishing knots — 'half' of all knots will share the same invariant value. Once Z_6S^1 was shown to be nonorientable in Corollary 62, the hope of establishing thelemic circles as a useful invariant was lost. The remaining possibilities allowed for $|(\mathcal{H}/\mathbb{Z}_6)_K|$ to be an impractical, nontrivial modulo two invariant, or a trivial invariant that establishes a geometrically appealing property that is common to all knots.

Chapter 7

Conclusion

The study of cocircularities on knots has led to the establishment of two types of knot invariants. The collection of five-point cocircularities of the satanic variety has strong and surprising connections to the second-order Vassiliev invariant. While many properties of this invariant are well-understood, a geometric interpretation was unknown until the authors of [BCSS] provided one in terms of quadriseccants on long knots. However, their extension of this result to closed knots is in some ways unnatural. Here, a simpler proof of the quadriseccant result for long knots is given, as well as a more appealing extension of this result to closed knots. This result is intuitively clear from the corresponding information regarding alternating quadriseccants of long knots (given in Chapter 4, and [BCSS]). While the work in [BCSS] forms the foundation of the efforts in this thesis, the approach and methods of proof are significantly different. As a result, we obtain a new perspective and a more detailed analysis of the behavior of these satanic circles.

This analysis easily extended to the examination of six-point cocircularities of knots. The methodology of proof in the five-point and quadriseccant case illuminated that the thelemic circles were exactly the type worth studying. After establishing the preliminary transversality results, it becomes apparent that cyclic permutations of thelemic points result in other thelemic points. Unfortunately, this cyclic permutation map is orientation-reversing (Corollary 62), which resulted in the loss of a signed thelemic circle count. While five-point cocircularities have the same cyclic permutation issues (a cyclic permutation of a satanic point is still satanic), in this case the map remains orientation-preserving, so orientability is maintained. Regardless, a non-oriented intersection number between the space of thelemic points and the configuration space of six points on the knot was still available for study. Here, a

computer algorithm can be used to easily detect the occurrences of thelemic points, and this data was used to show that the number of thelemic circles is always even on a sufficiently generic knot.

Moving onward to seven-point cocircularities is fruitless. The space of seven-point cocircularities in C_7S^3 is 13-dimensional, while the configuration space C_7K is 7-dimensional. Therefore, transversality between these two spaces in C_7S^3 results in an empty intersection — there are no seven-point (or more) cocircularities of generic knots. On the other side of the spectrum, four-point cocircularities are able to successfully be examined on a knot, but not without additional complications. Given transversality between the space of four-point cocircularities and C_4K within the ambient space of C_4S^3 , their intersection is a dimension 2 submanifold. However, there is no way to arrange four points (x_1, \dots, x_4) on a circle so that consecutive subscripts are not adjacent on the circle (a critical property of satanic and thelemic circles). Because of this, two consecutive points x_i and x_{i+1} can be arbitrarily close together on the knot, and may ultimately 'collide' in the limit to form a degenerate three-point cocircularity. This issue may be addressed by compactifying the configuration spaces C_4S^1 and C_4S^3 . The method of compactification is called the Fulton-MacPherson compactification, and a detailed description of this space can be found in [Si].

The approach presented in this paper can also be applied to many other geometric objects, rather than circles. For instance, consider the subspace of C_3S^3 consisting of points (x_1, x_2, x_3) that form the vertices of an equilateral triangle. This is a codimension 3 condition placed upon C_3S^3 . The configuration space of three points on a knot C_3K is of dimension three, so if transversality between these two spaces can be demonstrated, then we arrive at an invariant representing the number of equilateral triangles that appear on a given knot. Various geometric objects can be studied in a similar light, although the author has not extensively studied any objects other than cocircularities. This presents numerous open questions that are tractable and readily solvable.






Although the invariance of satanic and thelemic points have been presented, the study of these objects is not exhausted. The signed alternating quadriseccant count corresponds to the second Vassiliev invariant. A result by Denne ([D]) states that *every* nontrivial knot has an alternating quadriseccant — even those that take on a value of 0 by v_2 . A similar question can be asked of thelemic circles: does every nontrivial knot have a pair of thelemic circles? The answer is in the negative, as the trefoil does not always have thelemic circles. Additionally, the 5_1 knot does not

necessarily hold any thelemic circles. However, the number of thelemic circles seems to explode as the complexity of the knot increases. Is there a tangible criteria under which all knots have thelemic circles? If so, it is unlikely that such a criteria has much to do with the Vassiliev invariants, as the 5_1 knot is such that $v_2(5_1) = -5$ and $v_3(5_1) = 3$, which are large values when compared to other knots of similar complexity. Denne's argument for the existence of alternating quadrisecants invokes extensive surgery on knots, and it is conjectured that such techniques will be required to find a corresponding statement for thelemic circles. These questions provide numerous pathways to further study the geometric properties of knots. Knots are primarily geometric creatures, and the strengthening of the bond between knots and geometry provides insight to better comprehend the subtleties of knots.

Appendix A

Vassiliev Tables

The first few Vassiliev invariants are reasonably well understood, and their values have been explicitly computed for knots of low complexity. Here we present a table of some simple knots and list the values of v_2 and v_3 .

Knot Name [Ro]	Illustration	v_2 [CDM]	v_3 [CDM]
$0_1 = \bigcirc$ (unknot)		0	0
3_1 (trefoil)		1	-1
4_1 (figure-eight)		-1	0
5_1		3	-5
5_2		2	-3

Appendix B

Satanic Circle Code

In this appendix, a description of the algorithm utilized to detect satanic points is provided. Since the satanic points of a knot form a 1-dimensional submanifold of C_5S^3 , the code will find all satanic points that intersect a specific point on the knot. That is, a choice of $t_1 \in S^1$ will be fixed, and the program will locate the (finite number of) satanic points $\mathbf{x} = (x_1, \dots, x_5)$ of the knot such that $f^{-1}(x_1) = t_1$. Let ε be the injective radius of the tubular neighborhood of the knot $K = \text{im}f$. By Lemma 47, if \mathbf{x} is a satanic point on K , then $|x_i - x_j| \geq \varepsilon$, for all distinct $i, j \in \{1, 2, 3, 4, 5\}$. The domain of f is compact, so there exists a bound on $|df_x|$, which we will denote as F . If \mathbf{t} is the preimage of a satanic point, then $|t_i - t_j| \geq \varepsilon/F^5$ (where S^1 is considered as the interval $[0, 2\pi]$, with endpoints identified).

In practice it is often easier to consider knots as embeddings of a circle into \mathbb{R}^3 rather than S^3 , and such an approach will be taken here. By compactifying \mathbb{R}^3 , we obtain S^3 , and our knot in \mathbb{R}^3 becomes an embedding of S^1 into S^3 . Circles in S^3 , when projected stereographically into \mathbb{R}^3 become generalized circles in \mathbb{R}^3 — either a genuine circle or a line intersecting the point-at-infinity. The set of points in S^3 that form a coordinate of a satanic point in C_5S^3 determine a 1-parameter family of S^3 , while the set of points of S^3 that lie upon a satanic circle of the knot formulate a 2-parameter family of S^3 . Thus, almost every point in S^3 misses this family of satanic circles of a knot, and projecting down to \mathbb{R}^3 at such a point implies that all satanic circles of a knot embedded in \mathbb{R}^3 are genuine circles. In fact, a small neighborhood may be chosen about this projecting point in S^3 , so that no satanic circles intersect any point in this neighborhood. As a result, we may also ensure that the satanic circles do not have an excessively large radius, i.e. circles that are 'almost lines'.

In summation, our setup will be as follows: let $f : S^1 \rightarrow \mathbb{R}^3$ be an embedding,

with $|df|$ bounded above and below by values F_{\pm} (where F_- is the lower bound, and F_+ is the upper bound), and the image of f contained within a compact ball B of radius 1. A point $\mathbf{x} = (x_1, \dots, x_5) \in C_5\mathbb{R}^3$ is satanic if and only if the coordinates are cocircular or collinear, with no two adjacent points on the knot being adjacent on the common generalized circle. As with knots in S^3 , there exists some $\varepsilon > 0$ such that if \mathbf{x} is satanic with preimage $\mathbf{t} \in C_5S^1$, then $|x_i - x_j| \geq \varepsilon$, and $|t_i - t_j| \geq \varepsilon/F^5$ for all distinct $i, j \in \{1, 2, 3, 4, 5\}$. Fix a choice of $t_1 \in S^1$, and let $x_1 = f(t_1)$. We will attempt to compute all satanic points with first coordinate x_1 by applying Newton's method to a particular function that has its zeroes exactly at the satanic points of a knot.

Let

$$X = \{(x_2, x_3, x_4, x_5) \in B^4 : |x_i - x_j| \geq \varepsilon, \text{ for all distinct } i, j \in \{1, 2, 3, 4, 5\}\}$$

$$X_- = \{(x_2, x_3) \in B^2 : |x_i - x_j| \geq \varepsilon, \text{ for all distinct } i, j \in \{1, 2, 3\}\}$$

and define the intermediary functions $\ell, \alpha, \beta, \gamma : X_- \rightarrow \mathbb{R}$ by:

$$\begin{aligned} \ell(x_2, x_3) &= |(x_1 - x_2) \times (x_2 - x_3)| \\ \alpha(x_2, x_3) &= \frac{|x_2 - x_3|^2(x_1 - x_2) \cdot (x_1 - x_3)}{2 \cdot \ell(x_2, x_3)^2}, \\ \beta(x_2, x_3) &= \frac{|x_3 - x_1|^2(x_2 - x_3) \cdot (x_2 - x_1)}{2 \cdot \ell(x_2, x_3)^2}, \\ \gamma(x_2, x_3) &= \frac{|x_1 - x_2|^2(x_3 - x_1) \cdot (x_3 - x_2)}{2 \cdot \ell(x_2, x_3)^2}. \end{aligned}$$

The function ℓ detects when the points x_1, x_2, x_3 are close to collinearity. If $\ell(x_2, x_3)$ is small, then x_1, x_2, x_3 are nearly collinear. They cannot be close in distance, as $(x_2, x_3) \in X_-$. Thus, α, β and γ are not quite well-defined. If x_1, x_2, x_3 are collinear, then these functions take the value ∞ . We will address this issue later, for now assume that x_1, x_2, x_3 are not collinear. The points x_1, x_2, x_3 determine a unique circle with circumcenter

$$c : X_- \rightarrow \mathbb{R}^3 \quad c(x_2, x_3) = \alpha(x_2, x_3) \cdot x_1 + \beta(x_2, x_3) \cdot x_2 + \gamma(x_2, x_3) \cdot x_3$$

and circumradius

$$r : X_- \rightarrow (0, \infty) \quad r(x_2, x_3) = \frac{|x_1 - x_2||x_2 - x_3||x_3 - x_1|}{2 \cdot \ell(x_2, x_3)},$$

along with a unit normal vector determined by

$$\hat{v} : X_- \rightarrow \mathbb{R}^3 \quad \hat{v}(x_2, x_3) = \frac{(x_1 - x_2) \times (x_2 - x_3)}{\ell(x_2, x_3)}.$$

Let

$$T = \{(t_2, t_3, t_4, t_5) \in C_4S^1 : |t_i - t_j| \geq \varepsilon/F^5, \text{ for all distinct } i, j \in \{1, 2, 3, 4, 5\}\}$$

. The function Newton's method is applied to is $\omega : T \rightarrow \mathbb{R}^4$,

$$\omega(t_2, t_3, t_4, t_5) = \begin{bmatrix} \omega^{(1)}(t_2, t_3, t_4, t_5) \\ \omega^{(2)}(t_2, t_3, t_4, t_5) \\ \omega^{(3)}(t_2, t_3, t_4, t_5) \\ \omega^{(4)}(t_2, t_3, t_4, t_5) \end{bmatrix} = \begin{bmatrix} (f(t_4) - c(\mathbf{x}_-)) \cdot \hat{v}(\mathbf{x}_-) \\ (f(t_5) - c(\mathbf{x}_-)) \cdot \hat{v}(\mathbf{x}_-) \\ (f(t_4) - c(\mathbf{x}_-))^2 - r(\mathbf{x}_-)^2 \\ (f(t_5) - c(\mathbf{x}_-))^2 - r(\mathbf{x}_-)^2 \end{bmatrix},$$

where $\mathbf{t}_- = (t_2, t_3)$, and $\mathbf{x}_- = (x_2, x_3) = C_2f(\mathbf{t}_-)$. Then $\omega(t_2, t_3, t_4, t_5) = \mathbf{0}$ if and only if $f(t_4)$ and $f(t_5)$ lie on the genuine circle determined by x_1, x_2 and x_3 (the point (t_1, \dots, t_5) is not necessarily the preimage of a satanic point, but it is the preimage of a five-point cocircularity of the knot).

As mentioned, $\ell(x_2, x_3)$ approaches 0 as x_1, x_2, x_3 approach collinearity. For the purposes of our program, we will arbitrarily choose a very small value e . If, at any point during the running of Newton's method, two points x_2, x_3 are encountered with $\ell(x_2, x_3) < e$, then the points x_1, x_2, x_3 become nearly collinear, and any possible cocircularities have an excessively large radius. In this case, the program will output an error, and the entire knot must be discarded, or a smaller value of e must be chosen. Otherwise, the points x_1, x_2, x_3 will never approach collinearity in the course of Newton's method, which means that all satanic circles are genuine circles with a radius that is not too large. Since three generic points are not collinear, $\ell(x_2, x_3) < e$ is an anomaly for small values of e , and will generally not occur.

Once this minimum is established, positive lower and upper bounds may be computed for the derivatives of $\ell, \alpha, \beta, \gamma, r$, that depend solely on e and ε , as $X_- \subset B^2$ is compact. Such bounds will be computed for ℓ , and the other bounds follow suit.

The derivative of $(x_1 - x_2) \times (x_2 - x_3)$ with respect to (x_2, x_3) can be represented by the block matrix

$$\begin{bmatrix} M & N \end{bmatrix} \quad (\text{B.0.1})$$

with 3×3 blocks:

$$M = \begin{bmatrix} 0 & (x_{23} - x_{33}) & -(x_{22} - x_{32}) \\ -(x_{23} - x_{33}) & 0 & (x_{21} - x_{31}) \\ (x_{22} - x_{32}) & -(x_{21} - x_{31}) & 0 \end{bmatrix}$$

and

$$N = \begin{bmatrix} 0 & -(x_{13} - x_{23}) & (x_{12} - x_{22}) \\ (x_{13} - x_{23}) & 0 & -(x_{11} - x_{21}) \\ -(x_{12} - x_{22}) & (x_{11} - x_{21}) & 0 \end{bmatrix},$$

where $x_i = (x_{i1}, x_{i2}, x_{i3})$, for each $i \in \{1, 2, 3\}$. Thus, the derivative of $\ell(x_2, x_3)$ with respect to (x_2, x_3) is

$$\frac{(x_1 - x_2) \times (x_2 - x_3)}{|(x_1 - x_2) \times (x_2 - x_3)|} \cdot d((x_1 - x_2) \times (x_2 - x_3)).$$

Since the knot is entirely contained within a compact ball of radius 1, it follows that $2 \geq |x_{ij} - x_{i'j}|$ for each $i, i', j \in \{1, 2, 3\}$ with i, i' distinct. The value of each coordinate in $\frac{(x_1 - x_2) \times (x_2 - x_3)}{|(x_1 - x_2) \times (x_2 - x_3)|}$ cannot exceed 1, so a quick check can verify that

$$\frac{\left| \begin{bmatrix} 4 & 4 & 4 & 4 & 4 & 4 \end{bmatrix} \right|}{e} \leq \frac{10}{e} = L_+$$

is a suitable upper bound for the derivative of ℓ . On the other hand, one of the coordinates in the vector $\frac{(x_1 - x_2) \times (x_2 - x_3)}{|(x_1 - x_2) \times (x_2 - x_3)|}$ must exceed $\frac{1}{4}$. Assume, without loss to generality, that it is the first. Furthermore, assume the first row of the matrix (B.0.1) contains elements all between $\pm \varepsilon e / 4$. Then since, $|x_i - x_{i'}| \geq \varepsilon$, it follows that $|x_{21} - x_{31}|$ and $|x_{11} - x_{21}|$ are each greater than $\varepsilon / 4$ and less than ε . However, this also implies that x_1, x_2, x_3 are close to being collinear. Computing $(x_1 - x_2) \times (x_2 - x_3)$,

$$\left\| \begin{bmatrix} (x_{12} - x_{22}) & (x_{13} - x_{23}) \\ (x_{22} - x_{32}) & (x_{23} - x_{33}) \end{bmatrix} \right\| \leq \frac{e\varepsilon}{2}$$

$$\left| \begin{bmatrix} (x_{11} - x_{21}) & (x_{13} - x_{23}) \\ (x_{21} - x_{31}) & (x_{23} - x_{33}) \end{bmatrix} \right| \leq \frac{\varepsilon^2 e}{2}$$

$$\left| \begin{bmatrix} (x_{11} - x_{21}) & (x_{12} - x_{22}) \\ (x_{21} - x_{31}) & (x_{22} - x_{32}) \end{bmatrix} \right| \leq \frac{\varepsilon^2 e}{2},$$

and so $|(x_1 - x_2) \times (x_2 - x_3)| = \ell(x_2, x_3) \leq e\sqrt{\varepsilon^2 + 2\varepsilon^4}/4 < e$. This is a contradiction of our assumption that x_1, x_2, x_3 are such that $\ell(x_2, x_3) \geq e$. Therefore, it follows that one of the elements in the first row of (B.0.1) must have an absolute value greater than $\varepsilon e/4$. Therefore, a lower bound for the derivative of ℓ is

$$L_- = \frac{1}{4} \cdot \frac{\varepsilon e}{4} = \frac{\varepsilon e}{16}.$$

Let $A_{\pm}, B_{\pm}, G_{\pm}, R_{\pm}$ denote upper and lower bounds for $|d\alpha|, |d\beta|, |d\gamma|, |dr|$ respectively. From here, a positive upper and lower bound for each $|d\omega^{(i)}|$ may be computed, and will be denoted by $\Omega_{\pm}^{(i)}$, while the positive lower and upper bounds on $|\det d\omega|$ will be denoted by Ω_{\pm} . If $\mathbf{t}_1, \mathbf{t}_2 \in T$, then

$$(\Omega_+ - \Omega_-)|\mathbf{t}_1 - \mathbf{t}_2| \leq |d\omega_{\mathbf{t}_2} - d\omega_{\mathbf{t}_1}| \leq (\Omega_- + \Omega_+)|\mathbf{t}_1 - \mathbf{t}_2|.$$

Additionally,

$$\frac{1}{\Omega_+} \leq |(d\omega_{\mathbf{t}})^{-1}| \leq \frac{1}{\Omega_-}.$$

Now consider the value

$$\Omega^* = \frac{1}{2(\Omega_- + \Omega_+)(\Omega_-)^2},$$

and let $\mathbf{t} = (t_2, \dots, t_5) \in C_4 S^1$. If

$$|\omega(\mathbf{t})| \leq \Omega^*$$

then

$$|\omega(\mathbf{t})| |d\omega_{\mathbf{t}}^{-1}|^2 (\Omega_- + \Omega_+) \leq (\Omega^*) \left(\frac{1}{\Omega_-}\right)^2 (\Omega_- + \Omega_+) \leq \frac{1}{2}.$$

By Kantorovich's Theorem, there exists a unique root of ω within

$$|d\omega_{\mathbf{t}}^{-1}| |\omega(\mathbf{t})| \geq \frac{|\omega(\mathbf{t})|}{\Omega_+}$$

of \mathbf{t} , and Newton's method, when applied to ω at \mathbf{t} converges to it.

Otherwise, if

$$|\omega(\mathbf{t})| > \Omega^*$$

then since the 'speed' of ω is bounded above by Ω_+ , a root of ω cannot lie too close to \mathbf{t} . In particular, a solution cannot lie within distance

$$\frac{|\omega(\mathbf{t})|}{\Omega_+} > \frac{\Omega^*}{\Omega_+}$$

of \mathbf{t} .

Now choose a very small positive real $u > 0$ such that

$$u < \frac{\Omega^*}{\Omega_+},$$

and a collection of points $\mathbf{t}_1, \dots, \mathbf{t}_n$ in T such that each point is within distance u of some other point — that is, the balls of radius u about each \mathbf{t}_i together cover T . If $|\omega(\mathbf{t}_i)| \geq \Omega_+ u$ for each \mathbf{t}_i , then applying Newton's method to each \mathbf{t}_i results in two possible scenarios. First, if

$$|\omega(\mathbf{t}_i)| > \Omega^*,$$

then there are no solutions to ω within $u < \Omega^*/\Omega_+$ of \mathbf{t}_i . Alternatively, if

$$\Omega_+ u \leq |\omega(\mathbf{t}_i)| \leq \Omega^*,$$

then there exists a unique root of ω within

$$|d\omega_{\mathbf{t}}^{-1}| |\omega(\mathbf{t}_i)| \geq u$$

of \mathbf{t}_i . Therefore, running Newton's method on each \mathbf{t}_i will guarantee that we find all the solutions to $\omega(\mathbf{t}) = \mathbf{0}$. This assures that the program will either return an error or successfully find all five-point cocircularities intersecting t_1 .

Below is a description of the algorithm in pseudocode.

Once this output is generated, it is a simple matter to check each five-point cocircularity to determine if it is indeed satanic, or if it should be discarded. If the program is terminated, then no output is given, and either a change in e , u or the parametrization of the knot can potentially resolve the issue.

Algorithm 1 Detecting Satanic Points

- Input: $u, e, \varepsilon, f, F_{\pm}$
 - f is a smooth embedding of S^1 into \mathbb{R}^3 , parameterized by the interval $[0, 2\pi]$.
 - F_{\pm} are the upper and lower bounds for $|df|$.
 - ε is a positive real smaller than the injective radius of the tubular neighborhood of f .
 - e is a positive real; the minimum tolerance for $(x_1 - x_2) \times (x_2 - x_3)$ before quitting the program.
 - u is an arbitrary positive real.
 - Output: A list of preimages of five-point cocircularities that intersect $f(0)$.
-

- Partition $[0, 2\pi]$ evenly into n segments, where $2\pi/n < u$, letting $t_i = 2\pi i/n$.
 - Let $t_1 = 0$, and $x_1 = f(0)$.
 - FOR each $\{i_2, i_3, i_4, i_5\}$ such that $1 \leq i_2 < i_3 < i_4 < i_5 \leq n$:
 - Let $\mathbf{t} = (t_{i_2}, t_{i_3}, t_{i_4}, t_{i_5})$, $j = 0$, $\mathbf{x} = (x_2, x_3, x_4, x_5) = C_4 f(\mathbf{t})$, and $stoploop = false$.
 - If $|\omega(\mathbf{t})| > \Omega^*$: Let $stoploop = true$.
 - If $|\omega(\mathbf{t})| \leq \Omega_+ u$: TERMINATE PROGRAM
 - WHILE $j \leq 1000$ AND $stoploop = false$:
 - * If $|(x_1 - x_2) \times (x_2 - x_3)| < e$: TERMINATE PROGRAM.
 - * If $|\omega(\mathbf{t})| > \Omega^*$: Let $stoploop = true$.
 - * Let $\mathbf{h} = -d\omega_{\mathbf{t}}^{-1}(f(\mathbf{t}))$, and $\mathbf{t} = \mathbf{h} + \mathbf{t}$.
 - * Let $j = j + 1$.
 - If $stoploop = false$, OUTPUT \mathbf{t} .
-

Appendix C

Satanic Circle Gallery

Three examples of satanic points and circles are shown here in larger, more detailed images. The knots 4_1 , 5_1 , and 8_{14} are depicted, along with the collection of all satanic circles that intersect the arbitrarily chosen black dot on the knot. The knot names are derived from [Ro]. As indicated in Chapter 6, the preimages of the satanic points form a 1-manifold in C_5S^1 . Beneath each knot, a projection of this 1-manifold onto C_3S^1 is shown, where the space C_3S^1 is diffeomorphic to the filled torus, $S^1 \times (0, 1)^2$. The second-order Vassiliev invariant agrees with the number of times this curve winds around the circle. The image of the projected curve is comprised of a series of approximately 1000 points. As a result, there are 'gaps' in some of the curves. In actuality, these gaps in the curve do not appear, and the strand is a smooth curve in the filled torus.

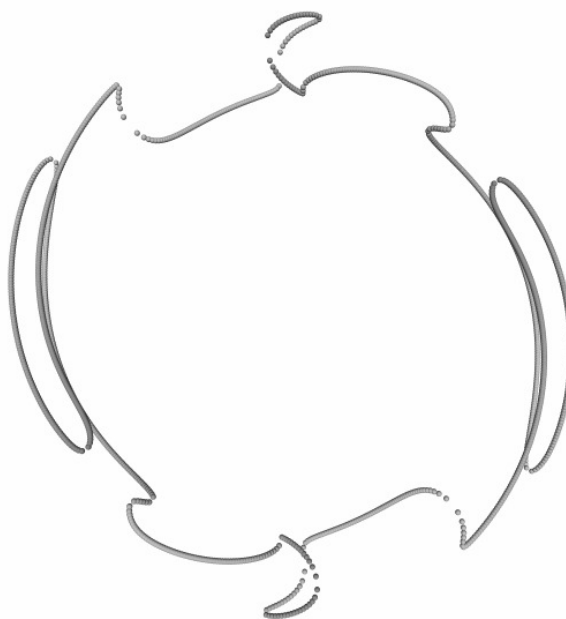
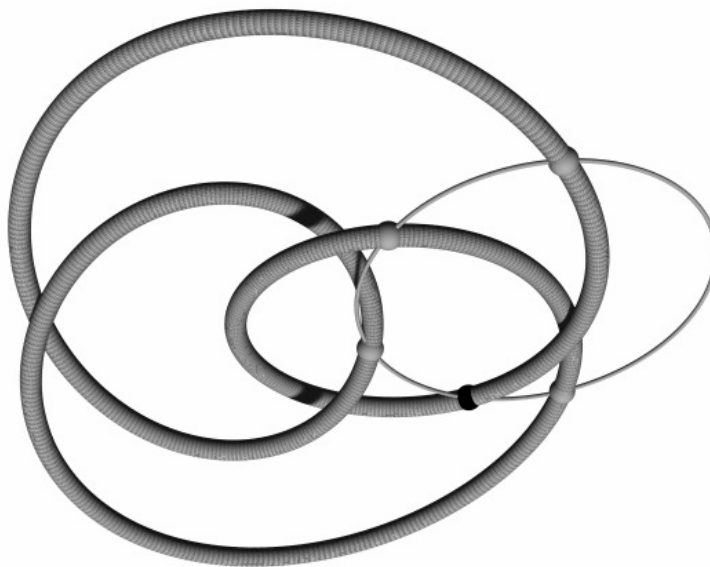


Figure C.0.1: The 4_1 (figure-eight) knot. $v_2(4_1) = -1$.

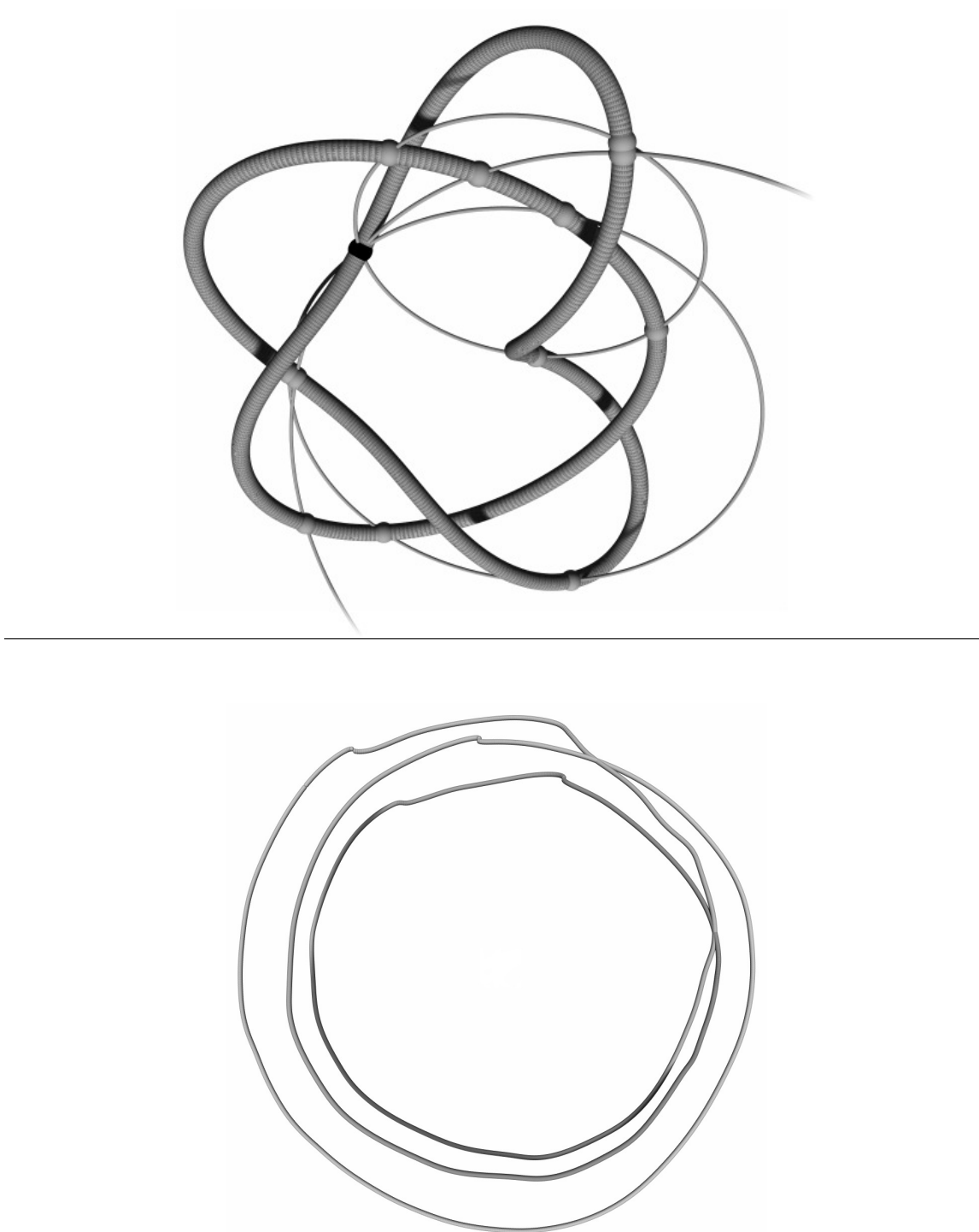


Figure C.0.2: The 5_1 knot. $v_2(5_1) = 3$.

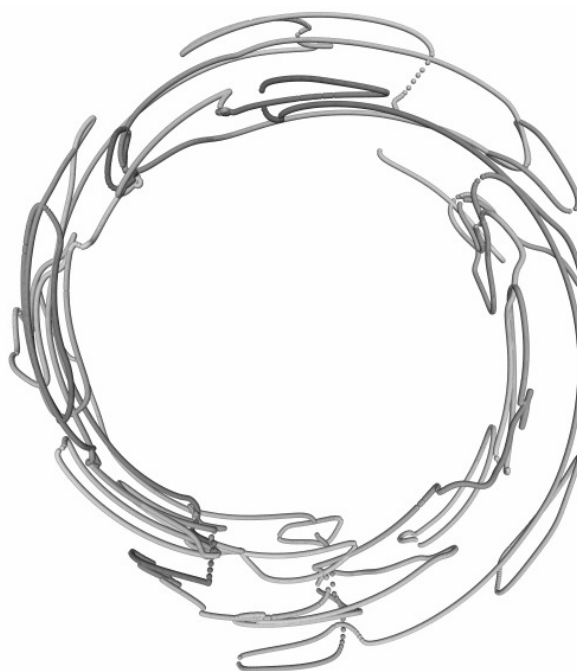
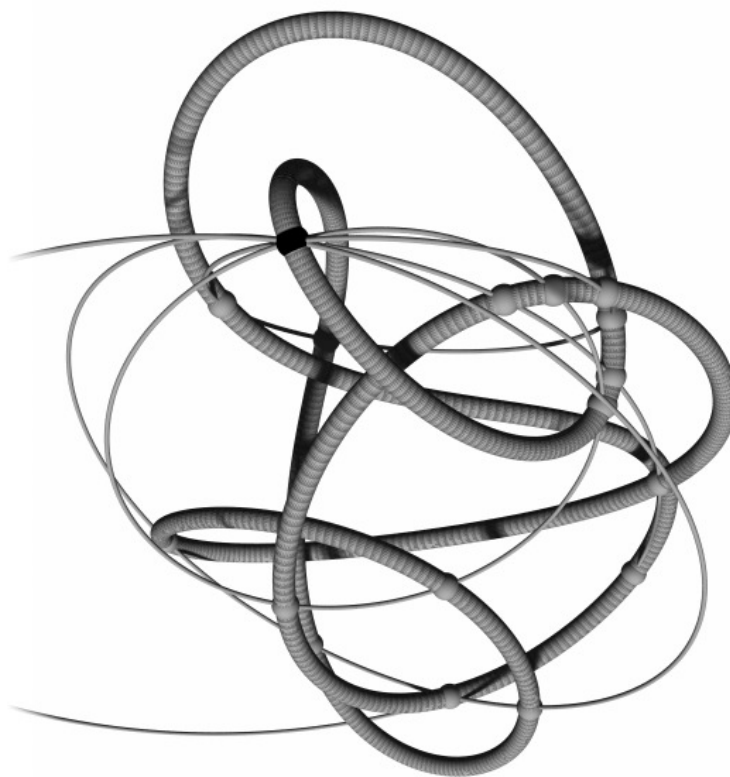


Figure C.0.3: The 8_{14} knot. $v_2(8_{14}) = 0$

Appendix D

Thelemic Circle Code

Detecting thelemic circles is largely done in the same manner as detecting satanic circles of a knot. In the satanic case, the code was only able to detect satanic circles that intersected a particular $t_1 \in S^1$. Here, the thelemic circles determine a 0-manifold in $C_6\mathbb{R}^3$, and we are able to detect all thelemic circles at once. Much of the setup from Appendix B is retained. Let f be a knot embedded in \mathbb{R}^3 contained within a compact ball B of radius 1, such that if $\mathbf{t} \in C_6S^1$ is the preimage of a thelemic point \mathbf{x} of the knot, then $|t_i - t_j| \geq \varepsilon/F^6$, where i, j are distinct elements of $\{1, 2, 3, 4, 5, 6\}$, and F is the upper bound on $|df|$.

Let

$$X = \{\mathbf{x} \in B^6 : |x_i - x_j| \geq \varepsilon, i, j \in \{1, \dots, 6\} \text{ distinct}\}$$

$$X_- = \{(x_1, x_2, x_3) \in B^3 : |x_i - x_j| \geq \varepsilon, i, j \in \{1, 2, 3\} \text{ distinct}\}$$

be subspaces of B^6 and B^3 , and define $\ell, \alpha, \beta, \gamma : X_- \rightarrow \mathbb{R}$ by

$$\begin{aligned} \ell(x_1, x_2, x_3) &= |(x_1 - x_2) \times (x_2 - x_3)| \\ \alpha(x_1, x_2, x_3) &= \frac{|x_2 - x_3|^2 (x_1 - x_2) \cdot (x_1 - x_3)}{2 \cdot \ell(x_2, x_3)^2}, \\ \beta(x_1, x_2, x_3) &= \frac{|x_3 - x_1|^2 (x_2 - x_3) \cdot (x_2 - x_1)}{2 \cdot \ell(x_2, x_3)^2}, \\ \gamma(x_1, x_2, x_3) &= \frac{|x_1 - x_2|^2 (x_3 - x_1) \cdot (x_3 - x_2)}{2 \cdot \ell(x_2, x_3)^2}. \end{aligned}$$

Furthermore, let

$$\begin{aligned}
c : X_- \rightarrow \mathbb{R}^3 & \quad c(x_1, x_2, x_3) = \alpha(x_1, x_2, x_3) \cdot x_1 + \beta(x_1, x_2, x_3) \cdot x_2 + \gamma(x_1, x_2, x_3) \cdot x_3 \\
r : X_- \rightarrow (0, \infty) & \quad r(x_1, x_2, x_3) = \frac{|x_1 - x_2||x_2 - x_3||x_3 - x_1|}{2 \cdot \ell(x_1, x_2, x_3)} \\
\hat{v} : X_- \rightarrow \mathbb{R}^3 & \quad \hat{v}(x_1, x_2, x_3) = \frac{(x_1 - x_2) \times (x_2 - x_3)}{\ell(x_1, x_2, x_3)}.
\end{aligned}$$

be functions that compute the circumcenter, circumradius, and a unit normal vector to the plane determine uniquely by the (noncollinear) points x_1, x_2, x_3 . As in Appendix B, an arbitrarily small value e is established as a lower bound on $\ell(x_1, x_2, x_3)$ — if ℓ drops below this value, then our program will terminate, so we will always assume that $\ell(x_1, x_2, x_3) \geq e$. As a result, lower and upper bounds may be computed for $|d\ell|, |d\alpha|, |d\beta|, |d\gamma|$, and $|dr|$.

The Newton function will again be represented by $\omega : T \rightarrow \mathbb{R}^6$, where $T = \{\mathbf{t} \in C_6S^1 : |t_i - t_j| \geq \varepsilon/F^6\}$, and defined as

$$\omega(\mathbf{t}) = \begin{bmatrix} \omega^{(1)}(\mathbf{t}) \\ \omega^{(2)}(\mathbf{t}) \\ \omega^{(3)}(\mathbf{t}) \\ \omega^{(4)}(\mathbf{t}) \\ \omega^{(5)}(\mathbf{t}) \\ \omega^{(6)}(\mathbf{t}) \end{bmatrix} = \begin{bmatrix} (f(t_4) - c(\mathbf{x}_-)) \cdot \hat{v}(\mathbf{x}_-) \\ (f(t_5) - c(\mathbf{x}_-)) \cdot \hat{v}(\mathbf{x}_-) \\ (f(t_6) - c(\mathbf{x}_-)) \cdot \hat{v}(\mathbf{x}_-) \\ (f(t_4) - c(\mathbf{x}_-))^2 - r(\mathbf{x}_-)^2 \\ (f(t_5) - c(\mathbf{x}_-))^2 - r(\mathbf{x}_-)^2 \\ (f(t_6) - c(\mathbf{x}_-))^2 - r(\mathbf{x}_-)^2 \end{bmatrix}.$$

The value \mathbf{x}_- is equal to $(x_1, x_2, x_3) = C_3 f(t_1, t_2, t_3)$. Then $\omega(\mathbf{t}) = \mathbf{0}$ if and only if $f(t_4), f(t_5)$ and $f(t_6)$ lie on the same circle as x_1, x_2, x_3 . Upper and lower bounds Ω_{\pm} may be placed on $|\det d\omega|$. If

$$|\omega(\mathbf{t})| \leq \Omega^*$$

then

$$|\omega(\mathbf{t})| |d\omega_{\mathbf{t}}^{-1}|^2 (\Omega_- + \Omega_+) \leq (\Omega^*) \left(\frac{1}{\Omega_-}\right)^2 (\Omega_- + \Omega_+) \leq \frac{1}{2}.$$

and by Kantorovich's Theorem, a unique root of ω exists within

$$|d\omega_{\mathbf{t}}^{-1}| |\omega(\mathbf{t})| \geq \frac{|\omega(\mathbf{t})|}{\Omega_+}$$

of \mathbf{t} , and Newton's method on ω will converge to it from \mathbf{t} .

Otherwise, if

$$|\omega(\mathbf{t})| > \Omega^*$$

then since $|\det d\omega|$ is bounded above by Ω_+ , a root of ω cannot lie too close to \mathbf{t} . In particular, a solution cannot lie within

$$\frac{|\omega(\mathbf{t})|}{\Omega_+} > \frac{\Omega^*}{\Omega_+}$$

of \mathbf{t} .

By choosing a very small positive real

$$u < \frac{\Omega^*}{\Omega_+},$$

and a collection of points $\mathbf{t}_1, \dots, \mathbf{t}_n$ in T where the union of balls of radius u about \mathbf{t}_i covers T , we may guarantee that all six-point cocircularities of the knot may be found via Newton's method, as long as $|\omega(\mathbf{t}_i)| \geq \Omega_+ u$ for each \mathbf{t}_i . As if

$$|\omega(\mathbf{t}_i)| > \Omega^*,$$

then there are no solutions to ω within $u < \Omega^*/\Omega_+$ of \mathbf{t}_i , and if

$$\Omega_+ u \leq |\omega(\mathbf{t}_i)| \leq \Omega^*,$$

then there exists a unique root of ω within

$$|d\omega_{\mathbf{t}}^{-1}| |\omega(\mathbf{t}_i)| \geq u$$

of \mathbf{t}_i . Running Newton's method on each \mathbf{t}_i guarantees that all solutions to $\omega(\mathbf{t}) = \mathbf{0}$ will be found.

Below is a description of the algorithm in pseudocode.

This program, if successfully run, outputs a list of all six-point cocircularities, and a quick check of each one can verify whether it is thelemic. If the program fails, adjusting the values of u , e or f can result in a successful implementation.

Algorithm 2 Detecting Thelemic Points

- Input: $u, e, \varepsilon, f, F_{\pm}$
 - f is a smooth embedding of S^1 into \mathbb{R}^3 , parameterized by the interval $[0, 2\pi]$.
 - F_{\pm} are the upper and lower bounds for $|df|$.
 - ε is a positive real smaller than the injective radius of the tubular neighborhood of f .
 - e is a positive real; the minimum tolerance for $(x_1 - x_2) \times (x_2 - x_3)$ before quitting the program.
 - u is an arbitrary positive real.
- Output: A list of preimages of six-point cocircularities.

-
- Partition $[0, 2\pi]$ evenly into n segments, where $2\pi/n < u$, letting $t_i = 2\pi i/n$.
 - FOR each $\{i_1, i_2, i_3, i_4, i_5, i_6\}$ such that $1 \leq i_1 < i_2 < i_3 < i_4 < i_5 < i_6 \leq n$:
 - Let $\mathbf{t} = (t_{i_1}, t_{i_2}, t_{i_3}, t_{i_4}, t_{i_5}, t_{i_6})$, $j = 0$, $\mathbf{x} = (x_1, x_2, x_3, x_4, x_5, x_6) = C_6 f(\mathbf{t})$, and $stoploop = false$.
 - If $|\omega(\mathbf{t})| > \Omega^*$: Let $stoploop = true$.
 - If $|\omega(\mathbf{t})| \leq \Omega_+ u$: TERMINATE PROGRAM
 - WHILE $j \leq 1000$ AND $stoploop = false$:
 - * If $|(x_1 - x_2) \times (x_2 - x_3)| < e$: TERMINATE PROGRAM.
 - * If $|\omega(\mathbf{t})| > \Omega^*$: Let $stoploop = true$.
 - * Let $\mathbf{h} = -d\omega_{\mathbf{t}}^{-1}(f(\mathbf{t}))$, and $\mathbf{t} = \mathbf{h} + \mathbf{t}$.
 - * Let $j = j + 1$.
 - If $stoploop = false$, OUTPUT \mathbf{t} .
-

Appendix E

Thelemic Circle Gallery

Below are three examples of thelemic circles on knots in greater detail. The knots selected are 4_1 , 5_2 , and 6_2 . In each example, an even number of thelemic circles appear, agreeing with Theorem 65.

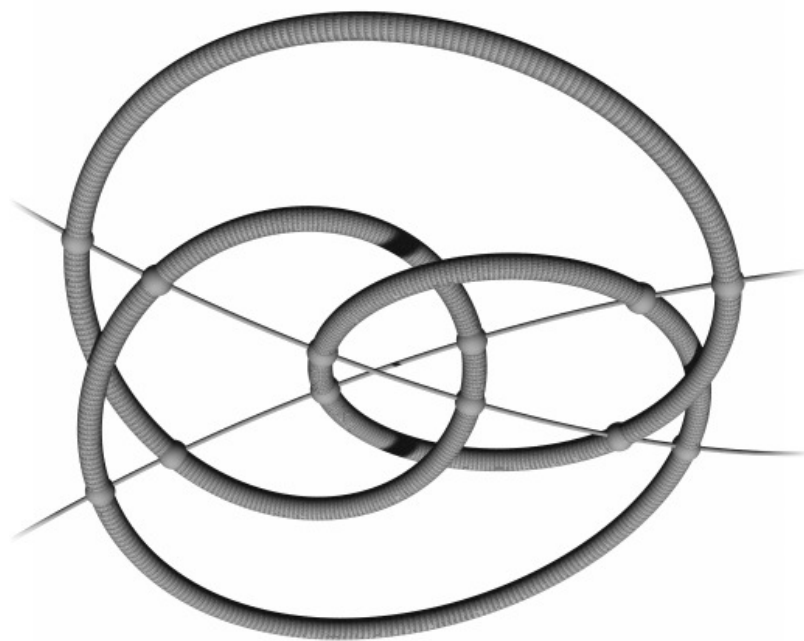


Figure E.0.1: The 4_1 knot.

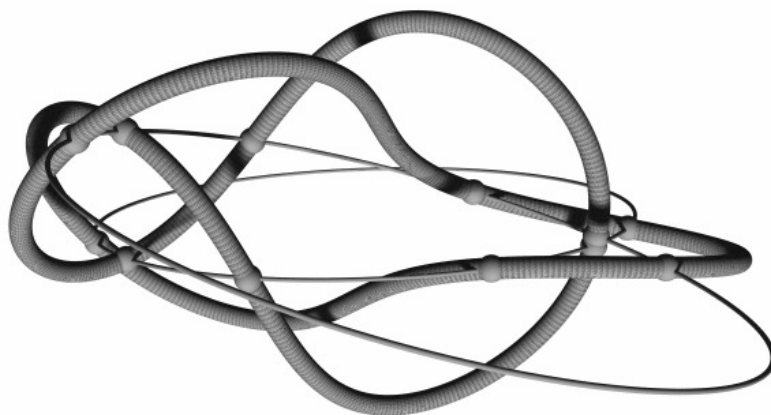


Figure E.0.2: The 5_2 knot.

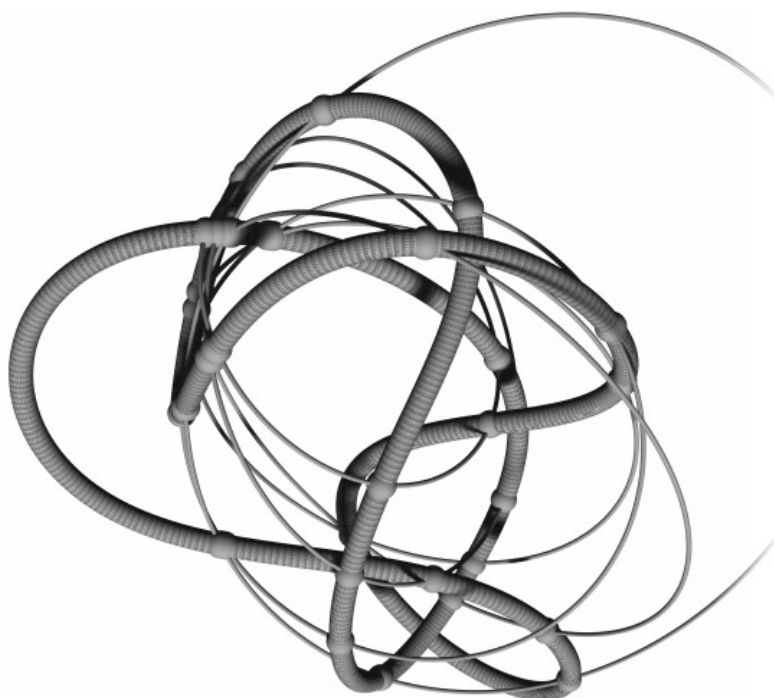


Figure E.0.3: The 6_2 knot.

Bibliography

- [B-N] D. Bar-Natan. *On the Vassiliev knot invariants*. *Topology* 34 (1995), no. 2, 423–472.
- [BCSS] R. Budney; J. Conant; K. P. Scannell; D. P. Sinha. *New perspectives on self-linking*. *Adv. Math.* **191** (2005), no. 1, 78–113.
- [Co] H. S. M. Coxeter. *Introduction to geometry*. Second edition. John Wiley & Sons, Inc., New York-London-Sydney, 1969. xviii+469 pp.
- [CDM] S. Chmutov, S. Duzhin, J. Mostovoy. *Introduction to Vassiliev knot invariants*. Pre-print (2010).
- [D] E. J. Denne. *Alternating quadriseccants of knots*. Thesis (Ph.D.)—University of Illinois at Urbana-Champaign. ProQuest LLC, Ann Arbor, MI, 2004. 119 pp.
- [Gi] B. Gilbert. *Ideal Knots, KnotAtlas*. http://katlas.org/wiki/Ideal_knots, April 9, 2009.
- [GP] V. Guillemin and A. Pollack, *Differential topology*, Prentice-Hall, Inc., Englewood Cliffs, 1974.
- [Ha] J. Hass. *Algorithms for recognizing knots and 3-manifolds*. *Knot theory and its applications*. *Chaos Solitons Fractals* **9** (1998), no. 4-5, 569–581.
- [Hi] M. W. Hirsch. *Differential topology*. Corrected reprint of the 1976 original. *Graduate Texts in Mathematics*, 33. Springer-Verlag, New York, 1994. x+222 pp.
- [L] J. M. Lee. *Introduction to smooth manifolds*. *Graduate Texts in Mathematics*, 218. Springer-Verlag, New York, 2003. xviii+628 pp.
- [M] P. W. Michor. *Topics in differential geometry*. *Graduate Studies in Mathematics*, 93. American Mathematical Society, Providence, RI, 2008. xii+494 pp.

- [P] M. Polyak. "Enumerative geometry and finite type invariants". MPI+Technion (2008).
- [Re] K. Reidemeister. *Knot theory*. Translated from the German by Leo F. Boron, Charles O. Christenson and Bryan A. Smith. BCS Associates, Moscow, Idaho, 1983. xv+143 pp.
- [Ro] D. Rolfsen. *Knots and links*. Mathematics Lecture Series, No. 7. Publish or Perish, Inc., Berkeley, Calif., 1976. ix+439 pp.
- [Sa] A. Sard. *The measure of the critical values of differentiable maps*. Bull. Amer. Math. Soc. **48**, (1942). 883–890.
- [Si] D. P. Sinha. *Manifold-theoretic compactifications of configuration spaces*. Selecta Math. (N.S.) **10** (2004), no. 3, 391–428.
- [V] V. A. Vassiliev. *Combinatorial formulas for cohomology of knot spaces*. Mosc. Math. J. **1** (2001), no. 1, 91–123.